

Aus dem Berlin-Brandenburger Centrum für Regenerative Therapien (BCRT)
der Medizinischen Fakultät Charité – Universitätsmedizin Berlin

DISSERTATION

„Expansion of human induced pluripotent stem cells (hiPSCs)
in 3D bioreactors for extracorporeal liver support”

zur Erlangung des akademischen Grades
Doctor medicinae (Dr. med.)

vorgelegt der Medizinischen Fakultät
Charité – Universitätsmedizin Berlin

von Selina Greuel
aus Bergisch Gladbach

Datum der Promotion: 06.03.2020

INHALTSVERZEICHNIS

ZUSAMMENFASSUNG DER PUBLIKATIONSPROMOTION	2
ABSTRACT (deutsch)	2
ABSTRACT (englisch).....	3
INTRODUCTION.....	4
Scientific background.....	4
Aim of the thesis	5
MATERIALS AND METHODS	6
2D culture and pre-expansion of undifferentiated hiPSCs.....	6
Expansion of undifferentiated hiPSCs in 3D bioreactors	6
Continuous measurement of oxygen.....	7
Calculation of the oxygen uptake rate (OUR).....	7
Calculation of the specific oxygen uptake rate (sOUR).....	7
Analysis of biochemical parameters	8
CellTiter-Blue® Cell Viability Assay.....	8
Simulation of hiPSC growth in a perfusion-based bioreactor model.....	8
Gene expression analysis of pluripotency and differentiation resp. stage-specific markers.....	9
Immunofluorescence studies	9
Culture medium testing in HUVEC cultures	10
Statistical evaluation	10
RESULTS	10
Cell metabolism and online oxygen monitoring of hiPSCs during expansion in 3D bioreactors.....	10
Quantification of hiPSCs after expansion in 3D bioreactors	12
Analysis of pluripotency and differentiation markers of hiPSCs during and after expansion in 3D bioreactors	13
Effect of culture media variations on human umbilical vein endothelial cell (HUVEC) cultures	14
DISCUSSION	15
CONCLUSION	18
REFERENCES	18
EIDESSTATTLICHE VERSICHERUNG	22
ANTEILSERKLÄRUNG AN DEN BETEILIGTEN PUBLIKATIONEN	23
ORIGINALARBEITEN ALS PROMOTIONSLEISTUNG	24
CURRICULUM VITAE	71
KOMPLETTE PUBLIKATIONSLISTE	73
DANKSAGUNG	74

ZUSAMMENFASSUNG DER PUBLIKATIONSPROMOTION

ABSTRACT (deutsch)

Akutes Leberversagen führt zu einem lebensbedrohlichen klinischen Zustand; therapeutische Möglichkeiten sind derzeit limitiert auf unterstützende Verfahren und die Lebertransplantation als Ultima Ratio. Die Verwendung von aus humanen induzierten pluripotenten Stammzellen (hiPSCs) gebildeten Hepatozyten, sog. *hepatocyte-like cells* (HLCs), stellt eine vielversprechende therapeutische Alternative dar, für die jedoch ausreichende Zellmengen in hoher Qualität und Reinheit benötigt werden.

Ziel des ersten Teils dieser Arbeit war es, die Expansion von hiPSCs in perfusionsbasierten 3D-Hohlfaser-Bioreaktoren in Kombination mit einem nicht-invasiven Online-Monitoring-Verfahren von Sauerstoff zur Kulturüberwachung zu untersuchen. Die erste Studie beschäftigt sich mit dem Einfluss der initialen Zelldichte auf das quantitative sowie qualitative Expansionsergebnis. Die Analyse der Expansionsraten, ermittelt durch Zellzählung und den CellTiter-Blue® Assay, ergab eine mehr als 100-fache Expansion in Bioreaktoren mit einer geringeren initialen Zelldichte ($2,9 - 3,3 \times 10^6$ Zellen/mL). Bioreaktoren, die mit einer höheren Zellzahl befüllt wurden ($16,6 \times 10^6$ Zellen/mL), zeigten hingegen nur eine 28-fache Expansion. Außerdem wurde anhand von Genexpressionsanalysen und immunhistologischen Untersuchungen in diesen Bioreaktoren auch eine höhere Rate einer spontanen, ungezielten Differenzierung festgestellt. Aus den Ergebnissen lässt sich schließen, dass eine eher geringe Zelldichte im Bereich von 3×10^6 Zellen/mL sowohl quantitativ als auch qualitativ zu besseren Expansionsergebnissen als eine höhere Zelldichte führt. In der zweiten Studie wurde die Verwendung einer kontinuierlichen Sauerstoffmessung zur engmaschigen Überwachung des Expansionsprozesses untersucht. Die errechneten Sauerstoffaufnahmeraten (*OURs*), Glukoseverbrauchsraten (*GCRs*) und Laktatproduktionsraten (*LPRs*) zeigten eine hoch signifikante Korrelation ($p < 0.0001$) und wiesen somit darauf hin, dass Sauerstoff in gleichem Maße wie Glukose zum Monitoring der hiPSC-Expansion in dem untersuchten Bioreaktorsystem geeignet ist, jedoch mit dem zusätzlichen Vorteil, die Kulturentwicklung in Echtzeit darzustellen.

Mit diesen beiden Studien wurden erfolgreich die Bedingungen für eine optimierte Expansion von hiPSCs in 3D-Bioreaktoren unter kontinuierlicher Online-Sauerstoffüberwachung etabliert.

Inhalt des zweiten Teils dieser Arbeit waren grundlegende Untersuchungen zu einer Verbesserung der leberspezifischen Funktionen von HLCs durch Kokultur mit *human umbilical vein endothelial cells* (HUVECs). Ziel war es, eine Mediumzusammensetzung zu ermitteln, die sowohl die hepatische Differenzierung der hiPSCs, als auch den Erhalt der kokultivierten HUVECs unterstützt. Die Ergebnisse zeigten, dass sowohl eine Mischung aus *hepatocyte culture medium*

(HCM) und *endothelial growth medium* (EGM) in einem 1:1-Verhältnis, als auch eine Mischung aus HCM und EGM-Zusätzen (ohne das EGM Basalmedium) für die HUVEC-Kultur geeignet sind. Damit wurden erfolgreich geeignete Mediumzusammensetzungen für nachfolgende Experimente zur Kokultur von hiPSCs mit HUVECs identifiziert.

ABSTRACT (englisch)

Acute liver failure (ALF) is a life-threatening condition, which to date can only be treated by supportive care or liver transplantation. The use of hiPSC-derived hepatocyte-like cells (HLCs) offers a promising therapeutic alternative which, however, requires sufficient hiPSC quantities at high cell quality and purity.

Therefore, the aim of the first part of this thesis was to investigate the expansion of hiPSCs in perfusion-based, 3D hollow-fiber bioreactors combined with non-invasive online monitoring of oxygen for culture surveillance.

The first study examines the effect of the initial cell density on the quantitative and qualitative expansion outcome. Analysis of the expansion rates, which were determined by cell counting and performing the CellTiter-Blue® Assay, revealed a more than 100-fold expansion at low initial cell densities ($2,9 - 3,3 \times 10^6$ cells/mL) compared to a 28-fold expansion at higher initial cell densities ($16,6 \times 10^6$ cells/mL). Furthermore, a higher rate of spontaneous cell differentiation occurred in bioreactors inoculated with higher cell densities. To conclude, lower initial cell densities in the range of 3×10^6 cells/mL lead to better quantitative and qualitative expansion results compared to higher initial cell densities.

In the second study, the use of continuous measurement of oxygen for online culture control was evaluated. Calculated oxygen uptake rates (*OURs*), glucose consumption rates (*GCRs*) and lactate production rates (*LPRs*) revealed a highly significant correlation ($p < 0.0001$), indicating that oxygen is equivalent to glucose as parameter for hiPSC expansion while providing an accurate real-time monitoring of the hiPSC culture development.

As a result of both studies, the conditions for an optimized expansion of hiPSCs in 3D bioreactors under continuous online surveillance of oxygen were successfully established.

Subject of the second part of this thesis were basic studies on the co-cultivation of hiPSCs with human umbilical vein endothelial cells (HUVECs) for an improvement of the hepatic differentiation of hiPSCs. The study was aimed at determining a medium composition supporting both, the hepatic differentiation of hiPSCs as well as the maintenance of co-cultured HUVECs. The results revealed that a mixture of hepatocyte culture medium (HCM) and endothelial growth medium (EGM) at a 1:1 ratio, as well as a mixture of HCM and EGM supplements (without the

base medium) supported the maintenance of HUVEC cultures. Thus, suitable medium compositions for following experiments on co-cultures of hiPSCs and HUVECs were successfully identified.

INTRODUCTION

Scientific background

The liver is the central organ responsible for detoxification, synthesis of proteins (such as albumin) and metabolism of small molecules. Liver failure constitutes a life-threatening condition.¹ Acute liver failure (ALF) in particular has a very variable clinical progression, and the mortality rate is high. In the United States, deaths upon ALF without transplantation occur in 30% of adults.² To date, treatment options for patients with ALF (or acute-on-chronic liver failure) are limited to supportive care, or liver transplantation.³ To overcome this limitation, several bioartificial liver support devices have been developed.⁴ Sauer and colleagues, for example, successfully treated a 26-year old patient suffering from primary graft non-function of a liver transplant using an extracorporeal liver support technology charged with primary human liver cells.⁵ However, the availability of primary human liver cells is limited. A major approach to address this challenge is the use of human induced pluripotent stem cells (hiPSCs). In contrast to human embryonic stem cells, which are subject to ethical concerns with regards to their retrieval and clinical use, hiPSCs can be generated from adult tissue cells by introducing specific genes encoding transcription factors.⁶ Generated hiPSCs can then be used as a cell source for subsequent differentiation into the desired cell type, such as hiPSC-derived hepatocyte-like cells (HLCs). However, for supplying clinical therapies with hiPSC derivatives, large quantities are needed. As 3D bioreactors enable large-scale cultures of hiPSCs in a closed system, their use is better suitable for achieving high cell numbers as compared to conventional 2D cultures, which lack in scalability and production yields.^{7,8} To date, typically achieved cell numbers lay between 2.00 and 2.85×10^8 hiPS cells upon expansion in bioreactors, with expansion rates ranging from the four to sevenfold.^{9,10} Despite these promising results, at least 5×10^9 to 10^{10} hepatic cells would be necessary for treatment of hepatic failure with an extracorporeal liver device.^{7,11} In order to further optimize the expansion process in 3D systems, it is important to consider those factors that potentially influence hiPSC expansion and differentiation in 3D culture systems, such as the cell inoculum density.^{8,12}

Besides large cell quantities, expanded hiPSCs need to be of high purity, with cells preserving their pluripotency characteristics, as well as their expansion and differentiation potential for subsequent differentiation and clinical use.¹³ The continuous control of the expansion is of great importance in order to instantly detect stagnation in culture growth or early changes in cell fate,

and as a consequence being able to intervene promptly. In the biotechnological industries, measurement of oxygen is commonly used for bioprocess control.¹⁴ In recent studies, it has been shown that the measurement of oxygen can also be utilized for monitoring growth in mammalian 3D tissue cultures.^{15,16} However, studies using oxygen measurements for surveillance of stem cell cultures, especially hiPSC cultures, are limited.^{9-10,17}

A further challenge that has to be addressed in hiPSC-based liver support systems is a sufficient differentiation grade of the cells in such systems. Thus, hiPSC-derived HLCs resulting from subsequent directed hepatic differentiation need to be of high maturity and must provide high functionality for effectively treating patients with ALF. Currently, research groups have successfully produced hiPSC-derived HLCs with up to 85% of differentiated cells expressing several hepatic markers.¹⁸ Despite these promising results, the cell functionality as determined by their urea and albumin production, is in a range of only 10% of the functionality of primary human hepatocytes.¹⁹ Furthermore, cytochrome P450 (CYP) isoenzyme activities of resulting HLCs are nearly 30-fold lower compared to those of primary human hepatocytes.¹⁹ However, it has been shown that the co-culture with non-parenchymal cells improves the hepatic functionality of HLCs derived by hiPSCs.²⁰ For utilizing such co-cultures, a medium composition needs to be determined that supports the growth resp. maintenance of both cell types.

Aim of the thesis

The aim of the first part of this thesis was to explore the expansion of hiPSCs in 3D hollow-fiber bioreactors in view of future clinical applications. Two main aspects were investigated:

In the first study, the effect of the inoculum density on the expansion procedure and expansion outcome was analyzed (Greuel, et al., 2019a). The second study examined the feasibility of continuous oxygen monitoring for 3D culture control during the hiPSC expansion process (Greuel et al., 2019b). Based on the results, suitable conditions for an optimized expansion of hiPSCs in 3D bioreactors under continuous online surveillance of oxygen were determined.

The aim of the second part of this thesis was to investigate different media variations with respect to supporting the maintenance of human umbilical vein endothelial cells (HUVECs), while enabling growth and hepatic differentiation of co-cultured hiPSCs (Freyer et al., 2017). As a result, promising medium compositions for use in co-culture models for improved differentiation of hiPSC-derived HLCs were identified.

MATERIALS AND METHODS

2D culture and pre-expansion of undifferentiated hiPSCs

Before bioreactor inoculation, the hiPSC line DF6-9-9T²¹ (WiCell Research Institute, Madison, WI, USA) was grown under feeder-free conditions on six-well culture plates or T175 culture flasks (both BD Falcon, San José, CA) coated with 8.68 $\mu\text{g}/\text{cm}^2$ Matrigel (growth factor reduced, Corning, NY, USA) and passaged after reaching a confluency of approx. 70% using EDTA (Versene, 0.48mM, Gibco® by Thermo Fisher Scientific, Waltham, MA, USA). The culture medium mTeSR^{TM1} (Stemcell Technologies, Vancouver, BC, Canada) was used, supplemented with 10.000 units/mL penicillin and 10 mg/mL streptomycin (Pen Strep, Gibco® by Life Technologies/ Thermo Fisher Scientific).

Expansion of undifferentiated hiPSCs in 3D bioreactors

The 3D hollow-fiber bioreactor, with a cell compartment volume of either 3 or 17 mL, is characterized by a capillary structure, which mimics the *in vivo* mass transport of nutrients and oxygen for an optimized nutrient supply, enabling high density cell cultures in the extracapillary space.²² The bioreactors were integrated into a perfusion device with electronic temperature control, pumps for medium feed and medium recirculation, and a gas mixing unit for air resp. CO₂ supply.

Following pre-expansion, a number of either 10 x 10⁶ (resulting in a cell density of 3,3 x 10⁶ cells/mL in 3 mL bioreactors) or 50 x 10⁶ hiPSCs (resulting in a cell density of 16,6 x 10⁶ cells/mL in 3 mL bioreactors or a cell density of 2,9 x 10⁶ cells/mL in the 17 mL bioreactor) were inoculated into precoated bioreactors (8.68 $\mu\text{g}/\text{cm}^2$ Matrigel, Corning). The medium recirculation rate was set to 10 mL/min (3 mL bioreactors) resp. 20 mL/min (17 mL bioreactor), whereas the medium feed was initially set to 1 mL/h (3 mL bioreactors) resp. 2 mL/h (17 mL bioreactor). Feed rates were adapted daily, depending on glucose consumption rates, and reached up to 12 mL/h (3 mL bioreactors) or 40 mL/h (17 mL bioreactor). The gas perfusion rate was maintained at 20 mL/min (3 mL bioreactors) resp. 40 mL/min (17 mL bioreactor) throughout the culture period; CO₂ was added at a percentage of up to 5% for pH regulation. Bioreactor cultures were maintained over a time period of 15 days and compared to 2D cultures and embryoid bodies with respect to the expression of pluripotency and differentiation markers.

Embryoid bodies were built by placing 2 x 10⁶ hiPSCs into an AggreWell 800 plate (Stemcell Technologies); the following day, formed embryoid bodies were cultured in E6-medium²³ for 15

days on non-treated 12-well culture plates (Costar®, Corning®, NY, USA) for expression analysis or Lumox plates (Sarstedt, Nümbrecht, Germany) for immunohistochemical staining.

Continuous measurement of oxygen

A chemical optical oxygen sensor, built for performing oxygen measurements in fluids (O₂ Flow-Through Cell FTC-PSt3-S, PreSens, Regensburg, Germany), was incorporated into the perfusion circuit behind the medium outflow of the bioreactor. Thereby, the sensor did not interfere with the cultured cells. Oxygen values were automatically measured at 10-minute-intervals during the 15-day bioreactor culture period and controlled by a custom-built software, provided by StemCell Systems GmbH, Berlin, Germany.

Calculation of the oxygen uptake rate (OUR)

Mean *OUR* values of the bioreactors (μmol/h) were calculated as described previously²⁴ for time intervals of 24 hours. For *OUR* calculation, equation (1) was used, where the term $k_L a \times (C^* - C)$ represents the volumetric oxygen transfer rate (*OTR*) from the gas capillaries to the bioreactor (μmol/L/h); $k_L a$ is the volumetric oxygen transfer coefficient (h⁻¹), C^* (μmol/L) the saturation constant for dissolved oxygen concentration in the liquid medium, and C (μmol/L) the dissolved oxygen concentration in the medium at time point t during the culture period of 15 days. The oxygen uptake rate (*OUR*) is expressed by the term $q_{O_2} \times N$. The term dC/dt (μmol/L/h) refers to the accumulation of oxygen in the liquid phase over a defined period dt . The $k_L a$ was determined as described elsewhere (Greuel et al., 2019b).

$$OTR \times V - q_{O_2} \times N = k_L a \times (C^* - C) - q_{O_2} \times N = \left(\frac{dC}{dt}\right) \times V \quad (1)$$

Calculation of the specific oxygen uptake rate (sOUR)

Two hours after cell inoculation as well as on the final day of the experiment (day 15), the continuous supply of gas as well as nutrients was paused for 1 hour. During that time period, oxygen measurements were performed every 2 minutes instead of every 10 minutes in order to accurately detect the decline in oxygen concentration. For evaluation of the oxygen consumption during that time period, the measured value after 1 hour was subtracted from the initial value before pausing fresh medium and gas supply.

In order to obtain specific oxygen uptake rates, equation (2) was used, where the term $k_L a \times (C^* - C) - \left(\frac{dC}{dt}\right)$ refers to the oxygen uptake during the 60 minutes, and N refers to the

cell numbers obtained by cell counting (day 0) or the CellTiter-Blue® Cell Viability Assay (day 15).

$$sOUR = \frac{k_L a \times (C^* - C) - \left(\frac{dC}{dt}\right)}{N} \quad (2)$$

Analysis of biochemical parameters

The metabolic activity of cultured cells was analyzed by daily measurements of glucose and lactate concentrations in samples from the recirculating medium with a blood gas analyzer (ABL 700, Radiometer, Copenhagen, Denmark). Glucose consumption rates (*GCRs*) and lactate production rates (*LPRs*) were calculated based on daily collected raw data of glucose and lactate, as previously described.²⁵ The yield coefficient of lactate from glucose was calculated by dividing lactate production rates by glucose consumption rates.

Further clinical parameters were analyzed by Labor Berlin GmbH, using clinical chemistry analyzers. Potential cell damage was assessed by measuring the lactate dehydrogenase (LDH) release, and beginning differentiation was detected by measuring alpha-fetoprotein (AFP) levels in the culture perfusate. AFP levels were analyzed every five days, or more frequently when concentrations were above the detection limit.

CellTiter-Blue® Cell Viability Assay

The CellTiter-Blue® Cell Viability Assay (CTB, Promega GmbH, Mannheim, Germany) was performed at the end of the experiment for indirect cell quantification according to the manufacturer's instructions. A concentration of 2.5% CTB was applied to the bioreactor recirculation. Samples were taken every 15 minutes, and after 60 minutes a stop solution consisting of 3% sodium dodecyl sulfate (SDS, Carl Roth GmbH + Co. KG, Karlsruhe, Germany) and 97% dimethyl sulfoxide (DMSO, Sigma-Aldrich/Merck, Darmstadt, Germany) was added to the samples for inhibition of an ongoing conversion of resazurin to resorufin. Fluorescence measurements were performed at 560 nm (excitation) and 590 nm (emission) using the Infinite M200 Pro plate reader (Tecan Group Ltd., Männedorf, Switzerland). Indirect cell quantification was undertaken based on a calibration curve, which was built by correlating a defined number of cells with obtained CTB gradients.

Simulation of hiPSC growth in a perfusion-based bioreactor model

A compartmentalized model for the 3D hollow-fiber bioreactor was built by Prof. Carl-Fredrik Mandenius (Linköping University, Sweden) in MATLAB (MathWorks, Massachusetts, USA) using the toolbox SIMUPLOT (KTH, Stockholm, Sweden). Established mass balances and kinetic

equations frequently used in bioreactor engineering were applied; experimental data obtained from the bioreactor runs were used to fit the values of these parameters.

Gene expression analysis of pluripotency and differentiation resp. stage-specific markers

The RNA isolation and subsequent cDNA synthesis were performed as previously described²⁶ using the PureLink™ RNA Mini Kit (Life Technologies) and the High Capacity cDNA Reverse Transcription Kit (Applied Biosystems, Foster City, CA). The produced cDNA was prepared for quantitative real-time polymerase chain reaction (qRT-PCR; Mastersyler ep Realplex 2; Eppendorf, Wesseling-Berzdorf, Germany) according to the manufacturer's instructions using the polymerase chain reaction (PCR) Master mix (Applied Biosystems; Foster City, CA, USA). The following human specific primers and probes (Taqman Gene Expression Assays; Life Technologies/ Thermo Fisher Scientific) were used in hiPSC cultures: Alpha Fetoprotein (*AFP*), C-X-C Motif Chemokine Receptor 4 (*CXCR4*), GATA Binding Protein 2 (*GATA2*), Nanog Homeobox (*Nanog*), Neurofilament Light (*NEFL*), Paired Box 6 (*PAX6*), POU Class 5 Homeobox 1 (*POU5F1*), SRY-Box 17 (*SOX17*) and T-Box Transcription Factor T (*T*). For HUVEC cultures, the following two primers and probes were used: platelet and endothelial cell adhesion molecule 1 (PECAM1) and von Willebrand factor (VWF). Expression values of measured genes were normalized to expression values of the house-keeping gene glyceraldehyde-3-phosphate dehydrogenase (GAPDH) and fold changes of expression levels were calculated using the $\Delta\Delta C_T$ method.²⁷

Immunofluorescence studies

Upon termination of bioreactor cultures, sections of the capillary bed containing cell material were removed and prepared for immunofluorescence staining by fixating the samples with 4% formaldehyde (Herbeta Arzneimittel, Berlin, Germany), followed by dehydration, paraffinization and cutting into 2.5 to 5 μm thick slides. Afterwards, slides were deparaffinized and rehydrated; antigen-retrieval was performed by boiling the samples in citrate buffer (pH of 6.0), followed by antibody staining as previously described.²⁵ Samples were incubated with primary antibodies specific for the following antigens: Alpha-fetoprotein (AFP), Marker Of Proliferation (MKI67), Nestin (NES), POU Class 5 Homeobox 1 (POU5F1), Vimentin (VIM) and Alpha Smooth Muscle Actin (α -SMA). For HUVEC cultures, antibodies against the platelet and endothelial cell adhesion molecule 1 (PECAM1) and von Willebrand factor (VWF) were employed. Nuclei were counterstained with Dapi. As secondary antibodies, Alexa Fluor 488 anti-mouse and Alexa Fluor 594 anti-rabbit (Life Technologies) were applied.

Culture medium testing in HUVEC cultures

Cryopreserved HUVECs (PromoCell GmbH, Heidelberg, Germany) were cultivated on cell culture dishes (Thermo Fisher Scientific), using endothelial cell growth medium (EGM, PromoCell GmbH), consisting of basal medium and EGM supplements, as well as gentamycin added at a concentration of 0.05 mg/mL (Merck, Darmstadt, Germany). The cells were passaged according to the manufacturer's instructions when they reached a confluence of approx. 95%.

For testing of different culture media, HUVECs were seeded at a density of 4×10^3 cells/cm² and cultured over 14 days using either 100% endothelial growth medium (EGM, positive control), 100% hepatocyte culture medium (HCM), HCM and EGM at a ratio of 1:1 (HCM + EGM) or HCM enriched with endothelial cell growth supplements (HCM + EGM supplements). The media compositions were compared with regards to microscopic cell evaluation, glucose consumption and lactate production as well as gene expression and immunocytochemical staining of the endothelial markers platelet and endothelial cell adhesion molecule 1 (PECAM1) and von Willebrand factor (VWF).

Statistical evaluation

Statistical analysis was performed using GraphPad Prism 7.0 for Windows (GraphPad Software, SanDiego, CA). Data are presented as means \pm standard error of the mean (SEM), unless stated otherwise. Correlation analysis was performed using the Pearson correlation coefficient for comparison of the *OUR* and *GCR* resp. *LPR* in each bioreactor group. Differences in the oxygen consumption and *sOUR* on day 0 and day 15 between the two 3 mL bioreactor groups and time points, as well as differences between both 3 mL bioreactor groups regarding quantification data, areas under curves (AUCs) and peak times of biochemical parameters were detected using the unpaired, two-tailed Student's *t*-test. The effects of different media variations on HUVEC cultures were also detected using the unpaired, two-tailed Student's *t*-test; the area under the curve was calculated for the time courses of biochemical parameters beforehand.

RESULTS

Cell metabolism and online oxygen monitoring of hiPSCs during expansion in 3D bioreactors

The time courses of glucose consumption and lactate production revealed significant differences between the two 3 mL bioreactor groups; in 3 mL bioreactors inoculated with 50×10^6 cells, the area under curve (AUC) was significantly larger ($p < 0.05$), and the tipping point was achieved significantly earlier ($p < 0.05$) as compared to 3 mL bioreactors inoculated with 10×10^6 cells ($p < 0.05$). The metabolic parameters for the 17 mL bioreactor revealed maximum values that were

more than three times as high compared to maximum values obtained in 3 mL bioreactors inoculated with 50×10^6 cells. In conclusion, higher cell densities led to a significantly higher overall glucose metabolism in 3 mL bioreactors; the highest values for energy metabolism were achieved in the 17 mL bioreactor.

The online oxygen curves were generated from oxygen measurements at 10-minute-intervals; for clarity purposes, the time courses of online oxygen measurements are compared exemplarily for one bioreactor of each group. In both 3 mL bioreactors, oxygen curves decreased during the first 7 days, followed by constant oxygen levels until the end of bioreactor cultures. However, the overall drop of oxygen was more profound in the 3 mL bioreactor inoculated with 50×10^6 cells (a $100 \mu\text{mol/L}$ drop) compared to the bioreactor inoculated with 10×10^6 cells (a $75 \mu\text{mol/L}$ drop). The oxygen curve for the 17 mL bioreactor showed a decrease of oxygen throughout the culture until day 14. Also, the overall oxygen drop value was the highest compared to both 3 mL bioreactors with a value of $155 \mu\text{mol/L}$. These results indicate that the cell growth is strongest in the 17 mL bioreactor and takes place until the end of the 15-day culture period, whereas a growth stagnation is reached in both 3 mL bioreactors after approximately 7 days.

In order to compare the ability of predicting the culture performance of online oxygen measurement with that of glucose and lactate, the *OURs* were compared to the *GCRs* and *LPRs*, which showed similar time courses. The correlation analysis between *OUR* and *GCR* or *OUR* and *LPR* values revealed a high significance for all bioreactor groups ($p < 0.0001$), indicating that oxygen is equally as suitable as glucose and lactate for reflecting the culture development.

The measured oxygen consumption revealed a distinct increase between the day of inoculation and day 15 for all of the tested bioreactor types and conditions. Significant differences were observed in oxygen consumption between both 3 mL bioreactor groups on day 0, and between day 0 and day 15 within the 3 mL bioreactors inoculated with 10×10^6 cells. Specific oxygen uptake rates revealed a significant decrease in oxygen uptake per cell at the end of cell cultures compared to the day of cell inoculation. This decrease was most pronounced in 3 mL bioreactors inoculated with 10×10^6 cells with a *sOUR* of $140 \pm 8 \text{ fmol/cell/h}$ on day 0 and $15 \pm 3 \text{ fmol/cell/h}$ on day 15 ($p < 0.01$), followed by the 3 mL bioreactors inoculated with 50×10^6 cells with *sOUR* values of $84 \pm 26 \text{ fmol/cell/h}$ on day 0 and $15 \pm 2 \text{ fmol/cell/h}$ on day 15 ($p < 0.05$). Uptake values of the 17 mL bioreactor were 101 fmol/cell/h on the day of cell inoculation and 10 fmol/cell/h on the final day of the experiment.

These results show that cell cultures consume considerably more oxygen at the end of the expansion procedure; however, the oxygen consumption per cell decreases.

In order to gain a deeper insight into the energy metabolism of the cultured cells, the yield coefficient of lactate from glucose was calculated, which was below 1.8 for all bioreactors during the entire culture indicating a generation of ATP mainly from oxidative phosphorylation. The highest recorded value was on the first day of culture in the 3 mL bioreactors inoculated with 10×10^6 cells (1.67 ± 0.02), whereas the lowest value was on day 6 for the 17 mL bioreactor (1.14). However, the ratio of *OURs* [$\mu\text{mol/h}$] to *GCRs* [$\mu\text{mol/h}$] showed a constant increase during the entire culture for both 3 mL bioreactors (maximum of 0.3 in 3 mL bioreactors inoculated with 50×10^6 cells), indicating that no more than 5% of the glucose metabolism occurred under usage of oxygen.

Quantification of hiPSCs after expansion in 3D bioreactors

The cell quantification based on the CellTiter-Blue® Cell Viability Assay (CTB), which was performed on the final day of the experiment, revealed the highest achieved cell number for the 17 mL bioreactor (5.39×10^9 cells), followed by the 3 mL bioreactors inoculated with 50×10^6 cells ($1.40 \times 10^9 \pm 37.96$) and with 10×10^6 cells ($1.10 \times 10^9 \pm 21.04$). Cell yields were significantly different ($p < 0.05$) between the two 3 mL bioreactor groups. Expansion rates revealed a 28-fold increase in 3 mL bioreactors inoculated with 50×10^6 cells. In contrast, an over 100-fold increase in cell number was observed for 3 mL bioreactors inoculated with 10×10^6 cells and for the 17 mL bioreactor.

These results indicate that lower cell densities, although leading to a lower absolute cell yield after the expansion procedure (in 3 mL bioreactors), lead to a much more efficient expansion with a more than 100-fold increase in cell number. Cell expansion in the 17 mL bioreactor led to a production of 5.39×10^9 hiPSCs.

The model simulation, which was carried out by Prof. Carl-Fredrik Mandenius (Linköping University, Sweden), was built in order to predict the cell growth course from the inoculation cell number and the final cell number. Rate parameters and inhibition constants in the simulation model were fitted to the experimental data from the three bioreactor conditions. The rate “constants” are essentially changing dynamically during bioreactor runs due to the cells’ gradual transformation. These changes in cell growth resp. culture development were, in contrast to most models, incorporated into the model simulation and thereby, the simulation gives a realistic impression of the time courses of culture parameters during the expansion procedure.

Analysis of pluripotency and differentiation markers of hiPSCs during and after expansion in 3D bioreactors

Release rates of lactate dehydrogenase (LDH), indicating potential cell death, increased in both 3 mL bioreactor groups with culture progression, but were significantly higher in 3 mL bioreactors inoculated with 50×10^6 cells throughout the culture period compared to 3 mL bioreactors inoculated with 10×10^6 cells ($p < 0.0001$). For the 17 mL bioreactor, LDH release showed a similar time course as the 3 mL bioreactors inoculated with 50×10^6 cells, while absolute values were three times as high. The albumin precursor alpha-fetoprotein (AFP), indicating beginning differentiation, showed an exponential increase from day 12 onwards for 3 mL bioreactors inoculated with 50×10^6 cells. In contrast, there was no AFP detectable in perfusates of 3 mL bioreactors inoculated with 10×10^6 cells during the entire culture period. For the 17 mL bioreactor, a slight increase was measured from day 14 onwards. These results indicate that higher initial cell densities lead to earlier and more distinct onset differentiation processes.

For the characterization of hiPSCs after expansion in 3D bioreactors, the gene expression of pluripotency and differentiation markers relative to the undifferentiated state were analyzed. The expression data of the two pluripotency markers *POU5F1* and *NANOG* revealed only slight changes in the pluripotency of bioreactor cultures. In contrast, a distinct reduction in *POU5F1* and *NANOG* expression was detected in embryoid bodies.

Regarding differentiation markers, the strongest increases in gene expression were observed for the endodermal lineage marker *AFP* with highest values being detected for embryoid bodies and for 3 mL bioreactors inoculated with 50×10^6 cells. Gene expression measurements for the other two endodermal markers, *SOX17* and *CXCR4*, revealed an increase compared to the undifferentiated state in both 3 mL bioreactor groups. However, the expression of *CXCR4* showed the highest value in embryoid bodies, which was significantly higher compared to both 3 mL bioreactor groups ($p < 0.05$). Also, the expression data for the ectodermal marker *NEFL* showed the strongest increase in embryoid bodies, with expression values being significantly higher compared both 3 mL bioreactor groups ($p < 0.001$). In contrast, values for *T*, a marker for early mesodermal differentiation, revealed the highest expression values in both 3 mL bioreactor groups and the lowest ones in embryoid bodies.

To summarize, gene expression profiles indicate beginning differentiation processes in bioreactor cultures, which were most pronounced in 3 mL bioreactors inoculated with higher cell densities (50×10^6 cells). However, the expression of both pluripotency markers was higher, and expression

of the majority of differentiation markers was lower in bioreactor cultures as compared to the embryoid bodies.

Staining with the pluripotency marker POU5F1 and the proliferation marker MKI67 showed that the vast majority of cells in 3 mL bioreactors inoculated with 10×10^6 cells and in the 17 mL bioreactor were positive for POU5F1 and MKI67. In contrast, only approximately half of the cells in 3 mL bioreactors inoculated with 50×10^6 cells were positive for those markers. The marker α -SMA, indicating mesodermal differentiation, was mostly negative in all bioreactor groups. In contrast, staining of α -SMA was clearly positive in embryoid bodies and interestingly, the stained structures appeared filament-like. The marker for the endodermal lineage AFP was detectable in the majority of cells in embryoid bodies and in a number of cells in both 3 mL bioreactor groups. In contrast, cells expanded in the 17 mL bioreactor appeared negative for AFP. The marker for the ectodermal lineage nestin was detected in embryoid bodies and, again, filament-like structures were visible. Only a small number of cells in 3 mL bioreactors or the 17 mL bioreactor were positive for nestin.

In summary, the majority of cultured cells in bioreactors expressed both, the pluripotency marker and the proliferation marker, whereas only a small fraction of cells was positive for differentiation markers; most pronounced beginning differentiation processes in bioreactors occurred in 3 mL bioreactors inoculated with 50×10^6 cells. However, the expression of differentiation markers in those bioreactors was lower than in embryoid body cultures, which partially formed filament-like structures.

Effect of culture media variations on human umbilical vein endothelial cell (HUVEC) cultures

The use of pure hepatocyte culture medium (HCM) without any addition of endothelial cell growth medium (EGM) led to rapid HUVEC disintegration and detachment, whereas the use of pure EGM, used as a positive control, resulted in constantly increasing glucose consumption and lactate production during the 15-day culture period. However, when mixing HCM and EGM at a 1:1 ratio, values for glucose consumption and lactate production of HUVEC cultures were almost similar compared to HUVEC cultures using pure EGM. Also, EGM, as well as the HCM and EGM 1:1 mixture both led to an increase in endothelial cell markers platelet and endothelial cell adhesion molecule 1 (PECAM1) and von Willebrand factor (VWF) expression by the 3 to 4-fold. In contrast, a mixture of HCM and EGM supplements (without the base medium) resulted in considerably lower glucose metabolism in HUVECs as well as slightly lower expression values for the endothelial markers PECAM1 and VWF. Immunocytochemical analysis mirrored these

observations. The results indicate that both HCM and EGM mixtures are suitable for downstream hiPSC and HUVEC co-culture experiments, the mixture of HCM and EGM at a 1:1 ratio being the preferred medium composition with regards to HUVEC maintenance.

DISCUSSION

The generation of hiPSC-derived hepatocyte-like cells (HLCs) offers a unique opportunity for treatment of acute liver failure (ALF). In order to enable such hiPSC-based therapies, sufficient cell numbers at high cell quality and purity are necessary. Therefore, the first part of this thesis aims to establish suitable conditions for optimized hiPSC expansion in 3D bioreactors with continuous culture surveillance via online oxygen measurement.

In the first study, the influence of the initial hiPSC density on the expansion procedure, expansion yield and pluripotency state of the cells was investigated (Greuel et al., 2019a). Higher inoculation numbers resp. cell densities (3 mL bioreactors inoculated with 50×10^6 cells) led to a higher metabolic activity, and expansion occurred faster compared to lower inoculation numbers (3 mL bioreactors inoculated with 10×10^6 cells or the 17 mL bioreactor), as indicated by glucose metabolism values. This observation may be explained by a greater cell-cell signaling, leading to an increased cell proliferation and expansion rate.^{28,29} Similar findings have been reported by Meng et al.,³⁰ who reported that the strongest increase in viable cell density occurred with the highest cell inoculation number when inoculating three different cell densities into stirred-suspension bioreactors.

However, the results of this study show that higher inoculation numbers also lead to cells more prone to beginning differentiation processes, as indicated by increasing alpha-fetoprotein (AFP) release rates towards the end of bioreactor cultures, as well as gene expression and immunohistochemistry data obtained upon termination of the bioreactor cultures. These differentiation tendencies can be explained by an upper cellularity limit of the bioreactor cell compartment,³¹ and/or large aggregate sizes resulting in a reduced nutrient and oxygen supply in the central regions of the aggregates.³² The observed differentiation tendencies may be prevented by applying a dissociation protocol as performed in a study by Abecasis et al.,¹⁷ or harvesting cells from the cell compartment as soon as cell cultures reach a growth plateau, as reported by Knöspel et al.²⁶

With regards to the expansion yields, bioreactors inoculated with higher cell numbers achieved higher absolute expansion yields compared to bioreactors inoculated with lower cell numbers. However, when relating the achieved cell numbers to the initial cell numbers, higher initial cell

densities led only to a 28-fold expansion, whereas lower initial cell densities led to an over 100-fold expansion. The cell quantities achieved in the 17 mL bioreactor (5.39×10^9 cells) would be sufficient for single-patient treatments for myocardial infarction and treatment of diabetes.⁷ To date, such relevant cell numbers have only been achieved by Kwok et al., who gained 2×10^9 hiPSCs after 14 days of stirred suspension culture,³³ and Abecasis et al., who obtained 10^{10} pluripotent hiPSCs within 11 days of 3D culture and three sequential passages.¹⁷ The implementation of a dissociation protocol into this study may not only prevent spontaneous differentiation processes, but furthermore improve the expansion rates of cultured hiPSCs. In addition, an up-scale from the 17 mL bioreactor to bioreactors with a culture volume of 800 mL will most likely lead to a production of sufficient cell numbers ($>10^{10}$ cells) for treating patients with hepatic failure.³⁴

The second study investigates the feasibility of using non-invasive online oxygen measurement for monitoring cell growth and activity during hiPSC expansion in 3D bioreactors (Greuel et al., 2019b).

The recorded oxygen time courses of the tested bioreactor conditions demonstrate the feasibility of online oxygen measurement for hiPSC expansion monitoring. Also, the variations in growth behaviors between the bioreactor conditions were reflected in the *OUR*, *GCR* and *LPR*. The *OUR* and *GCR* values as well as *OUR* and *LPR* values showed significant linear correlations, especially in the 3 mL bioreactor inoculated with 10×10^6 cells and in the 17 mL bioreactor (R-squared > 0.9). These results are supported by other studies displaying a high correlation between glucose consumption and cell growth,³¹ as well as oxygen values and cell number.³⁵ As the glucose metabolism is well established³⁶ and commonly used as cell culture parameter,^{9-10,17} the results emphasize the feasibility of using online oxygen measurement for monitoring hiPSC cultures.

The *sOUR* values observed in this study are in accordance with results reported by Abaci et al.,³⁷ who presented a *sOUR* of 127.1 fmol/cell/h for hiPSCs under atmospheric oxygen conditions. In the same study, oxygen levels of 5% resulted in a decrease of the *sOUR* to 56.2 fmol/cell/h, and oxygen levels of 1% led to a decrease to 11.9 fmol/cell/h.³⁷ These observations support the assumption that an oxygen depletion, e.g. due to large aggregate size, leads to a decrease in cell metabolism per cell.

This change in cell metabolism was, in contrast to most models, also incorporated into the simulation model as an inhibition constant for growth. Therefore, the model provided an accurate and precise reflection of the culture dynamics (especially with regards to the course of cell numbers) between the beginning and the end of the 15-day culture period.

Based on the collected data, further calculations regarding the energy metabolism of the cultured hiPSCs were made. The yield coefficient of lactate from glucose $Y(q_{lac}/q_{glc})$, with values in a range of 1.2 – 1.7, was approximately in the range of results presented by Kropp et al.,⁹ who observed a yield coefficient of 2 for their hiPSC line.

It has been reported that fibroblasts, which are the source of the hiPSC line used in this study, have a yield coefficient of 0.62,³⁸ whereas embryonic stem cells, which have immature mitochondria and mainly rely on glycolysis, showed a yield coefficient of 1.8 to 2.8:^{9,39} with a yield coefficient of 1.2 – 1.7, the herein used hiPSC line lays in between these two cell types. This observation is in line with findings reported by Varum et al.,⁴⁰ who described a mixed mitochondrial phenotype for hiPSCs, resembling the original somatic cells.

To conclude, continuous measurements of oxygen not only facilitate real-time, non-invasive monitoring of hiPSC cultures during expansion, but also, in conjunction with glucose and lactate measurements, enable to draw conclusions regarding the hiPSC metabolism.

The third study was aimed at examining different media variations with respect to supporting the maintenance of human umbilical vein endothelial cells (HUVECs), while enabling growth and hepatic differentiation of co-cultured hiPSCs. Therefore, hepatocyte culture medium (HCM), which is known to support the hepatic differentiation of hiPSCs, was combined with endothelium growth medium (EGM) in different mixtures for evaluation in HUVEC cultures.

The results showed that a 1:1 mixture of HCM and EGM media lead to similar HUVEC growth and maintenance results, as indicated by the glucose metabolism and expression of endothelial cell markers, compared to pure EGM, which is the standard medium used for HUVEC cultivation. In contrast, the use of HCM mixed with only EGM supplements instead of the complete EGM medium (basal medium + supplements) enabled HUVEC maintenance, but on a reduced level. This observation may be a result of higher glucose concentrations in the HCM + EGM supplements mixture (10 mM), compared to the HCM + EGM mixture (7 mM), as it has been reported that high glucose concentrations increase apoptosis and oxidative stress in endothelial cells.⁴¹ As the mixture of HCM + EGM supplements also supported the maintenance of HUVECs, albeit not being as efficient as EGM or HCM + EGM at a 1:1 ratio, both HCM + EGM mixtures can be seen as being suitable for subsequent hiPSC and HUVEC co-culture studies. With regards to an optimized HUVEC maintenance, the 1:1 mixture of HCM + EGM media may preferably be used.

CONCLUSION

In summary, hiPSCs were successfully expanded in 3D hollow-fiber bioreactors using different cell inoculation conditions and bioreactor sizes. The findings also show that the inoculum density has a significant influence on the growth behavior and the differentiation state of the cells in 3D bioreactors, with low initial inoculum densities resulting in higher quality hiPSCs at sufficient cell quantities. This finding is particularly important with regards to a clinical translation, as expanded hiPSCs need to be of high quantity and quality for subsequent differentiation and clinical use. Additional repeated cell harvesting or cell aggregate dissociation may further improve the results.

The continuous measurement of oxygen during bioreactor cultures has proven to be feasible as culture surveillance method, while also enabling an assessment of the metabolic state of the cultured cells. The method allows for automated, non-invasive, applicable and affordable real-time monitoring of oxygen and thus facilitates the translation of hiPSC-based therapies to clinical use.

Regarding the preliminary experiments for HUVEC maintenance during hiPSC co-culture and hepatic differentiation, two suitable media compositions were identified supporting HUVEC maintenance and expression of endothelial markers. These results provide an important basis for successful HUVEC and hiPSC co-culture experiments, which are intended to enhance the hepatic functionality of hiPSC-derived hepatocyte-like cells.

REFERENCES

- 1: Mokdad AA, Lopez AD, Shahraz S, Lozano R, Mokdad AH, Stanaway J, Murray CJ, Naghavi M. Liver cirrhosis mortality in 187 countries between 1980 and 2010: a systematic analysis. *BMC Med.* 2014; 12:145. doi: 10.1186/s12916-014-0145-y.
- 2: Lee WM, Squires RH Jr, Nyberg SL, Doo E, Hoofnagle JH. Acute liver failure: Summary of a workshop. *Hepatology.* 2008; 47:1401-15. doi: 10.1002/hep.22177.
- 3: Villarreal JA, Sussman NL. Extracorporeal Liver Support in Patients with Acute Liver Failure. *Tex Heart Inst J.* 2019; 46: 67-68. doi: 10.14503/THIJ-18-6744.
- 4: Nussler AK, Zeilinger K, Schyschka L, Ehnert S, Gerlach JC, Yan X, Lee SM, Ilowski M, Thasler WE, Weiss TS. Cell therapeutic options in liver diseases: cell types, medical devices and regulatory issues. *J Mater Sci Mater Med.* 2011; 22: 1087-99. doi: 10.1007/s10856-011-4306-7.
- 5: Sauer IM, Zeilinger K, Pless G, Kardassis D, Theruvath T, Pascher A, Goetz M, Neuhaus P, Gerlach JC. Extracorporeal liver support based on primary human liver cells and albumin dialysis-treatment of a patient with primary graft non-function. *J Hepatol.* 2003; 39: 649-53.

- 6: Takahashi K, Yamanaka S. Induction of pluripotent stem cells from mouse embryonic and adult fibroblast cultures by defined factors. *Cell*. 2006; 126: 663-76.
- 7: Serra M, Brito C, Correia C, Alves PM. Process engineering of human pluripotent stem cells for clinical application. *Trends Biotechnol*. 2012; 30: 350-9. doi: 10.1016/j.tibtech.2012.03.003.
- 8: Kropp C, Massai D, Zweigerdt R. Progress and challenges in large-scale expansion of human pluripotent stem cells. *Process Biochemistry*. 2017; 59: 244-254. doi: 10.1016/j.procbio.2016.09.032.
- 9: Kropp C, Kempf H, Halloin C, Robles-Diaz D, Franke A, Scheper T, Kinast K, Knorpp T, Joos TO, Haverich A, Martin U, Zweigerdt R, Olmer R. Impact of Feeding Strategies on the Scalable Expansion of Human Pluripotent Stem Cells in Single-Use Stirred Tank Bioreactors. *Stem Cells Transl Med*. 2016; 5: 1289-1301.
- 10: Olmer R, Lange A, Selzer S, Kasper C, Haverich A, Martin U, Zweigerdt R. Suspension culture of human pluripotent stem cells in controlled, stirred bioreactors. *Tissue Eng Part C Methods*. 2012; 18: 772-84.
- 11: Demetriou AA, Rozga J, Podesta L, Lepage E, Morsiani E, Moscioni AD, Hoffman A, McGrath M, Kong L, Rosen H, et al. Early clinical experience with a hybrid bioartificial liver. *Scand J Gastroenterol Suppl*. 1995; 208: 111-7.
- 12: Abbasalizadeh S, Larijani MR, Samadian A, Baharvand H. Bioprocess development for mass production of size-controlled human pluripotent stem cell aggregates in stirred suspension bioreactor. *Tissue Eng Part C Methods*. 2012; 18: 831-51. doi: 10.1089/ten.TEC.2012.0161.
- 13: Wang Y, Cheng L, Gerecht S. Efficient and scalable expansion of human pluripotent stem cells under clinically compliant settings: a view in 2013. *Ann Biomed Eng*. 2014; 42: 1357-72. doi: 10.1007/s10439-013-0921-4.
- 14: Alford JS. Bioprocess control: Advances and challenges. *Computers and Chemical Engineering*. 2006; 30: 1464-1475. doi: 10.1016/j.compchemeng.2006.05.039.
- 15: Mahfouzi SH, Amoabediny G, Doryab A, Safiabadi-Tali SH, Ghanei M. Noninvasive Real-Time Assessment of Cell Viability in a Three-Dimensional Tissue. *Tissue Eng Part C Methods*. 2018; 24:197-204. doi: 10.1089/ten.TEC.2017.0371.
- 16: Weyand B, Nöhre M, Schmäzlin E, Stolz M, Israelowitz M, Gille C, von Schroeder HP, Reimers K, Vogt PM. Noninvasive Oxygen Monitoring in Three-Dimensional Tissue Cultures Under Static and Dynamic Culture Conditions. *Biores Open Access*. 2015; 4: 266-77. doi: 10.1089/biores.2015.0004.
- 17: Abecasis B, Aguiar T, Arnault É, Costa R, Gomes-Alves P, Aspegren A, Serra M, Alves PM. Expansion of 3D human induced pluripotent stem cell aggregates in bioreactors: Bioprocess intensification and scaling-up approaches. *J Biotechnol*. 2017; 246: 81-93. doi: 10.1016/j.jbiotec.2017.01.004.

- 18: Si-Tayeb K, Noto FK, Nagaoka M, Li J, Battle MA, Duris C, North PE, Dalton S, Duncan SA. Highly efficient generation of human hepatocyte-like cells from induced pluripotent stem cells. *Hepatology*. 2010; 51: 297-305. doi: 10.1002/hep.23354.
- 19: Song Z, Cai J, Liu Y, Zhao D, Yong J, Duo S, Song X, Guo Y, Zhao Y, Qin H, Yin X, Wu C, Che J, Lu S, Ding M, Deng H. Efficient generation of hepatocyte-like cells from human induced pluripotent stem cells. *Cell Res*. 2009; 19: 1233-42. doi: 10.1038/cr.2009.107.
- 20: Takebe T, Sekine K, Enomura M, Koike H, Kimura M, Ogaeri T, Zhang RR, Ueno Y, Zheng YW, Koike N, Aoyama S, Adachi Y, Taniguchi H. Vascularized and functional human liver from an iPSC-derived organ bud transplant. *Nature*. 2013; 499: 481-4. doi: 10.1038/nature12271.
- 21: Yu J, Hu K, Smuga-Otto K, Tian S, Stewart R, Slukvin II, Thomson JA. Human induced pluripotent stem cells free of vector and transgene sequences. *Science*. 2009; 324: 797-801. doi: 10.1126/science.
- 22: Gerlach JC, Lübberstedt M, Edsbagge J, Ring A, Hout M, Baun M, Rossberg I, Knöspel F, Peters G, Eckert K, Wulf-Goldenberg A, Björquist P, Stachelscheid H, Urbaniak T, Schatten G, Miki T, Schmelzer E, Zeilinger K. Interwoven four-compartment capillary membrane technology for three-dimensional perfusion with decentralized mass exchange to scale up embryonic stem cell culture. *Cells Tissues Organs*. 2010; 192: 39-49. doi: 10.1159/000291014.
- 23: Lin Y, Chen G. Embryoid body formation from human pluripotent stem cells in chemically defined E8 media. 2014. *StemBook* [Internet]. Cambridge, MA: Harvard Stem Cell Institute; 2008. Available from <http://www.ncbi.nlm.nih.gov/books/NBK424234/>. Accessed March 8, 2019
- 24: Garcia-Ochoa F, Gomez E. Bioreactor scale-up and oxygen transfer rate in microbial processes: an overview. *Biotechnol Adv*. 2009; 27: 153-76. doi: 10.1016/j.biotechadv.2008.10.006.
- 25: Hoffmann SA, Müller-Vieira U, Biemel K, Knobloch D, Heydel S, Lübberstedt M, Nüssler AK, Andersson TB, Gerlach JC, Zeilinger K. Analysis of drug metabolism activities in a miniaturized liver cell bioreactor for use in pharmacological studies. *Biotechnol Bioeng*. 2012; 109: 3172-81. doi: 10.1002/bit.24573.
- 26: Knöspel F, Freyer N, Stecklum M, Gerlach JC, Zeilinger K. Periodic harvesting of embryonic stem cells from a hollow-fiber membrane based four-compartment bioreactor. *Biotechnol Prog*. 2016; 32 :141-51. doi: 10.1002/btpr.2182.
- 27: Livak KJ, Schmittgen TD. Analysis of relative gene expression data using real-time quantitative PCR and the 2(-Delta Delta C(T)) Method. *Methods*. 2001; 25: 402-8.
- 28: Li L, Bennett SA, Wang L. Role of E-cadherin and other cell adhesion molecules in survival and differentiation of human pluripotent stem cells. *Cell Adh Migr*. 2012; 6: 59-70. doi: 10.4161/cam.19583.
- 29: Nelson CM, Chen CS. Cell-cell signaling by direct contact increases cell proliferation via a PI3K-dependent signal. *FEBS Lett*. 2002; 514: 238-42.

- 30: Meng G, Liu S, Poon A, Rancourt DE. Optimizing Human Induced Pluripotent Stem Cell Expansion in Stirred-Suspension Culture. *Stem Cells Dev.* 2017; 26: 1804-1817. doi: 10.1089/scd.2017.0090.
- 31: Simmons AD, Williams C 3rd, Degoix A, Sikavitsas VI. Sensing metabolites for the monitoring of tissue engineered construct cellularity in perfusion bioreactors. *Biosens Bioelectron.* 2017; 90: 443-449. doi: 10.1016/j.bios.2016.09.094.
- 32: Murphy KC, Hung BP, Browne-Bourne S, Zhou D, Yeung J, Genetos DC, Leach JK. Measurement of oxygen tension within mesenchymal stem cell spheroids. *J R Soc Interface.* 2017;14. pii: 20160851. doi: 10.1098/rsif.2016.0851.
- 33: Kwok CK, Ueda Y, Kadari A, Günther K, Ergün S, Heron A, Schnitzler AC, Rook M, Edenhofer F. Scalable stirred suspension culture for the generation of billions of human induced pluripotent stem cells using single-use bioreactors. *J Tissue Eng Regen Med.* 2018; 12: e1076-e1087. doi: 10.1002/term.2435.
- 34: Tzanakakis ES, Hess DJ, Sielaff TD, Hu WS. Extracorporeal tissue engineered liver-assist devices. *Annu Rev Biomed Eng.* 2000; 2: 607-32.
- 35: Santoro R, Krause C, Martin I, Wendt D. On-line monitoring of oxygen as a non-destructive method to quantify cells in engineered 3D tissue constructs. *J Tissue Eng Regen Med.* 2012; 6: 696-701. doi: 10.1002/term.473.
- 36: Tsao YS, Cardoso AG, Condon RG, Voloch M, Lio P, Lagos JC, Kearns BG, Liu Z. Monitoring Chinese hamster ovary cell culture by the analysis of glucose and lactate metabolism. *J Biotechnol.* 2005; 118: 316-27.
- 37: Abaci HE, Truitt R, Luong E, Drazer G, Gerecht S. Adaptation to oxygen deprivation in cultures of human pluripotent stem cells, endothelial progenitor cells, and umbilical vein endothelial cells. *Am J Physiol Cell Physiol.* 2010; 298: C1527-37. doi: 10.1152/ajpcell.00484.2009.
- 38: Lemons JM, Feng XJ, Bennett BD, Legesse-Miller A, Johnson EL, Raitman I, Pollina EA, Rabitz HA, Rabinowitz JD, Coller HA. Quiescent fibroblasts exhibit high metabolic activity. *PLoS Biol.* 2010; 8: e1000514. doi: 10.1371/journal.pbio.1000514.
- 39: Fernandes TG, Fernandes-Platzgummer AM, da Silva CL, Diogo MM, Cabral JM. Kinetic and metabolic analysis of mouse embryonic stem cell expansion under serum-free conditions. *Biotechnol Lett.* 2010; 32: 171-9. doi: 10.1007/s10529-009-0108-0.
- 40: Varum S, Rodrigues AS, Moura MB, Momcilovic O, Easley CA 4th, Ramalho-Santos J, Van Houten B, Schatten G. Energy metabolism in human pluripotent stem cells and their differentiated counterparts. *PLoS One.* 2011; 6: e20914. doi: 10.1371/journal.pone.0020914.
- 41: Piconi L., Quagliario L., Assaloni R., Da Ros R., Maier A., Zuodar G., Ceriello A. Constant and intermittent high glucose enhances endothelial cell apoptosis through mitochondrial superoxide overproduction. *Diabetes Metab. Res. Rev.* 2006; 22: 198–203. doi: 10.1002/dmrr.613.

EIDESSTATTLICHE VERSICHERUNG

„Ich, Selina Greuel, versichere an Eides statt durch meine eigenhändige Unterschrift, dass ich die vorgelegte Dissertation mit dem Thema: „Expansion of human induced pluripotent stem cells (hiPSCs) in 3D bioreactors for extracorporeal liver support“ selbstständig und ohne nicht offengelegte Hilfe Dritter verfasst und keine anderen als die angegebenen Quellen und Hilfsmittel genutzt habe.

Alle Stellen, die wörtlich oder dem Sinne nach auf Publikationen oder Vorträgen anderer Autoren beruhen, sind als solche in korrekter Zitierung (siehe „Uniform Requirements for Manuscripts (URM)“ des ICMJE -www.icmje.org) kenntlich gemacht. Die Abschnitte zu Methodik (insbesondere praktische Arbeiten, Laborbestimmungen, statistische Aufarbeitung) und Resultaten (insbesondere Abbildungen, Graphiken und Tabellen) entsprechen den URM (s.o) und werden von mir verantwortet.

Meine Anteile an den ausgewählten Publikationen entsprechen denen, die in der untenstehenden gemeinsamen Erklärung mit dem/der Betreuer/in, angegeben sind. Sämtliche Publikationen, die aus dieser Dissertation hervorgegangen sind und bei denen ich Autor bin, entsprechen den URM (s.o) und werden von mir verantwortet.

Die Bedeutung dieser eidesstattlichen Versicherung und die strafrechtlichen Folgen einer unwahren eidesstattlichen Versicherung (§156,161 des Strafgesetzbuches) sind mir bekannt und bewusst.“

Datum

Unterschrift

ANTEILSERKLÄRUNG AN DEN BETEILIGTEN PUBLIKATIONEN

Selina Greuel hatte folgenden Anteil an den folgenden Publikationen:

Publikation 1: **Greuel S**, Hanci G, Böhme M, Miki T, Schubert F, Sittinger M, Mandenius CF, Zeilinger K, Freyer N. Effect of inoculum density on human induced pluripotent stem cell (hiPSC) expansion in 3D bioreactors. Cell Prolif. 2019 May 8:e12604. doi: 10.1111/cpr.12604. [Epub ahead of print] IF: 4.936

Beitrag im Einzelnen:

- Konzeption, Planung und Durchführung der Experimente
- Datenauswertung
- Literaturrecherche
- Schreiben des Artikels

Publikation 2: **Greuel S**, Freyer N, Hanci G, Böhme M, Miki T, Werner J, Schubert F, Sittinger M, Zeilinger K, Mandenius CF. Online measurement of oxygen enables continuous non-invasive evaluation of human induced pluripotent stem cell (hiPSC) culture in a perfused 3D hollow-fiber bioreactor. J Tissue Eng Regen Med. 2019 Apr 29. doi: 10.1002/term.2871. [Epub ahead of print] IF: 4.089

Beitrag im Einzelnen:

- Konzeption, Planung und Durchführung der Experimente
- Datenauswertung
- Literaturrecherche
- Schreiben des Artikels

Publikation 3: Freyer N, **Greuel S**, Knöspel F, Strahl N, Amini L, Jacobs F, Monshouwer M, Zeilinger K. Effects of Co-Culture Media on Hepatic Differentiation of hiPSC with or without HUVEC Co-Culture. Int J Mol Sci. 2017 Aug 7;18(8). pii: E1724. doi: 10.3390/ijms18081724. IF: 3.687


Beitrag im Einzelnen:

- Durchführung der Medientestung in HUVEC-Monokulturen
- Datenauswertung der Medientestung in HUVEC-Monokulturen
- Literaturrecherche
- Schreiben des Artikels gemeinsam mit Nora Freyer

Unterschrift, Datum und Stempel des betreuenden Hochschullehrers/der betreuenden Hochschullehrerin

Unterschrift des Doktoranden/der Doktorandin

Effect of inoculum density on human-induced pluripotent stem cell expansion in 3D bioreactors

Selina Greuel¹  | Güngör Hanci¹ | Mike Böhme¹ | Toshio Miki² | Frank Schubert³ | Michael Sittinger⁴ | Carl-Fredrik Mandenius⁵ | Katrin Zeilinger¹ | Nora Freyer¹

¹Bioreactor Group, Berlin-Brandenburg Center for Regenerative Therapies (BCRT), Charité – Universitätsmedizin Berlin, Berlin, Germany

²Department of Surgery, Keck School of Medicine, University of Southern California, Los Angeles, California

³StemCell Systems GmbH, Berlin, Germany

⁴Tissue Engineering Laboratory, Berlin-Brandenburg Center for Regenerative Therapies (BCRT), Department of Rheumatology and Clinical Immunology, Charité – Universitätsmedizin Berlin, Berlin, Germany

⁵Division of Biotechnology, Department of Physics, Chemistry and Biology (IFM), Linköping University, Linköping, Sweden

Correspondence

Selina Greuel, Berlin-Brandenburg Center for Regenerative Therapies (BCRT), Charité – Universitätsmedizin Berlin, Berlin, Germany.
Email: selina.greuel@charite.de

Funding information

Bundesministerium für Bildung und Forschung, Grant/Award Number: 13GW0129A

Abstract

Objective: For optimized expansion of human-induced pluripotent stem cells (hiPSCs) with regards to clinical applications, we investigated the influence of the inoculum density on the expansion procedure in 3D hollow-fibre bioreactors.

Materials and Methods: Analytical-scale bioreactors with a cell compartment volume of 3 mL or a large-scale bioreactor with a cell compartment volume of 17 mL were used and inoculated with either 10×10^6 or 50×10^6 hiPSCs. Cells were cultured in bioreactors over 15 days; daily measurements of biochemical parameters were performed. At the end of the experiment, the CellTiter-Blue[®] Assay was used for culture activity evaluation and cell quantification. Also, cell compartment sections were removed for gene expression and immunohistochemistry analysis.

Results: The results revealed significantly higher values for cell metabolism, cell activity and cell yields when using the higher inoculation number, but also a more distinct differentiation. As large inoculation numbers require cost and time-extensive pre-expansion, low inoculation numbers may be used preferably for long-term expansion of hiPSCs. Expansion of hiPSCs in the large-scale bioreactor led to a successful production of 5.4×10^9 hiPSCs, thereby achieving sufficient cell amounts for clinical applications.

Conclusions: In conclusion, the results show a significant effect of the inoculum density on cell expansion, differentiation and production of hiPSCs, emphasizing the importance of the inoculum density for downstream applications of hiPSCs. Furthermore, the bioreactor technology was successfully applied for controlled and scalable production of hiPSCs for clinical use.

1 | INTRODUCTION

The application of human-induced pluripotent stem cells (hiPSCs) has shown high potential in the field of clinical therapies¹ and pharmaceutical drug development,² as this cell type is suitable for generating disease-specific models and patient-specific therapies.^{3–6} However, the utilization of hiPSC models in drug

discovery requires high cell quantities of hiPSCs and their derivatives at a constant quality.^{7,8} This can hardly be achieved by using conventional 2D cell cultures due to insufficient cell production yields, lack in scalability and difficulty of controlling cell culture parameters.^{9,10} In contrast, the use of 3D culture models offers the opportunity of large-scale expansion of hiPSCs under controlled conditions.^{9,11} For production of large cell quantities fulfilling the

This is an open access article under the terms of the Creative Commons Attribution License, which permits use, distribution and reproduction in any medium, provided the original work is properly cited.

© 2019 The Authors. *Cell Proliferation* Published by John Wiley & Sons Ltd

required quality standards, it is important to consider those factors that potentially influence hiPSC expansion and differentiation in 3D culture systems. Such factors include feeding strategies, coating materials, culture media and the cell inoculum density.⁹ In the present study, the effect of the inoculum density on cell expansion and differentiation of hiPSCs cultured in perfused hollow-fibre-based 3D bioreactors was investigated. For this purpose, 10×10^6 hiPSCs resp. 3.3×10^6 cells/mL, or 50×10^6 hiPSCs resp. 16.6×10^6 cells/mL were inoculated into analytical-scale bioreactors with a cell compartment volume of 3 mL (AS) and cultured over a period of 15 days. Both conditions were compared in terms of biochemical parameters, cell activity and cell yields, gene expression analysis and immunohistochemical staining. Changes in the differentiation state of hiPSCs expanded in bioreactors were detected by gene expression and immunofluorescence analysis, where hiPSCs forming embryoid bodies served as differentiation control. The feasibility of scaling up of hiPSC expansion was tested in a large-scale 3D bioreactor with a cell compartment volume of 17 mL (LS) using an inoculation number of 50×10^6 cells, resp. 2.9×10^6 cells/mL.

2 | MATERIALS AND METHODS

2.1 | Bioreactor system/technology

The 3D four-compartment hollow-fibre bioreactor used in this study is based on three independent, interwoven hollow-fibre capillary bundles, two for supplying nutrient media by countercurrent perfusion and one for gas exchange. The space between these capillary bundles (extracapillary space) serves as cell compartment. The capillary system is integrated into a polyurethane housing. The cells, grown in the cell compartment, were constantly supplied with nutrients and oxygen. The bioreactor types used in this study had a cell compartment volume of 3 mL (analytical-scale, AS) or 17 mL (large-scale, LS); specific data regarding compartment measurements as well as perfusion conditions are displayed in Table 1. Both bioreactor types, the AS and LS bioreactor, are constructed identically in

TABLE 1 Specifications of bioreactor compartments and perfusion parameters

	Analytical-scale	Large-scale
Volume of bioreactor compartments		
Total inner volume of the bioreactor	5.1 cm ³	26 cm ³
Total volume of capillaries	2.2 cm ³	8.9 cm ³
Volume of cell compartment	2.9 cm ³	17.1 cm ³
Perfusion parameters		
Recirculation rate	10 mL/min	20 mL/min
Feed rate	1-12 mL/h	2-40 mL/h
Air	20 mL/min	40 mL/min
CO ₂	0-1 mL/min	0-2 mL/min

respect of their capillary configuration (Figure 1); they only differ in length and number of capillaries. A detailed description of the bioreactor technology can be found elsewhere.^{12,13} The bioreactors were connected to a perfusion device consisting of pumps for medium feed and medium recirculation.

2.2 | Pre-expansion of hiPSCs in 2D cultures

The hiPSC line DF6-9-9T¹⁴ (WiCell Research Institute, Madison, WI, USA) was cultured feeder-free on six-well culture plates or T175 culture flasks (both BD Falcon, San José, CA, USA), which were pre-coated with 8.68 µg/cm² Matrigel (growth factor reduced, Corning, NY, USA). The culture medium mTeSRTM1 (Stemcell Technologies, Vancouver, BC, Canada) was used, supplemented with 10 000 units/mL penicillin and 10 mg/mL streptomycin (Pen Strep, Gibco® by Life Technologies/Thermo Fisher Scientific). After thawing, 1 mmol/L ROCK inhibitor (Y-27632; Abcam, Cambridge, UK) was added to the culture medium to increase single-cell survival. Passages for pre-expansion were performed at 70% confluence using 0.48 mmol/L EDTA (Versene, Gibco® by Thermo Fisher Scientific, Waltham, MA, USA).

2.3 | Expansion of hiPSCs in 3D bioreactors

Following pre-expansion, either 10×10^6 (AS 10) or 50×10^6 (AS 50, LS 50) hiPSCs were inoculated as single-cell suspension into pre-coated bioreactors (8.68 µg/cm² Matrigel, Corning) and cultured over 15 days. The initial cell numbers used in this study are based on previous studies on the hepatic differentiation of hiPSCs in the AS bioreactor, where 100×10^6 cells were inoculated.¹⁵ Thus, an initial cell number of 10×10^6 cells, resp. 3.3×10^6 cells/mL in AS 10 provides the spatial conditions for at least a 10-fold cell expansion, while an initial cell number of 50×10^6 resp. a cell density of 16.6×10^6 cells/mL in AS 50 should enable at least a 2-fold expansion. The latter was chosen to investigate the influence of a high initial cell density on the expansion procedure. For the feasibility testing of an up-scale of the hiPSC expansion, the LS bioreactor was inoculated with a cell number of 50×10^6 resp. a cell density of 2.9×10^6 cells/mL, as this equals the conditions of AS 10. To ensure single-cell survival at the beginning of the experiment, 1 mmol/L ROCK inhibitor (Y-27632; Abcam) was included into the culture medium as bolus injection and was rinsed out within the first 24 hours of bioreactor cultures.

The bioreactors were placed into a heating chamber constantly kept at 37°C. The medium recirculation rate was set to 10 mL/min (AS) resp. 20 mL/min (LS), whereas the medium feed was initially set to 1 mL/h (AS) resp. 2 mL/h (LS) and adapted daily to up to 12 mL/h (AS) or 40 mL/h (LS), depending on the glucose consumption rates. Thereby, glucose levels were kept above 4.4 mmol/L throughout the culture period. The gas perfusion rate was constantly maintained at 20 mL/min (AS) resp. 40 mL/min (LS); CO₂ was added at a percentage of up to 5% for pH regulation to approximately 7.2 (Table 1).

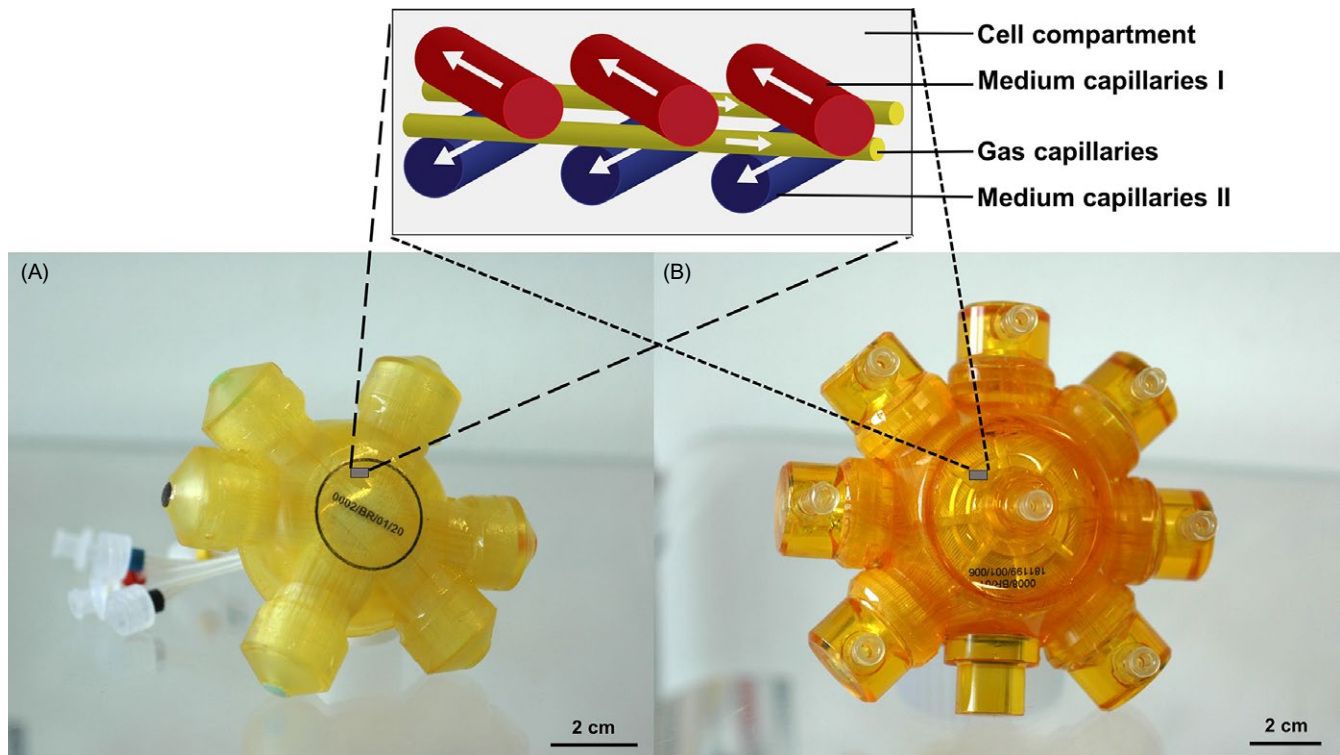


FIGURE 1 Bioreactor types used for the expansion of hiPSCs with their capillary structure. The picture shows the analytical-scale bioreactor (A) with a cell compartment volume of 3 mL and the large-scale bioreactor (B) with a cell compartment volume of 17 mL. The schematic image on top shows a section of the capillary structure inside the bioreactor, consisting of the following four compartments: medium capillaries I (red) and II (blue) for countercurrent medium perfusion, gas capillaries (yellow) and the space surrounding the capillaries, which serves as the cell compartment (white). The scale bars correspond to 2 cm

2.4 | Biochemical parameters

The metabolic activity of cultured cells was analysed by daily measurements of biochemical parameters in samples from the recirculating medium. Glucose and lactate concentrations were determined by means of a blood gas analyser (ABL 700; Radiometer, Copenhagen, Denmark). Potential cell damage was assessed by measuring the release of lactate dehydrogenase (LDH) using an automated clinical chemistry analyser (Cobas® 8000; Roche Diagnostics, Mannheim, Germany) provided by Labor Berlin GmbH. In addition, beginning differentiation was detected by measurement of alpha-fetoprotein (AFP) levels in the culture perfusate, using a clinical chemistry analyser (Cobas® 8000; Roche Diagnostics) provided by Labor Berlin GmbH. AFP levels were analysed every 5 days, or more frequently when concentrations were above the detection limit.

2.5 | CellTiter-Blue® Cell Viability Assay

Cell activity was evaluated, and cells quantified by performing the CellTiter-Blue® Cell Viability Assay (CTB; Promega GmbH, Mannheim, Germany) on day 15 of bioreactor cultures and parallel 2D cell cultures. The CTB reagent was applied at a concentration of 2.5% to the bioreactor recirculation with an incubation period of 60 minutes. The feed supply of bioreactors was paused during the measurement period. Samples of 300 µL were taken every

15 minutes from the supernatant and transferred to three wells of a 96-well plate (Greiner Bio-One GmbH, Frickenhausen, Germany); further conversion of resazurin to resorufin in the samples was stopped by adding 50 µL of 3% sodium dodecyl sulphate (SDS, Carl Roth GmbH + Co. KG, Karlsruhe, Germany) in dimethyl sulfoxide (DMSO, Sigma-Aldrich/Merck, Darmstadt, Germany) per well as stop solution. Fluorescence measurements took place at a wavelength of 560 nm (excitation) and 590 nm (emission) using the Infinite M200 Pro plate reader (Tecan Group Ltd., Männedorf, Switzerland). For cell quantification and growth characterization, a calibration curve was generated by correlating defined cell numbers to the resulting CTB gradients (data not shown).

2.6 | Embryoid body formation

Embryoid bodies were generated by transferring a number of 2×10^6 hiPSCs in 2 mL mTeSR supplemented with ROCK inhibitor (Y-27632, 1 mmol/L; Abcam) into a well of an AggreWell 800 plate (Stemcell Technologies). The plate was centrifuged at 500 g for 3 minutes and incubated overnight at 37°C and 5% CO₂. On the following day, the formed embryoid bodies were removed from the plate using a trimmed pipette tip with a 1 mL pipette and transferred to wells of non-treated 12-well culture plates (Costar®, Corning®, NY, USA) for expression analysis or to Lumox plates (Sarstedt, Nümbrecht, Germany) for immunohistochemical

staining. Also, the mTeSR medium was replaced with E6-medium,¹⁶ consisting of 96.8% DMEM-F12 (Gibco®; Thermo Fisher Scientific), 2% insulin-transferrin-selenium (Gibco®; Thermo Fisher Scientific), 1% Pen Strep (Gibco®; Thermo Fisher Scientific) and 0.2% L-Ascorbic Acid (Sigma-Aldrich/Merck). Embryoid bodies were cultured over 15 days in total; during the culture period, half of the medium was removed and replaced with fresh E6-medium three times per week.

2.7 | Gene expression analysis

Gene expression analysis was performed as described previously^{15,17} using human-specific primers and probes as listed in Table 2. Expression values of measured genes were normalized to expression values of the housekeeping gene glyceraldehyde-3-phosphate dehydrogenase (GAPDH), and fold changes of expression levels were calculated using the $\Delta\Delta C_t$ method.¹⁸

2.8 | Immunohistochemistry analysis

Upon termination of bioreactor cultures, sections of the capillary bed containing cell material were removed and prepared for immunofluorescence staining as described previously.¹⁹ Nuclei were counterstained with Dapi (blue). The antibodies used for immunohistochemistry are displayed in Table 3.

2.9 | Statistical evaluation

Statistical analysis was performed using GraphPad Prism 7.0 for Windows (GraphPad Software, San Diego, CA, USA). Data are presented as means \pm standard error of the mean (SEM) from three or four runs at each inoculum density for AS, or as single values for LS. For evaluation of differences in growth behaviour between AS 10 and AS 50, the areas under curves (AUCs) and the tipping points (ie time when peak values of the curves were reached) were calculated and compared using the unpaired, two-tailed Student's *t* test. Gene expression data were compared between AS 10 and AS 50, corresponding 2D cultures and embryoid bodies by one-way analysis of

variance (ANOVA). Slope values obtained in the CellTiter-Blue® Cell Viability Assay as well as cell quantification data, population doublings and doubling times were compared using the unpaired, two-tailed Student's *t* test.

3 | RESULTS

3.1 | Metabolic activity of hiPSCs during bioreactor expansion

For comparative evaluation of the hiPSC growth behaviour in the two analytical-scale bioreactors (AS) and the large-scale bioreactor (LS), glucose and lactate were measured as indicators for the energy metabolism of the cells. Time courses of glucose consumption and lactate production revealed significant differences between AS 10 and AS 50 (Figure 2A,B). The area under curve (AUC) of AS 50 was significantly larger compared with the AUC of AS 10 ($P < 0.05$). Also, the tipping point was achieved significantly earlier in AS 50 with day 7 for both, glucose and lactate, compared with day 12 for glucose and day 11 for lactate in AS 10 ($P < 0.05$ for glucose and lactate). The metabolic parameters for LS 50 (Figure 2E,F) revealed maximum values that were more than three times as high compared with maximum values obtained in AS 50. Release rates of LDH, indicating potential cell death, increased in AS 10 and AS 50 with culture progression, but were significantly higher in AS 50 throughout the culture period compared with AS 10 (Figure 2C; $P < 0.0001$). For LS 50 (Figure 2G), LDH release showed a similar time course as AS 50, while absolute values were three times as high as in AS 50. The albumin precursor AFP, indicating beginning differentiation, showed an exponential increase from day 12 onwards for AS 50 (Figure 2D). In contrast, there was no AFP detectable in perfusates of AS 10 during the entire culture period (Figure 2D). For LS 50 (Figure 2H), a slight increase was measured from day 14 onwards, but maximum values were almost five times lower than those observed in AS 50.

In conclusion, higher cell densities led to a significantly higher overall cell activity in AS bioreactors; however, higher cell densities also led to beginning differentiation as indicated by increasing AFP levels in AS 50. The highest values for energy metabolism were achieved in LS 50, being more than three times as high compared with maximum values obtained in AS 50.

3.2 | Gene expression profiles of hiPSC cultures

For the characterization of hiPSCs after expansion in 3D bioreactors, the gene expression of pluripotency as well as differentiation markers relative to the undifferentiated state were analysed. The expression data of the two pluripotency markers *POU5F1* and *NANOG* (Figure 3A,B) revealed only slight changes in pluripotency of bioreactor cultures and 2D cultures compared with the undifferentiated state. For the embryoid bodies, however, a distinct reduction in *POU5F1* and *NANOG* expression was detected, which was significant for *POU5F1* compared with 2D cultures ($P < 0.05$). Regarding differentiation markers, the strongest increases in gene expression were

TABLE 2 Applied biosystems TaqMan gene expression assays®

Gene symbol	Gene name	Assay ID
<i>AFP</i>	Alpha-fetoprotein	Hs00173490_m1
<i>CXCR4</i>	C-X-C Motif Chemokine Receptor 4	Hs00607978_s1
<i>GATA2</i>	GATA Binding Protein 2	Hs00231119_m1
<i>NANOG</i>	Nanog Homeobox	Hs02387400_g1
<i>NEFL</i>	Neurofilament Light	Hs00196245_m1
<i>PAX6</i>	Paired Box 6	Hs00240871_m1
<i>POU5F1</i>	POU Class 5 Homeobox 1	Hs00999632_g1
<i>SOX17</i>	SRY-Box 17	Hs00751752_s1
<i>T</i>	T-Box Transcription Factor T	Hs00610080_m1

TABLE 3 Antibodies used for immunofluorescence staining

	Protein symbol	Species	Manufacturer	Final conc. ($\mu\text{g/mL}$)
Primary antibody				
Alpha-fetoprotein	AFP	Mouse	Santa Cruz	2
Marker of proliferation	MKI67	Mouse	BD Biosciences	10
Nestin	NES	Rabbit	Santa Cruz	2
POU Class 5 Homeobox 1	POU5F1	Rabbit	Santa Cruz	2
Vimentin	VIM	Rabbit	Santa Cruz	2
Alpha smooth muscle actin	α -SMA	Mouse	Sigma-Aldrich	10-30
Secondary antibody				
Alexa Fluor 488 anti-mouse		Goat	Life Technologies	2
Alexa Fluor 594 anti-rabbit		Goat	Life Technologies	2

observed for the endodermal lineage marker *AFP* (Figure 3C) with highest values being detected for embryoid bodies and for AS 50. Gene expression measurements for the other two endodermal markers, *SOX17* (Figure 3D) and *CXCR4* (Figure 3E) revealed an increase compared with the undifferentiated state in AS 10 and AS 50. For *SOX17*, the increase was most pronounced in AS 10 and AS 50 and lowest in LS 50. The expression of *CXCR4* showed the highest value for the embryoid bodies, which was significantly higher compared with AS 10 and AS 50 ($P < 0.05$) as well as the 2D cultures ($P < 0.01$). Expression data for the ectodermal marker *PAX6* (Figure 2F) revealed a comparable increase in AS 10 and AS 50, while LS 50 had a noticeable lower increase in *PAX6* expression. The expression data for the second marker of the ectodermal lineage, *NEFL* (Figure 3G), showed the strongest increase for embryoid bodies, with expression values being significantly higher compared with AS 10 and AS 50 as well as the 2D cultures ($P < 0.001$). Expression data for the mesodermal lineage marker *GATA2* (Figure 3H) showed a similar gene expression for all tested groups. In contrast, values for *T* (Figure 3I), another mesodermal marker, revealed the highest expression values in AS 10 and AS 50 and the lowest ones in the embryoid bodies. Expression values of AS 50 were significantly higher compared with 2D cultures and embryoid bodies ($P < 0.05$).

To summarize, gene expression profiles indicate beginning differentiation processes in bioreactor cultures, which were most pronounced in AS 50. However, in embryoid bodies, the expression of both pluripotency markers was lower, and expression of the majority of differentiation markers was higher compared with the bioreactor cultures.

3.3 | Cell activity of hiPSC cultures

The CellTiter-Blue[®] Cell Viability assay (CTB) was performed in all bioreactors as well as in 2D cultures, which were cultured in parallel to bioreactor cultures (Figure 4). The strongest increase during the assay performance was detected in LS 50. The curves of AS 10 and AS 50 were comparable, with the slope of AS 50 being significantly larger than the slope of AS 10 ($P < 0.05$). The curve of 2D cultures showed the lowest fluorescence values with a significantly

smaller slope compared with AS 10 ($P < 0.05$) and AS 50 ($P < 0.01$). Fluorescence measurements were above the detection limit after 15 minutes (LS 50) or 45 minutes (AS 10 and AS 50) and are therefore not included in the graph.

In conclusion, the highest cell activity was detectable in LS 50, followed by AS 50 and AS 10. The increase in cell activity of AS 50 was significantly larger than that of AS 10.

3.4 | Immunohistochemical characteristics of hiPSC cultures

Staining with the pluripotency marker POU5F1 (Figure 5A-E) and the proliferation marker MKI67 (Figure 5F-J) showed that undifferentiated cells and the vast majority of cells in AS 10 or LS 50 were positive for POU5F1 and MKI67. In contrast, only approximately half of the cells in AS 50 were positive for those markers. Staining of the embryoid bodies revealed about one third of the cells to be positive for POU5F1 and MKI67. The markers for the mesodermal lineage, α -SMA (Figure 5K-O) and vimentin (Figure 5P-T), were clearly positive in embryoid bodies and interestingly, the stained structures appeared filament-like. Staining of α -SMA in all other groups was mostly negative, whereas vimentin was positive in a few cells in undifferentiated hiPSCs and bioreactor cultures. The marker for the endodermal lineage AFP (Figure 5U-Y) was detectable in the majority of cells in the embryoid bodies and in parts of cells in AS 10 and AS 50. In contrast, undifferentiated hiPSCs and cells in LS 50 appeared negative for AFP. The marker for the ectodermal lineage, nestin (Figure 5Z-AD) was detected in embryoid bodies and, again, filament-like structures were visible. A small amount of cells in AS 10 or LS 50 were positive, whereas in AS 50, almost all cells were negative for nestin. In undifferentiated hiPSCs, nestin was not detectable.

In summary, the majority of cultured cells in bioreactors expressed both, the pluripotency marker and the proliferation marker, whereas only a small fraction of cells was positive for differentiation markers. Cells cultured as embryoid bodies showed a more distinct expression of differentiation markers, partially forming filament-like structures.

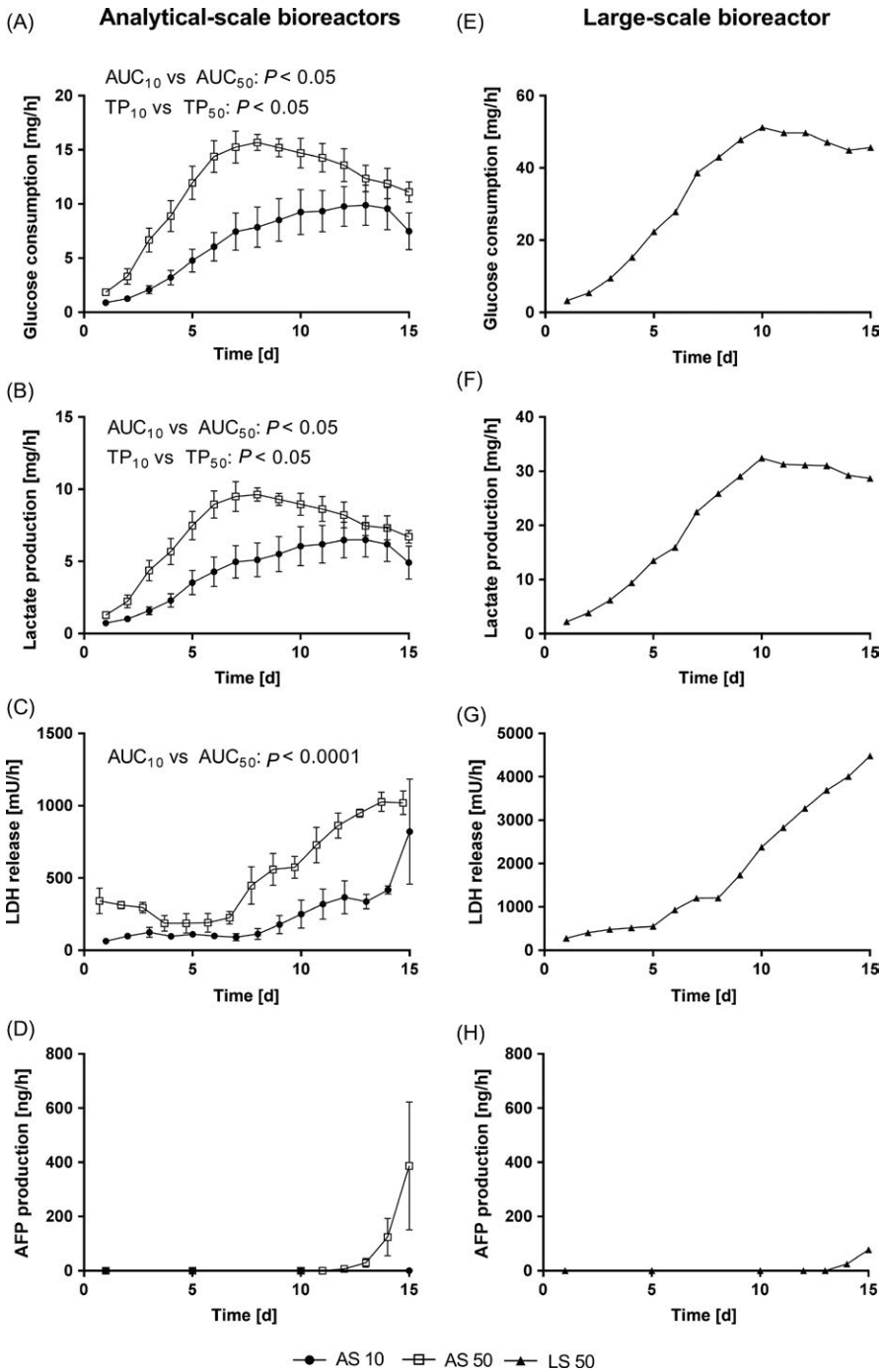


FIGURE 2 Comparison of clinical chemistry parameters during the culture of human-induced pluripotent stem cells over 15 days in analytical-scale bioreactors inoculated with either 10×10^6 (AS 10, $n = 4$) or 50×10^6 (AS 50, $n = 3$) cells, or the large-scale bioreactor inoculated with 50×10^6 (LS 50, $n = 1$) cells. Values are presented as mean \pm SEM (AS 10 and AS 50) or single values (LS 50). The two analytical-scale bioreactors were compared by means of the areas under the curves (AUCs) and the tipping points (TP). Differences were considered significant at $P < 0.05$

3.5 | Proliferation yields of hiPSCs expanded in bioreactors or 2D cultures

Based on the results of the CTB and a corresponding calibration curve obtained from 2D cultures (data not shown), cell numbers were determined on the final day of the bioreactor experiments or the final day of 2D cultures (Table 4). For AS 10, a mean cell number of $1.01 \times 10^9 \pm 21.04$ was achieved on day 15, which was significantly lower compared with the cell yield in AS 50 with cell numbers of $1.40 \times 10^9 \pm 37.96$ ($P < 0.05$). Cells cultured in LS 50 were expanded to 5.4×10^9 cells, which is the highest achieved

cell number. The determined cell numbers at the end of the 15-day bioreactor culture revealed an over 100-fold increase in cell number for AS 10 and for LS 50. In contrast, AS 50 showed a 28-fold increase. The achieved cell densities were 3.66×10^8 cells/mL for AS 10, 4.69×10^8 cells/mL for AS 50 and 3.17×10^8 cells/mL for LS 50. The population doubling of bioreactor cultures was similar in AS 10 (6.77 ± 0.03) and LS 50 (6.74), resulting in doubling times of 2.22 ± 0.01 days resp. 2.23 days. AS 50 revealed a significantly lower overall population doubling with 4.80 ± 0.04 ($P < 0.001$) and a significantly longer doubling time with 3.12 ± 0.02 days ($P < 0.001$) compared with AS 10. In 2D cultures, a cell number

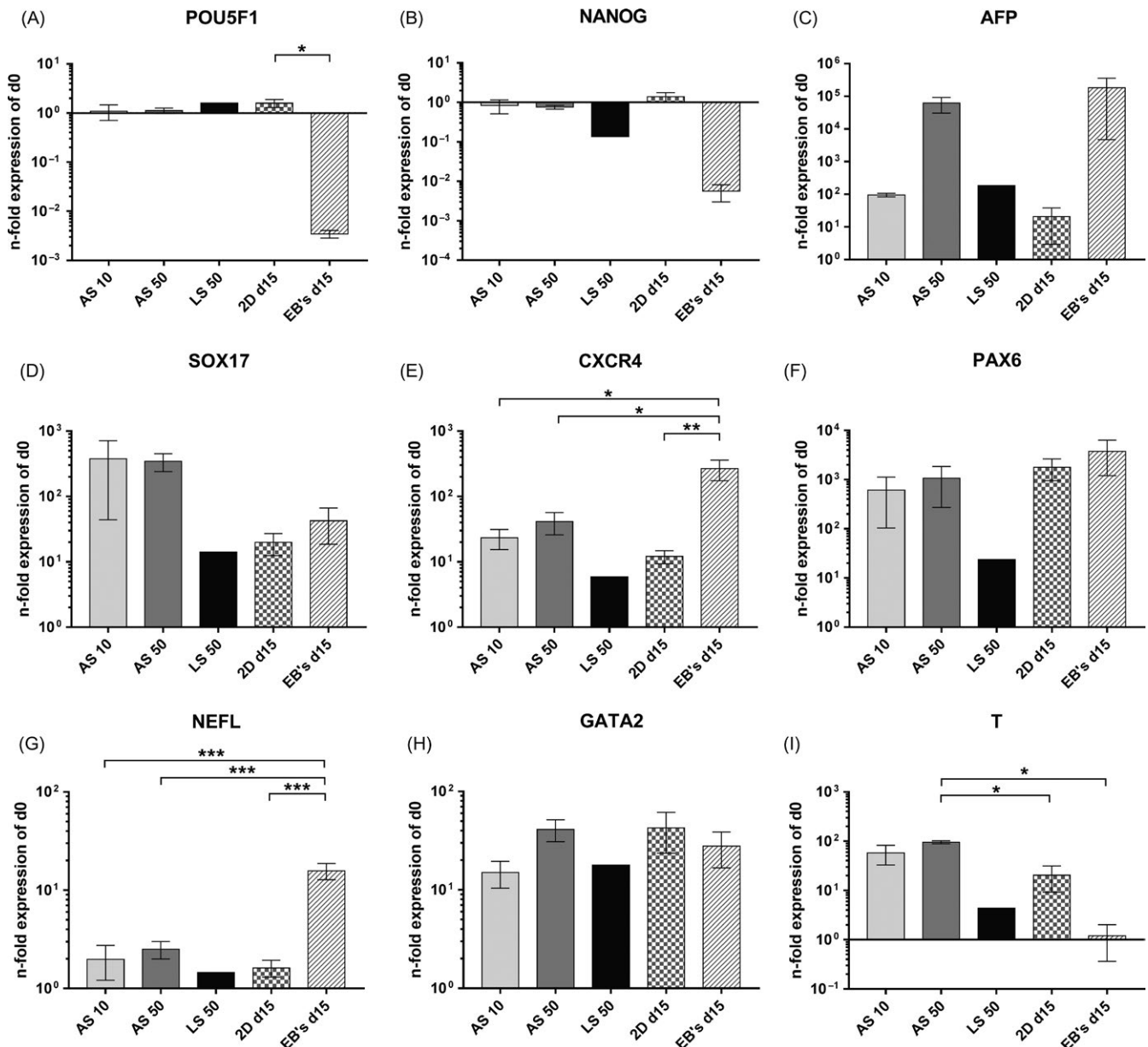


FIGURE 3 Gene expression analysis after 15 days of hiPSC culture in analytical-scale bioreactors inoculated with 10×10^6 (AS 10) or 50×10^6 (AS 50) cells, in the large-scale bioreactor inoculated with 50×10^6 cells (LS 50), on 2D culture plates, or after formation of embryoid bodies. The figure displays gene expression data of POU Class 5 Homeobox 1 (*POU5F1*, [A]), Nanog Homeobox (*NANOG*, [B]), Alpha-Fetoprotein (*AFP*, [C]), SRY-Box 17 (*SOX17*, [D]), C-X-C Motif Chemokine Receptor 4 (*CXCR4*, [E]), Paired Box 6 (*PAX6*, [F]), Neurofilament Light (*NEFL*, [G]), GATA Binding Protein 2 (*GATA2*, [H]) and T-Box Transcription Factor T (*T*, [I]). Expression data were normalized to the housekeeping gene Glyceraldehyde-3-Phosphate Dehydrogenase (*GAPDH*), and n-fold expression values were calculated relative to undifferentiated hiPSCs before inoculation on d0 using the $\Delta\Delta C_t$ method. Data are presented as mean \pm SEM (AS 10 $n = 3$; AS 50 $n = 3$; LS 50 $n = 1$; 2D d15 $n = 5$; EB's d15 $n = 3$). Differences between AS 10, AS 50 as well as 2D cultures and embryoid bodies were detected using the one-way ANOVA; calculated values were considered significant at * $P < 0.05$, ** $P < 0.01$ and *** $P < 0.001$

of $49.49 \times 10^6 \pm 9.02$ was achieved after a 15-day culture period, with a population doubling of 7.16 ± 0.30 and an average doubling time of 2.10 ± 0.09 days.

To conclude, a more than 100-fold increase in cell number was achieved in AS 10 and LS 50, whereas a 28-fold increase was reached in AS 50. Population doublings and doubling times reflected these results.

4 | DISCUSSION

Since the application of hiPSCs in the medical field requires large cell quantities at high-quality standards, it is of great interest to evaluate factors that influence hiPSC expansion in 3D culture systems. Therefore, the effect of the inoculum density on the hiPSC expansion procedure, cell differentiation and the cell yield was investigated in this study.

CellTiter-Blue® Cell Viability Assay

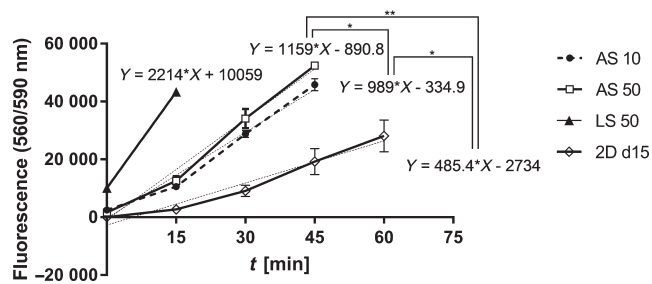


FIGURE 4 Comparison of CellTiter-Blue® fluorescence values over a time period of up to 60 minutes on the final day of the experiment (day 15). The figure shows measurements performed in analytical-scale bioreactors (AS) inoculated with 10×10^6 (AS 10, $n = 2$) or 50×10^6 (AS 50, $n = 3$) cells, the large-scale bioreactor (LS) inoculated with 50×10^6 cells (LS 50, $n = 1$) and 2D cultures (2D d15, $n = 4$). Differences in the gradients of the corresponding linear correlation were detected using the unpaired, two-tailed Student's t test and considered statistically significant at $*P < 0.05$ and $**P < 0.01$

For evaluation of the energy metabolism of hiPSCs cultured in bioreactors, glucose consumption and lactate production were determined. Analytical-scale (3 mL) bioreactors inoculated with 50×10^6 cells (AS 50) consumed glucose faster than analytical-scale bioreactors inoculated with 10×10^6 cells (AS 10), and growth stagnated significantly earlier. This observation can primarily be explained by the higher initial cell density in AS 50, resulting in higher overall glucose uptake and metabolic activity, but also by an increased cell-cell signalling, both leading to an increased cell proliferation and expansion rate.^{20,21} Similar findings have been reported by Meng et al,²² who observed the strongest increase in viable cell density at the highest cell inoculation number when inoculating three different cell densities in shape of cell aggregates into stirred suspension bioreactors. Additionally, Abaci et al²³ observed a sharp decrease in oxygen concentration in human embryonic stem cell (hESC) and iPSC cultures as a result of high cell seeding densities, indicating a corresponding increase in energy metabolism.

The observed shift from cell expansion towards maintenance, which occurred the earliest in AS 50 as indicated by the tipping point, is in line with results reported by Simmons et al,²⁴ who detected a plateau phase in cell growth and glucose consumption rates after approximately 1 week during 3D culture of rat mesenchymal stem cells. The observed stagnation of cell growth in that study was ascribed to the limited space for the cells in the 3D fibre mesh scaffolds which were placed into a flow perfusion bioreactor. Since AS 50 has the highest initial cell density in relation to the size of the bioreactor cell compartment, a growth stagnation due to space limitations appears likely in our study, too. However, growth limitations could also be caused by depletion of nutrients and oxygen in cell aggregates of larger size,²⁵ leading to cell differentiation or cell damage.²⁶ In order to evaluate potential cell damage and cell differentiation during cell culture, levels of LDH, an enzyme released during loss of plasma membrane integrity of cells,^{27,28} and alpha-fetoprotein (AFP), a marker for endodermal

differentiation,²⁹ were measured in the perfusates of bioreactor cultures. In AS 50 ($n = 3$), release of LDH was significantly higher compared with the LDH release in AS 10 ($n = 4$), which could be a result of both, upper cellularity limit of the cell compartment and/or large aggregate size. The release of AFP in AS 50 and LS 50 towards the end of the culture indicates beginning differentiation of the cells,³⁰ in parallel with the long plateau phase of approximately 8 resp. 5 days. Beginning differentiation was also indicated by the mRNA expression analysis, which was performed upon termination of bioreactor cultures. An upregulation of especially endodermal differentiation markers has been previously reported for 3D cultures of mouse embryonic stem cells by Knöspel, Freyer et al and was ascribed to reduced oxygen and nutrient supply in the centre of cell aggregates, amongst others.¹⁷ A large aggregate size may further explain elevated expression levels of *SOX17*, *CXCR4*, *PAX6*, *NEFL*, *GATA2* and *T* indicating a beginning undirected differentiation of hiPSCs. The tendency of elevated gene expression of differentiation markers, which occurred especially in AS 50, is in line with findings reported by Toyoda et al,³¹ who observed that the differentiation of hiPSCs into pancreatic bud-like progenitor cells was enhanced by high cell densities. However, for *CXCR4* and *NEFL*, expression levels of embryoid bodies were significantly higher than expression levels of the bioreactor or 2D cultures, indicating that the differentiation processes are minor compared with intended differentiation as performed in embryoid body cultures. Interestingly, the expression analysis for *T* revealed significantly lower expression levels for embryoid bodies compared with AS 50 and 2D cultures. Maximum levels for *T* in embryoid bodies built of human embryonic stem cells were measured between day 3 and 7,³²⁻³⁴ which explains the low levels of *T* expression in embryoid bodies in this study, which were analysed on day 15. Also, as *T* is a marker for early mesodermal differentiation, the hypothesis is supported that bioreactor cultures only show a beginning differentiation. Furthermore, immunohistochemical staining did not show a strong expression of any of the differentiation markers, especially when being compared with the staining patterns of the embryoid bodies. Nevertheless, beginning differentiation as well as cell death induced by cell compartment size limitations or aggregate size during hiPSC expansion could potentially be avoided by either harvesting cells from the cell compartment,¹⁷ or by performing passages during continuous expansion in 3D culture systems²⁶ as soon as cell cultures reach a growth plateau.

Results from the CellTiter-Blue® Cell Viability Assay underlined the results from glucose and lactate measurements with the additional finding that all bioreactors showed higher cell activity compared with corresponding 2D cultures, emphasizing the use of 3D culture systems instead of 2D cultures for hiPSC long-term expansion.

Studies on hiPSC expansion have been published using different culture models and inoculum densities, emphasizing that the ideal inoculum density and expansion efficiency varies depending on specific culture characteristics. For example, Kropp et al³⁵ used an inoculum density of 5×10^5 hiPS cells/mL for expansion in stirred tank bioreactors, whereas Olmer et al³⁶ used an initial cell density of only

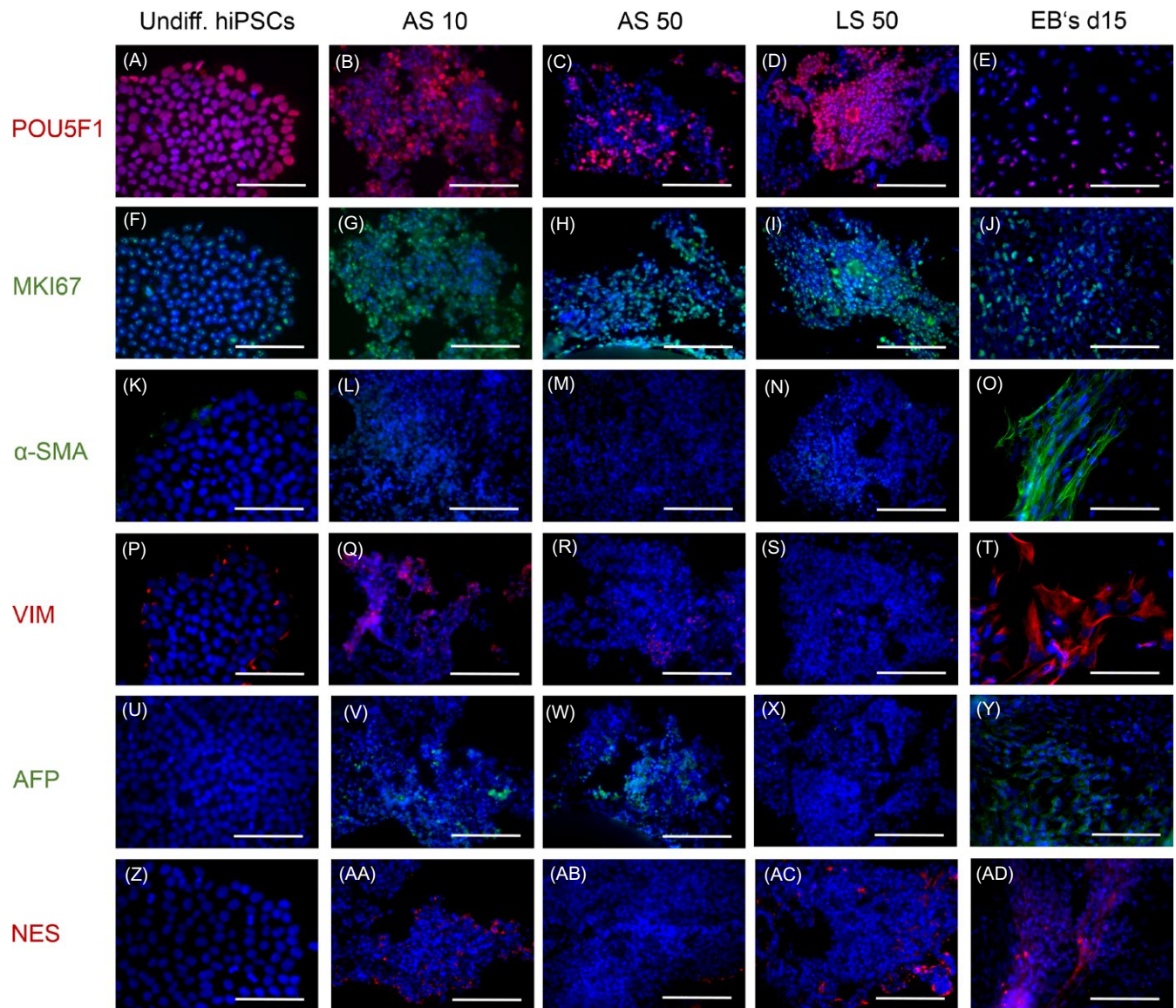


FIGURE 5 Immunohistochemical staining of undifferentiated human-induced pluripotent stem cells (hiPSCs) and hiPSCs after culture in analytical-scale bioreactors (AS) inoculated with 10×10^6 cells (AS 10) or 50×10^6 cells (AS 50), in the large-scale bioreactor (LS) inoculated with 50×10^6 cells (LS 50) and in embryoid bodies (EB's d 15). The figure shows staining of POU Class 5 Homeobox 1 (POU5F1, A-E), marker of proliferation (MKI67, F-J), α -smooth muscle actin (α -SMA, K-O) and vimentin (VIM, P-T), alpha-fetoprotein (AFP, U-Y) and nestin (NES, Z-AD). Nuclei were counterstained with Dapi (blue). Scale bars correspond to 100 μ m

TABLE 4 Cell quantification and growth characterization of cells cultured in bioreactors or 2D cultures after 15 days

	AS 10	AS 50	LS 50	2D
Cell number (mio)	$1097.73 \pm 21.04^*$	$1404.58 \pm 37.96^*$	5394.25	49.49 ± 9.02
Population doubling	$6.77 \pm 0.03^{***}$	$4.8 \pm 0.04^{***}$	6.74	7.16 ± 0.30
Doubling time (days)	$2.22 \pm 0.01^{***}$	$3.12 \pm 0.02^{***}$	2.23	2.10 ± 0.09

Differences between AS 10 and AS 50 bioreactors were considered significant at

* $P < 0.05$ and

*** $P < 0.001$.

5×10^4 hiPS cells/mL for expansion in stirred bioreactors. In these studies, hiPSC proliferation by the 4- to 6-fold was observed, reaching 2×10^6 to 3.5×10^6 cells/mL.^{35,36} In contrast, Lei et al³⁷ applied a hydrogel-based 3D culture system with inoculum densities between

2.5×10^5 and 2.5×10^6 cells/mL and reported a 20-fold hiPSC expansion with a resulting cell density of 2×10^7 cells/mL. The results of the present study show that the used four-compartment bioreactor enables a 100-fold expansion, reaching 4.69×10^8 cells/mL in

the bioreactor compartment. Initially developed for use as an extracorporeal liver support system and successfully applied as such,³⁸ the compartmentalized bioreactor provides a countercurrent “arteriovenous” media flow and decentralized gas perfusion via capillaries, thereby enhancing mass exchange for an optimized nutrient and oxygen supply for the cultured cells.³⁹ Also, cells are not affected by shear stress, which occurs for example if cells are cultured in stirred tank bioreactors,⁴⁰ and can cause cell damage.⁴¹

The total amount of cells produced in LS 50 (5.4×10^9 cells) would suffice for single-patient treatments in heart and liver therapies as well as treatment of diabetes.¹¹ Cell numbers of this relevance have to date been only achieved by Kwok et al,⁴² who produced 2×10^9 hiPSCs after 14 days of stirred suspension culture, and Abecasis et al,²⁶ who obtained 10^{10} pluripotent hiPSCs within 11 days of 3D culture and three sequential passages. The implementation of a dissociation protocol into our studies may even further improve the expansion rates and the maintenance of an undifferentiated state of cultured hiPSCs for long-term expansion procedures. Also, a larger number of repetitions, especially of the LS 50 run, are needed in order to verify the results of the study.

Several research groups observed that higher cell densities support differentiation processes of pluripotent stem cells.^{31,36,43-47} However, the majority of studies were performed in 2D culture models, where medium is usually exchanged discontinuously, and cells are limited to growing horizontally, instead of three-dimensionally. In contrast, perfused 3D cultures enable a continuous supply with nutrients and oxygen, while maintaining cell pluripotency.⁴⁸ In particular, the four-compartment hollow-fibre bioreactors used in this study aim to mimic the in vivo situation in the tissue, thereby enabling increased cell densities at physiological levels.¹⁷ Therefore, the results gained in 2D cultures may not be directly comparable to the 3D cultures used in the present study.

Furthermore, the results presented in 2D studies regarding critical cell densities varied, depending on the initial cell type and the desired differentiation outcome. For example, Selekmán et al⁴⁹ found that a human pluripotent stem cell density of 6500 cells/cm² is optimal for an epithelial differentiation considering the balance between purity and yield of cells. In contrast, initial seeding densities of dental and oral stem cells for neural induction in 2D cultures laid between 3000 cells/cm² and 20 000 cells/cm².⁵⁰

Overall, the expansion of hiPSCs in 3D hollow-fibre bioreactors was successful for different cell inoculation conditions and bioreactor sizes. The use of a larger bioreactor (17 mL) resulted in clinically relevant cell yields. The findings also show that the inoculum density has significant influence on the growth behaviour and the differentiation state of the cells in 3D bioreactors. A high cell inoculation number led to a faster expansion with higher maximum values for the glucose uptake and growth, but also to cells more prone to differentiation. In contrast, lower initial cell numbers led to slower expansion, but showed less differentiation and required less time and effort for pre-expansion of the inoculum to the 3D bioreactor. The latter is especially of relevance for efficient hiPSC expansion in large-scale bioreactors. Based on the described

results, we conclude that 3D perfusion bioreactors should be inoculated with low cell numbers for achieving a successful long-term hiPSC expansion for clinical purposes. In order to avoid differentiation, additional repeated cell harvesting or cell aggregate dissociation may be included into the expansion procedure.

ACKNOWLEDGMENTS

The work for this study was supported by the German Ministry for Education and Research (BMBF) in the context of “Förderung bilateraler Verbundprojekte US-amerikanischer und deutscher Forschergruppen zur Entwicklung und Validierung von Methoden und Verfahren für die Regenerative Medizin im Rahmen der Ausschreibungen des California Institute for Regenerative Medicine (CIRM)” within the funding network “EKLIPS” (FKZ:13GW0129A).

CONFLICT OF INTEREST

The authors have no conflict of interest to declare.

AUTHOR CONTRIBUTIONS

SG, NF, KZ, TM and CFM designed the experiments. SG, NF, GH and MB performed the experiments. SG and NF analysed the data. SG wrote the manuscript. FS was responsible for technical developments and bioreactor prototype design. MS supervised the study procedure. NF, KZ, MS, TM and CFM critically revised the manuscript.

ORCID

Selina Greuel  <https://orcid.org/0000-0001-5346-4499>

REFERENCES

- Schwartz SD, Regillo CD, Lam BL, et al. Human embryonic stem cell-derived retinal pigment epithelium in patients with age-related macular degeneration and Stargardt's macular dystrophy: follow-up of two open-label phase 1/2 studies. *Lancet*. 2015;385(9967):509-516. [https://doi.org/10.1016/S0140-6736\(14\)61376-3](https://doi.org/10.1016/S0140-6736(14)61376-3)
- Robinton DA, Daley GQ. The promise of induced pluripotent stem cells in research and therapy. *Nature*. 2012;481(7381):295-305. <https://doi.org/10.1038/nature10761>
- Centeno E, Cimarosti H, Bithell A. 2D versus 3D human induced pluripotent stem cell-derived cultures for neurodegenerative disease modelling. *Mol Neurodegener*. 2018;13(1):27. <https://doi.org/10.1186/s13024-018-0258-4>
- Di Baldassarre A, Cimetta E, Bollini S, Gaggi G, Ghinassi B. Human-induced pluripotent stem cell technology and cardiomyocyte generation: progress and clinical applications. *Cells*. 2018;7(6):E48. <https://doi.org/10.3390/cells7060048>
- Mondragon-Gonzalez R, Perlingeiro R. Recapitulating muscle disease phenotypes with myotonic dystrophy 1 induced pluripotent stem cells: a tool for disease modeling and drug discovery. *Dis Model Mech*. 2018;11(7):dmm034728. <https://doi.org/10.1242/dmm.034728>
- Wang Y, Jing Na, Su L, et al. Establishment of induced pluripotent stem cell line (ZZUi009-A) from an Alzheimer's disease patient

- carrying a PSEN1 gene mutation. *Stem Cell Res.* 2018;27:30-33. <https://doi.org/10.1016/j.scr.2017.12.005>
7. Hung S, Khan S, Lo CY, Hewitt AW, Wong R. Drug discovery using induced pluripotent stem cell models of neurodegenerative and ocular diseases. *Pharmacol Ther.* 2017;177:32-43. <https://doi.org/10.1016/j.pharmthera.2017.02.026>
 8. Mandenius CF. Biomechatronics for designing bioprocess monitoring and control systems: application to stem cell production. *J Biotechnol.* 2012;162(4):430-440. <https://doi.org/10.1016/j.jbiotec.2012.09.001>
 9. Kropp C, Massai D, Zweigerdt R. Progress and challenges in large-scale expansion of human pluripotent stem cells. *Process Biochem.* 2017;59:244-254. <https://doi.org/10.1016/j.procbio.2016.09.032>
 10. Steiner D, Khaner H, Cohen M, et al. Derivation, propagation and controlled differentiation of human embryonic stem cells in suspension. *Nat Biotechnol.* 2010;28(4):361-364. <https://doi.org/10.1038/nbt.1616>
 11. Serra M, Brito C, Correia C, Alves PM. Process engineering of human pluripotent stem cells for clinical application. *Trends Biotechnol.* 2012;30(6):350-359. <https://doi.org/10.1016/j.tibtech.2012.03.003>
 12. Zeilinger K, Schreiter T, Darnell M. Scaling down of a clinical three-dimensional perfusion multicompartment hollow fiber bioreactor developed for extracorporeal liver support to an analytical scale device useful for hepatic pharmacological in vitro studies. *Tissue Eng Part C Methods.* 2011;17(5):549-556. <https://doi.org/10.1089/ten.TEC.2010.0580>
 13. Schmelzer E, Mutig K, Schrade P, Bachmann S, Gerlach JC, Zeilinger K. Effect of human patient plasma ex vivo treatment on gene expression and progenitor cell activation of primary human liver cells in multi-compartment 3D perfusion bioreactors for extra-corporeal liver support. *Biotechnol Bioeng.* 2009;103(4):817-827. <https://doi.org/10.1002/bit.22283>
 14. Yu J, Hu K, Smuga-Otto K, et al. Human induced pluripotent stem cells free of vector and transgene sequences. *Science.* 2009;324(5928):797-801. <https://doi.org/10.1126/science.1172482>
 15. Freyer N, Knöspel F, Strahl N, et al. Hepatic differentiation of human induced pluripotent stem cells in a perfused three-dimensional multicompartment bioreactor. *Biores Open Access.* 2016;5(1):235-248. <https://doi.org/10.1089/biores.2016.0027>
 16. Lin Y, Chen G. Embryoid body formation from human pluripotent stem cells in chemically defined E8 media. 2014. StemBook [Internet]. Cambridge, MA: Harvard Stem Cell Institute; 2008. Available from <http://www.ncbi.nlm.nih.gov/books/NBK424234/>. Accessed March 8, 2019
 17. Knöspel F, Freyer N, Stecklum M, Gerlach JC, Zeilinger K. Periodic harvesting of embryonic stem cells from a hollow-fiber membrane based four-compartment bioreactor. *Biotechnol Prog.* 2016;32(1):141-151. <https://doi.org/10.1002/btpr.2182>
 18. Livak KJ, Schmittgen TD. Analysis of relative gene expression data using real-time quantitative PCR and the 2(-Delta Delta C(T)) Method. *Methods.* 2001;25(4):402-408.
 19. Knöspel F, Jacobs F, Freyer N, et al. In vitro model for hepatotoxicity studies based on primary human hepatocyte cultivation in a perfused 3D bioreactor system. *Int J Mol Sci.* 2016;17(4):584. <https://doi.org/10.3390/ijms17040584>
 20. Li L, Bennett SA, Wang L. Role of E-cadherin and other cell adhesion molecules in survival and differentiation of human pluripotent stem cells. *Cell Adh Migr.* 2012;6(1):59-70. <https://doi.org/10.4161/cam.19583>
 21. Nelson CM, Chen CS. Cell-cell signaling by direct contact increases cell proliferation via a PI3K-dependent signal. *FEBS Lett.* 2002;514(2-3):238-242.
 22. Meng G, Liu S, Poon A, Rancourt DE. Optimizing human induced pluripotent stem cell expansion in stirred-suspension culture. *Stem Cells Dev.* 2017;26(24):1804-1817. <https://doi.org/10.1089/scd.2017.0090>
 23. Abaci HE, Truitt R, Luong E, Drazer G, Gerecht S. Adaptation to oxygen deprivation in cultures of human pluripotent stem cells, endothelial progenitor cells, and umbilical vein endothelial cells. *Am J Physiol Cell Physiol.* 2010;298(6):C1527-C1537. <https://doi.org/10.1152/ajpcell.00484.2009>
 24. Simmons AD, Williams C 3rd, Degoix A, Sikavitsas VI. Sensing metabolites for the monitoring of tissue engineered construct cellularity in perfusion bioreactors. *Biosens Bioelectron.* 2017;90:443-449. <https://doi.org/10.1016/j.bios.2016.09.094>
 25. Murphy KC, Hung BP, Browne-Bourne S, et al. Measurement of oxygen tension within mesenchymal stem cell spheroids. *J R Soc Interface.* 2017;14(127):20160851. <https://doi.org/10.1098/rsif.2016.0851>
 26. Abecasis B, Aguiar T, Arnault É, et al. Expansion of 3D human induced pluripotent stem cell aggregates in bioreactors: bioprocess intensification and scaling-up approaches. *J Biotechnol.* 2017;246:81-93. <https://doi.org/10.1016/j.jbiotec.2017.01.004>
 27. Chan FK, Moriwaki K, De Rosa MJ. Detection of necrosis by release of lactate dehydrogenase activity. *Methods Mol Biol.* 2013;979:65-70. https://doi.org/10.1007/978-1-62703-290-2_7
 28. Denecker G, Vercammen D, Steemans M, et al. Death receptor-induced apoptotic and necrotic cell death: differential role of caspases and mitochondria. *Cell Death Differ.* 2001;8(8):829-840.
 29. Abe K, Niwa H, Iwase K, et al. Endoderm-specific gene expression in embryonic stem cells differentiated to embryoid bodies. *Exp Cell Res.* 1996;229(1):27-34.
 30. Stachelscheid H, Wulf-Goldenberg A, Eckert K, et al. Teratoma formation of human embryonic stem cells in three-dimensional perfusion culture bioreactors. *J Tissue Eng Regen Med.* 2013;7(9):729-741. <https://doi.org/10.1002/term.1467>
 31. Toyoda T, Mae S-I, Tanaka H, et al. Cell aggregation optimizes the differentiation of human ESCs and iPSCs into pancreatic bud-like progenitor cells. *Stem Cell Res.* 2015;14(2):185-197. <https://doi.org/10.1016/j.scr.2015.01.007>
 32. Pekkanen-Mattila M, Pelto-Huikko M, Kujala V, et al. Spatial and temporal expression pattern of germ layer markers during human embryonic stem cell differentiation in embryoid bodies. *Histochem Cell Biol.* 2010;133(5):595-606. <https://doi.org/10.1007/s00418-010-0689-7>
 33. Graichen R, Xu X, Braam SR, et al. Enhanced cardiomyogenesis of human embryonic stem cells by a small molecular inhibitor of p38 MAPK. *Differentiation.* 2008;76(4):357-370.
 34. Bettiol E, Sartiani L, Chicha L, Krause KH, Cerbai E, Jaconi ME. Fetal bovine serum enables cardiac differentiation of human embryonic stem cells. *Differentiation.* 2007;75(8):669-681.
 35. Kropp C, Kempf H, Halloin C, et al. Impact of feeding strategies on the scalable expansion of human pluripotent stem cells in single-use stirred tank bioreactors. *Stem Cells Transl Med.* 2016;5(10):1289-1301.
 36. Olmer R, Lange A, Selzer S, et al. Suspension culture of human pluripotent stem cells in controlled, stirred bioreactors. *Tissue Eng Part C Methods.* 2012;18(10):772-784.
 37. Lei Y, Jeong D, Xiao J, Schaffer DV. Developing defined and scalable 3D culture systems for culturing human pluripotent stem cells at high densities. *Cell Mol Bioeng.* 2014;7(2):172-183.
 38. Sauer IM, Zeilinger K, Pless G, et al. Extracorporeal liver support based on primary human liver cells and albumin dialysis-treatment of a patient with primary graft non-function. *J Hepatol.* 2003;39(4):649-653.
 39. Gerlach JC, Lübberstedt M, Edsbagge J, et al. Interwoven four-compartment capillary membrane technology for three-dimensional

- perfusion with decentralized mass exchange to scale up embryonic stem cell culture. *Cells Tissues Organs*. 2010;192(1):39-49. <https://doi.org/10.1159/000291014>
40. Galvanuskas V, Grincas V, Simutis R, Kagawa Y, Kino-Oka M. Current state and perspectives in modeling and control of human pluripotent stem cell expansion processes in stirred-tank bioreactors. *Biotechnol Prog*. 2017;33(2):355-364. <https://doi.org/10.1002/btpr.2431>
 41. Kinney MA, Sargent CY, McDevitt TC. The multiparametric effects of hydrodynamic environments on stem cell culture. *Tissue Eng Part B Rev*. 2011;17(4):249-262. <https://doi.org/10.1089/ten.TEB.2011.0040>
 42. Kwok CK, Ueda Y, Kadari A, et al. Scalable stirred suspension culture for the generation of billions of human induced pluripotent stem cells using single-use bioreactors. *J Tissue Eng Regen Med*. 2018;12(2):e1076-e1087. <https://doi.org/10.1002/term.2435>
 43. Kim E, Kim M, Hwang S-U, et al. Neural induction of porcine-induced pluripotent stem cells and further differentiation using glioblastoma-cultured medium. *J Cell Mol Med*. 2019;23(3):2052-2063. <https://doi.org/10.1111/jcmm.14111>
 44. Le M, Takahi M, Maruyama K, Kurisaki A, Ohnuma K. Cardiac differentiation at an initial low density of human-induced pluripotent stem cells. *Vitro Cell Dev Biol Anim*. 2018;54(7):513-522. <https://doi.org/10.1007/s11626-018-0276-0>
 45. Hsiao C, Lampe M, Nillasithanukroh S, Han W, Lian X, Palecek SP. Human pluripotent stem cell culture density modulates YAP signaling. *Biotechnol J*. 2016;11(5):662-675. <https://doi.org/10.1002/biot.201500374>
 46. Takizawa-Shirasawa S, Yoshie S, Yue F, et al. FGF7 and cell density are required for final differentiation of pancreaticamylase-positive cells from human ES cells. *Cell Tissue Res*. 2013;354(3):751-759. <https://doi.org/10.1007/s00441-013-1695-6>
 47. Lian X, Zhang J, Azarin SM, et al. Directed cardiomyocyte differentiation from human pluripotent stem cells by modulating Wnt/ β -catenin signaling under fully defined conditions. *Nat Protoc*. 2013;8(1):162-175. <https://doi.org/10.1038/nprot.2012.150>
 48. Almutawaa W, Rohani L, Rancourt DE. Expansion of human induced pluripotent stem cells in stirred suspension bioreactors. *Methods Mol Biol*. 2016;1502:53-61. https://doi.org/10.1007/7651_2015_311
 49. Selekmán JA, Grundl NJ, Kolz JM, Palecek SP. Efficient generation of functional epithelial and epidermal cells from human pluripotent stem cells under defined conditions. *Tissue Eng Part C Methods*. 2013;19(12):949-960. <https://doi.org/10.1089/ten.TEC.2013.0011>
 50. Heng BC, Lim LW, Wu W, Zhang C. An overview of protocols for the neural induction of dental and oral stem cells in vitro. *Tissue Eng Part B Rev*. 2016;22(3):220-250. <https://doi.org/10.1089/ten.TEB.2015.0488>

How to cite this article: Greuel S, Hanci G, Böhme M, et al. Effect of inoculum density on human-induced pluripotent stem cell expansion in 3D bioreactors. *Cell Prolif*. 2019;e12604. <https://doi.org/10.1111/cpr.12604>

Greuel S, Freyer N, Hanci G, Böhme M, Miki T, Werner J, Schubert F, Sittinger M, Zeilinger K, Mandenius CF. Online measurement of oxygen enables continuous noninvasive evaluation of human-induced pluripotent stem cell (hiPSC) culture in a perfused 3D hollow-fiber bioreactor. *J Tissue Eng Regen Med.* 2019 Jul;13(7):1203-1216.

<https://doi.org/10.1002/term.2871>



Article

Effects of Co-Culture Media on Hepatic Differentiation of hiPSC with or without HUVEC Co-Culture

Nora Freyer ^{1,*}, Selina Greuel ¹, Fanny Knöspel ¹, Nadja Strahl ¹, Leila Amini ¹, Frank Jacobs ², Mario Monshouwer ² and Katrin Zeilinger ¹

¹ Berlin-Brandenburg Center for Regenerative Therapies (BCRT), Charité—Universitätsmedizin Berlin, Campus Virchow-Klinikum, 13353 Berlin, Germany; selina.greuel@charite.de (S.G.); fanny.knoespel@gmx.de (F.K.); nadja.strahl@outlook.com (N.S.); leila.amini@charite.de (L.A.); katrin.zeilinger@charite.de (K.Z.)

² Janssen Research and Development, 2340 Beerse, Belgium; fjacobs1@its.jnj.com (F.J.); mmonshou@its.jnj.com (M.M.)

* Correspondence: nora.freyer@charite.de; Tel.: +49-30-450-559147

Received: 3 July 2017; Accepted: 2 August 2017; Published: 7 August 2017

Abstract: The derivation of hepatocytes from human induced pluripotent stem cells (hiPSC) is of great interest for applications in pharmacological research. However, full maturation of hiPSC-derived hepatocytes has not yet been achieved in vitro. To improve hepatic differentiation, co-cultivation of hiPSC with human umbilical vein endothelial cells (HUVEC) during hepatic differentiation was investigated in this study. In the first step, different culture media variations based on hepatocyte culture medium (HCM) were tested in HUVEC mono-cultures to establish a suitable culture medium for co-culture experiments. Based on the results, two media variants were selected to differentiate hiPSC-derived definitive endodermal (DE) cells into mature hepatocytes with or without HUVEC addition. DE cells differentiated in mono-cultures in the presence of those media variants showed a significant increase ($p < 0.05$) in secretion of α -fetoprotein and in activities of cytochrome P450 (CYP) isoenzymes CYP2B6 and CYP3A4 as compared with cells differentiated in unmodified HCM used as control. Co-cultivation with HUVEC did not further improve the differentiation outcome. Thus, it can be concluded that the effect of the used medium outweighed the effect of HUVEC co-culture, emphasizing the importance of the culture medium composition for hiPSC differentiation.

Keywords: human induced pluripotent stem cells (hiPSC); hepatic differentiation; human umbilical vein endothelial cells (HUVEC); co-culture

1. Introduction

Human induced pluripotent stem cells (hiPSC) hold great promise for application in cell therapies [1], but also in disease research [1,2] and drug toxicity testing with in vitro models [3]. In pharmacological research, there is a particular need for hepatic cells due to the central role of the liver in drug metabolism and toxicity [4,5]. Previous in vitro studies on hepatic drug toxicity using hepatocyte-like cells (HLC) differentiated from hiPSC showed promising results [6,7]. Despite these encouraging outcomes, the efficiency of the differentiation process of hiPSC towards functional HLC for further use, including hepatotoxicity assessment, remains low [8]. Several research groups managed to generate hiPSC-derived HLC with 60% [9] up to 80–85% [10] of differentiated cells being characterized by the expression of several hepatic markers, including albumin. However, hiPSC-derived HLC showed only 10% of the urea and albumin production capacity compared with primary human hepatocytes [9] and cytochrome P450 (CYP) isoenzyme activities of the generated HLC

were almost 30-fold lower than those of primary human hepatocytes [9]. Baxter et al. characterized human embryonic stem-cell derived HLC as being similar to fetal rather than to adult hepatocytes in terms of their metabolic profile [11]. Therefore, further improvement of the differentiation and maturation process is needed to generate fully functional HLC for clinical or in vitro use.

Current protocols for differentiation of hiPSC towards HLC mostly use a variation of a three-step differentiation protocol including differentiation into definitive endoderm (DE) cells, generation of hepatoblasts and further maturation into HLC [12]. DE differentiation is generally induced by the use of activin A [13,14] and Wnt3a [13,15]. Differentiation into hepatoblasts is supported by the addition of fibroblast growth factors (FGF) and bone morphogenetic proteins (BMP) [16,17] and hepatocyte maturation is induced by using hepatocyte growth factor (HGF) as well as oncostatin M (OSM) [18]. In addition to the optimization of the differentiation media and supplements, overexpression of hepatic transcription factors such as hepatocyte nuclear factor 4 α (HNF4A) [19] and manipulation of miRNA expression [20,21] were investigated aiming to improve hepatic maturation of hiPSC. Further support of the maturation of gained HLC was achieved by transferring the differentiation process to a 3D-culture system [6,22,23].

A promising approach to enhance the differentiation outcome and hepatic functionality of hiPSC-derived HLC can be seen in applying co-cultures with non-parenchymal liver cells. Matsumoto et al. observed that endothelial cells are essential for early organ development prior to the formation of a functioning local vasculature [24]. Takebe and colleagues recapitulated the early liver development by cultivating hiPSC-derived endodermal cells with human umbilical vein endothelial cells (HUVEC) and human mesenchymal stem cells. The observed expression profiles in the resulting hiPSC-liver buds were closer to native human liver tissue than hiPSC-derived HLC differentiated without HUVEC co-culture [25]. Since the cell behavior within such co-cultures relies on specific media compositions, special attention has to be given to the co-culture medium used to provide suitable conditions for all included cell types.

Within the scope to develop a co-culture model consisting of hiPSC-derived DE cells and HUVEC, a two-step approach was applied as shown in Figure 1. First, culture media used for endothelial cells or hepatocytes as well as mixtures thereof were tested in HUVEC mono-cultures. Based on the results, two of those media were selected to differentiate hiPSC-derived DE cells into mature hepatocytes in the presence or absence of HUVEC. Hepatic differentiation of hiPSC in mono- or co-cultures was assessed by measuring the protein and gene expression of stage-specific markers as well as the functionality of pharmacological relevant CYP isoenzymes.

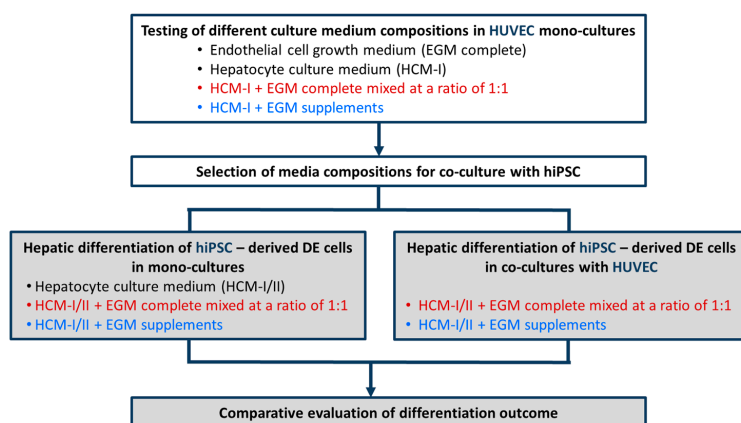


Figure 1. Schematic outline of experimental procedures for media testing in mono-cultures of human umbilical vein endothelial cells (HUVEC, white boxes) and for hepatic differentiation of hiPSC-derived definitive endodermal (DE) cells with or without HUVEC (grey boxes). Different mixtures of hepatocyte culture medium (HCM) and endothelial cell growth medium (EGM) were tested. Colors used for the different media compositions correspond to those used in the graphs.

2. Results

As a prerequisite for co-culture, a culture medium permitting endothelial cell maintenance during differentiation of hiPSC-derived DE cells towards the hepatic fate had to be determined. Therefore, HUVEC were cultured in the presence of 100% endothelial cell growth medium, consisting of basal medium and supplements (EGM complete), 100% hepatocyte culture medium (HCM-I), HCM-I and EGM complete mixed at a ratio of 1:1 (HCM-I + EGM complete) or HCM-I enriched with endothelial cell growth supplements (HCM-I + EGM supplements).

2.1. Effect of Culture Media Variations on Mono-Cultures of Human Umbilical Vein Endothelial Cells (HUVEC)

The use of pure HCM-I for HUVEC cultivation resulted in rapid cell disintegration and detachment and was therefore not further evaluated (data not shown). The results from HUVEC cultures treated with HCM-I + EGM complete, with HCM-I + EGM supplements or with EGM complete as control are shown in Figure 2. The curve progressions displaying glucose consumption rates of HUVEC cultivated in EGM complete or HCM-I + EGM complete were similar, showing an increase until day 4 and a slight decrease until day 6 followed by a slow, but stable increase until day 14 (Figure 2A). Values were only marginally lower in HCM-I + EGM complete than in EGM complete. In contrast, HUVEC grown in HCM-I + EGM supplements showed considerably lower glucose consumption rates over the whole culture period (Figure 2A). Values of lactate production mirrored those of glucose consumption (Figure 2B). Release of lactate dehydrogenase (LDH) as a marker for cell damage was detected at basal levels of maximally 3 U/L for all conditions (data not shown). Gene expression analysis of the endothelial cell markers platelet and endothelial cell adhesion molecule 1 (*PECAM1*) and von Willebrand factor (*VWF*) revealed a 3- to 3.5-fold increase in *PECAM1* gene expression and a 4-fold increase in *VWF* gene expression when using EGM complete or HCM-I + EGM complete (Figure 2C,D). In contrast, the expression levels of both, *PECAM1* and *VWF*, remained stable in HUVEC cultured in HCM-I + EGM supplements throughout the culture period of 14 days.

In accordance to the results of glucose and lactate measurement, cultures grown in EGM complete showed the highest cell density (Figure 3A), followed by those cultured in HCM-I + EGM complete (Figure 3B). Cultivation in HCM-I + EGM supplements resulted in a distinctly lower cell density as compared with the other media investigated (Figure 3C). Immunocytochemical staining of endothelial and hepatocyte markers was performed in HUVEC mono-cultures to evaluate the influence of the tested media on protein expression (Figure 3). Relative percentages of stained cells are provided in Table S1. In all conditions, the two endothelial cell markers *PECAM1* and *VWF* could clearly be observed, whereas the two hepatocyte markers *HNF4A* and cytokeratin 18 (*KRT18*) were not detectable (Figure 3D–I). However, the proportion of cells expressing endothelial cell markers differed between the conditions. Almost all cells ($91 \pm 6\%$) cultured in EGM complete were positive for *PECAM1* (Figure 3D), whereas only around 70% of the cells cultured in HCM-I + EGM complete or in HCM-I + EGM supplements showed *PECAM1* immunoreactivity (Figure 3E,F). Immunoreactivity for *VWF* was observed in approximately 80% of the cells when grown in EGM complete or in HCM-I + EGM complete (Figure 3G,H), while only $62 \pm 12\%$ of the cells cultured in HCM-I + EGM supplements appeared positive for this marker (Figure 3I).

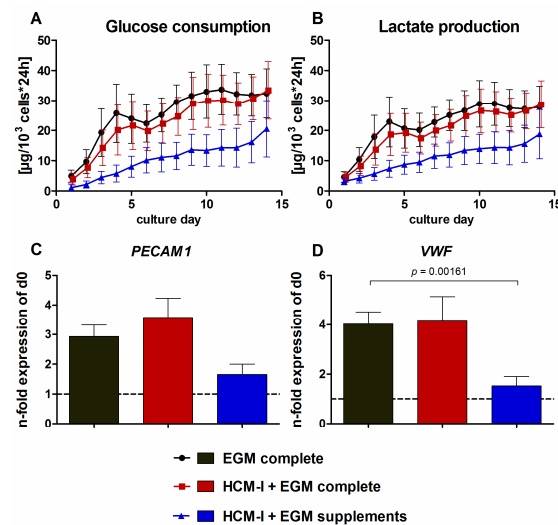


Figure 2. Effect of different media compositions on mono-cultures of human umbilical vein endothelial cells (HUVEC). The cells were cultured over 14 days in endothelial cell growth medium, consisting of basal medium and supplements (EGM complete), in a 1:1 mixture of hepatocyte culture medium and EGM complete (HCM-I + EGM complete) or in HCM enriched with endothelial cell growth supplements (HCM-I + EGM supplements). The graphs show time-courses of glucose consumption (A) and lactate production (B) as well as gene expression analyses of the endothelial cell markers platelet endothelial cell adhesion molecule 1 (*PECAM1*) (C) and von Willebrand factor (*VWF*) (D). Fold changes of mRNA expression were calculated relative to HUVEC before starting the experiments (d0) with normalization to glyceraldehyde-3-phosphate dehydrogenase (*GAPDH*) expression by the $\Delta\Delta C_t$ method. The area under the curve was calculated for time-courses of biochemical parameters and differences between groups were detected using the unpaired, two-tailed Student's *t*-test; for glucose consumption and lactate production $n = 6$, gene expression analysis $n = 3$, mean \pm standard error of the mean.

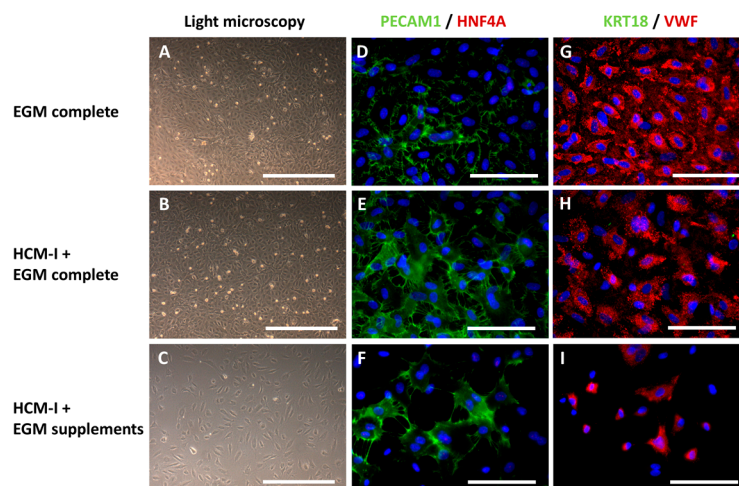


Figure 3. Light microscopy and immunocytochemical staining of mono-cultures of human umbilical vein endothelial cells (HUVEC) after cultivation over 14 days in endothelial cell growth medium, consisting of basal medium and supplements (EGM complete), hepatocyte culture medium and EGM complete mixed at a ratio of 1:1 (HCM-I + EGM complete) or HCM enriched with endothelial cell growth supplements (HCM-I + EGM supplements). The pictures show light microscopic photographs (A–C), staining of the endothelial cell marker platelet endothelial cell adhesion molecule 1 (*PECAM1*) and the hepatocyte marker hepatocyte nuclear factor 4 α (*HNF4A*) (D–F), staining of the hepatocyte marker cytokeratin 18 (*KRT18*) and the endothelial cell marker von Willebrand factor (*VWF*) (G–I). Nuclei were counter-stained with Dapi (blue). Scale bars correspond to 500 μm for light microscopy and to 100 μm for immunofluorescence.

2.2. Hepatic Differentiation of hiPSC-Derived Definitive Endoderm (DE) Cells with or without HUVEC Co-Cultivation Using Different Co-Culture Media

As maintenance and proliferation of endothelial cells might have positive effects on hepatic differentiation of hiPSC, both, HCM-I/II + EGM complete and HCM-I/II + EGM supplements, were tested for their suitability to induce hepatic differentiation in hiPSC-derived DE cells maintained in mono-culture or in co-culture with HUVEC. The results were compared with pure HCM-I/II, used as a positive control. HCM-II is based on HCM-I, but is further supplemented with OSM for the last four days of differentiation.

2.2.1. Morphological Characteristics of hiPSC-Derived Hepatocyte-like Cells (HLC) and Co-Cultured HUVEC

Light microscopic investigation at the end of hepatic differentiation showed that hiPSC-derived HLC maintained without HUVEC co-culture displayed a polygonal shape typical for hepatocytes in all tested media compositions (Figure 4A–C). Use of HCM-I/II + EGM complete resulted in a rather heterogeneous morphology showing large areas of overgrowth (Figure 4B), while HLC differentiated in HCM-I/II or HCM-I/II + EGM supplements appeared more homogeneous (Figure 4A,C). In co-culture experiments, using HCM-I/II + EGM complete or HCM-I/II + EGM supplements as culture media, the HUVEC grew in distinct areas between the hiPSC-derived DE cells until day 7 of the differentiation process (Figure 4D,E). Afterwards, HUVEC progressively infiltrated the hiPSC clusters and at the end of hepatic differentiation (day 17) they could hardly be discriminated from HLC (Figure 4F,G). In both medium conditions, HLC co-cultivated with HUVEC were less homogeneous in their morphology and culture behavior (Figure 4F,G) as compared with the corresponding hiPSC mono-cultures (Figure 4B,C).

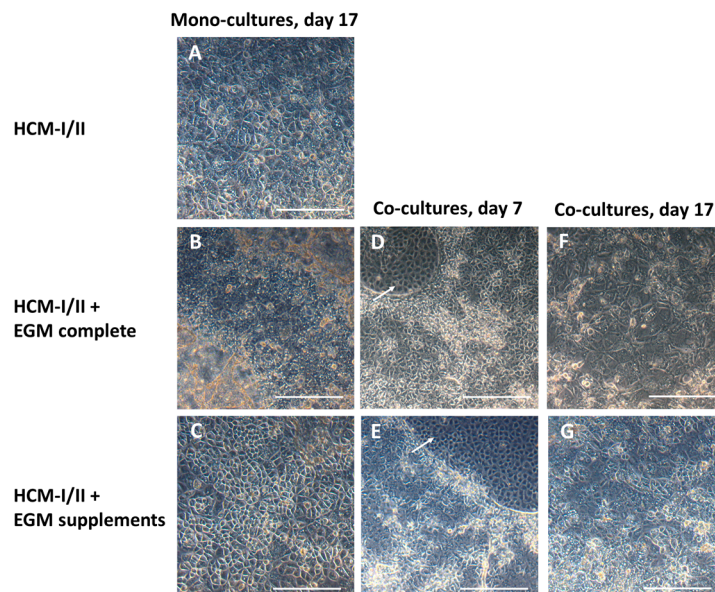


Figure 4. Morphology of human induced pluripotent stem cells (hiPSC) after hepatic differentiation over 17 days in different media and/or in co-culture with human umbilical vein endothelial cells (HUVEC). The pictures show hiPSC after hepatic differentiation in mono-culture over 17 days in hepatocyte culture medium (HCM-I/II) (A), in a 1:1 mixture of hepatocyte culture medium and endothelial cell growth medium EGM, consisting of basal medium and supplements (HCM-I/II + EGM complete) (B) or in HCM enriched with EGM supplements (HCM-I/II + EGM supplements) (C); hiPSC after hepatic differentiation in co-culture with HUVEC on day 7 of differentiation using HCM-I/II + EGM complete (D) or HCM-I/II + EGM supplements (E); hiPSC after hepatic differentiation in co-culture with HUVEC on day 17 of differentiation using HCM-I/II + EGM complete (F) or HCM-I/II + EGM supplements (G). HUVEC were growing in free spaces between the hiPSC (arrows). Scale bars correspond to 300 μ m.

2.2.2. Gene Expression of Stage-Specific and Endothelial Cell Markers

To evaluate the state of differentiation, mRNA expression of stage specific markers in HLC was analyzed relative to undifferentiated hiPSC. HUVEC cultured in EGM complete were used as a positive control for endothelial cell markers (Figure 5). The expression of the pluripotency gene POU domain, class 5, transcription factor 1 (*POU5F1*, Figure 5A) fell to less than 1% relative to undifferentiated hiPSC in all investigated conditions and was lowest in HUVEC mono-cultures. The fetal hepatocyte marker α -fetoprotein (*AFP*) had distinctly increased in all cultures except for the HUVEC. In particular, cultures differentiated in HCM-I/II + EGM supplements showed a distinct up-regulation of *AFP*, amounting to more than 10^7 -fold in both, HLC mono-cultures or co-cultures with HUVEC (Figure 5B). A similar expression pattern was observed for albumin (*ALB*) as a marker for mature hepatocytes, with a more than 10^5 -fold increase in the cultures differentiated in HCM-I/II + EGM supplements with or without HUVEC co-culture (Figure 5C). However, due to large variances in *AFP* and *ALB* expression, the differences between the investigated conditions were not significant (Figure 5B,C). As additional markers for mature hepatocytes, *KRT18* as well as *HNF4A* were investigated (Figure 5D,E). The expression levels of *KRT18* increased by around 10-fold for all tested conditions except for HUVEC mono-cultures which showed a comparable *KRT18* expression as undifferentiated hiPSC. A more pronounced increase by more than 10^4 -fold was observed for *HNF4A* gene expression in the presence of the different test media, which was significantly higher as compared with pure HCM-I/II ($p < 0.05$; Figure 5E). The expression of the endothelial cell marker *PECAM1* was minimally induced in HLC mono-cultures, whereas a more than 200-fold increase in expression was observed in HLC co-cultured with HUVEC, and HUVEC mono-cultures showed a more than 10^4 -fold higher *PECAM1* expression than undifferentiated hiPSC (Figure 5F).

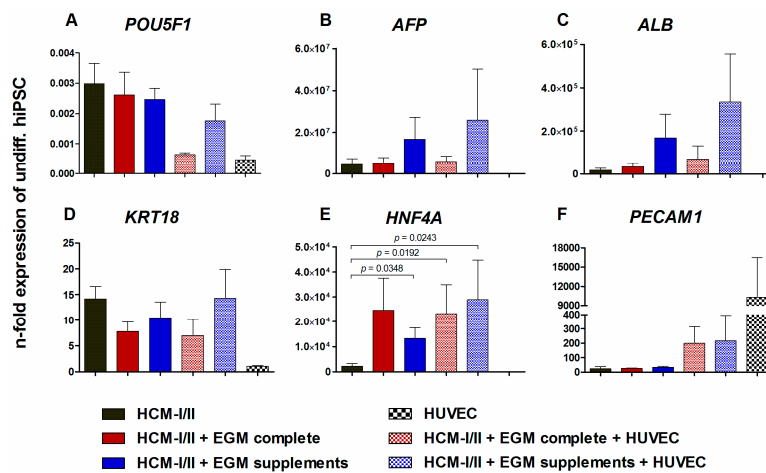


Figure 5. Effect of different media compositions and/or co-culture with human umbilical vein endothelial cells (HUVEC) on mRNA expression of stage-specific markers after hepatic differentiation of human induced pluripotent stem cells (hiPSC). Differentiation of definitive endodermal cells was performed over 14 days using hepatocyte culture medium (HCM-I/II), a 1:1 mixture of hepatocyte culture medium and endothelial cell growth medium, consisting of basal medium and supplements (HCM-I/II + EGM complete) or HCM enriched with endothelial cell growth supplements (HCM-I/II + EGM supplements) with or without HUVEC addition. In addition mRNA expression analysis was performed with HUVEC mono-cultures cultured in EGM complete as control. Graphs show POU class 5 homeobox 1 (*POU5F1*, A), α -fetoprotein (*AFP*, B), albumin (*ALB*, C), cytokeratin 18 (*KRT18*, D), hepatocyte nuclear factor 4 α (*HNF4A*, E) and platelet endothelial cell adhesion molecule 1 (*PECAM1*, F). Fold changes of mRNA expression were calculated relative to undifferentiated hiPSC with normalization to glyceraldehyde-3-phosphate dehydrogenase (*GAPDH*) expression by the $\Delta\Delta C_t$ method. Differences between HCM and all other groups and differences between test media and their corresponding co-cultures were detected with the unpaired, two-tailed Student's *t*-test, $n = 8$; Co-cultures: $n = 3$; mean \pm standard error of the mean.

2.2.3. Immunocytochemical Analysis of Stage-Specific and Endothelial Cell Markers

In order to confirm the results of the mRNA analysis, the protein expression of corresponding stage-specific markers in hiPSC-derived HLC was analyzed using immunocytochemical staining (Figure 6). Relative percentages of stained cells are provided in Table S2. In undifferentiated hiPSC cultures, almost all cells ($99 \pm 3\%$) were positive for the pluripotency marker POU5F1 (Figure 6A), whereas markers of differentiation (KRT18, HNF4A, PECAM1) were not detectable (Figure 6G,M,S). In contrast, the differentiated cultures showed no immunoreactivity for POU5F1 (Figure 6B–F). The hepatocyte marker KRT18 was clearly expressed in all differentiated cultures (Figure 6H–L). However, the percentage of KRT18 positive cells was $80 \pm 6\%$ in cultures incubated with pure HCM-I/II (Figure 6H), whereas in the other experimental groups the proportion of stained cells was distinctly lower, amounting to $60 \pm 17\%$ in HCM-I/II + EGM complete + HUVEC (Figure 6K) and less than 50% in the other groups resulting in a heterogeneous appearance (Figure 6I,J,L). Expression of the hepatocyte marker HNF4A was observed in all differentiated cell cultures with the highest percentage of positive cells ($60 \pm 30\%$) in HCM-I/II cultures (Figure 6N), followed by HCM-I/II + EGM complete cultures with $28 \pm 19\%$ (Figure 6O). All other groups showed 20% or less HNF4A positive cells (Figure 6P–R). The endothelial cell marker PECAM1 was only expressed in HLC cultures differentiated in co-culture with HUVEC (Figure 6W–X), showing a percentage of more than 20% positive cells, while mono-cultures of hiPSC were devoid of PECAM1 (Figure 6S–V).

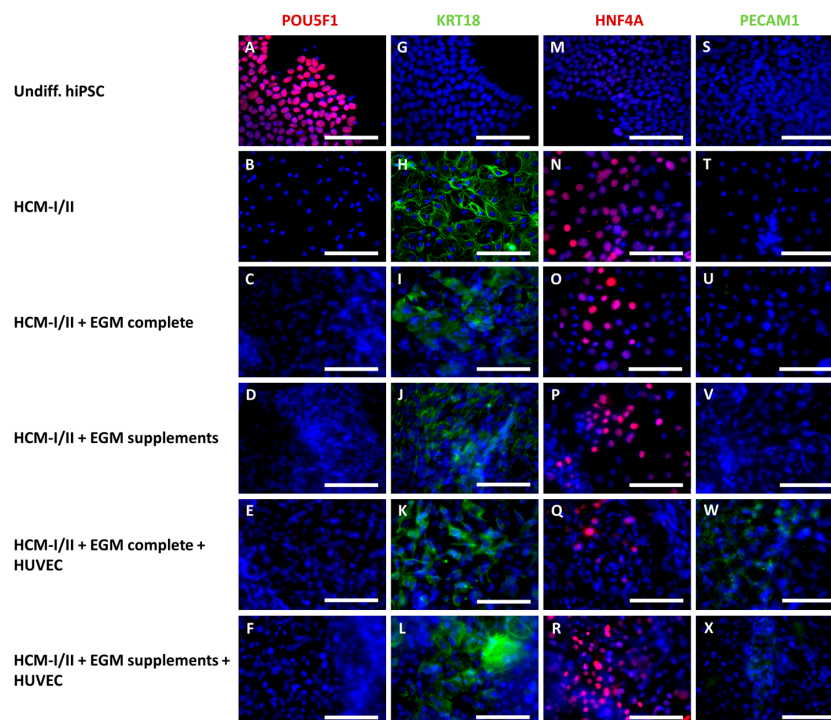


Figure 6. Immunocytochemical staining of human induced pluripotent stem cells (hiPSC) after hepatic differentiation in different media compositions and/or in co-culture with human umbilical vein endothelial cells (HUVEC). Differentiation of definitive endodermal cells was performed over 14 days using hepatocyte culture medium (HCM-I/II), a 1:1 mixture of hepatocyte culture medium and endothelial cell growth medium, consisting of basal medium and supplements (HCM-I/II + EGM complete) or HCM enriched with endothelial cell growth supplements (HCM-I/II + EGM supplements) with or without HUVEC addition. The pictures show the pluripotency marker POU class 5 homeobox 1 (POU5F1, A–F); the hepatocyte markers cytokeratin 18 (KRT18, G–L) and hepatocyte nuclear factor 4 α (HNF4A, M–R) and the endothelial cell marker platelet endothelial cell adhesion molecule 1 (PECAM1, S–X). Nuclei were counter-stained with Dapi (blue). Scale bars correspond to 100 μm .

2.2.4. Secretion of α -Fetoprotein (AFP), Albumin and Urea

The capacity of the cells for synthesis of liver-specific proteins was evaluated by measuring the secretion of the fetal albumin precursor protein AFP and of albumin into the culture supernatant (Figure 7). Secretion of AFP was detectable in all culture conditions from differentiation day 7 onwards (Figure 7A). In the HCM-I/II control culture, AFP secretion increased until day 11 reaching a maximum value of 560 ± 137 ng/h/ 10^6 initial cells and remained stable afterwards. In contrast, a continuous increase of AFP secretion until the end of the differentiation process on day 17 was observed in both, mono-cultures and co-cultures, treated with HCM-I/II + EGM complete or HCM-I/II + EGM supplements. AFP secretion rates over time, as calculated by the area under the curve, significantly ($p < 0.05$) exceeded the release of this protein in HCM-I/II control cultures, amounting to the 6- to 10-fold on day 17 as compared with HCM-I/II. Mean values of the two co-cultures showed a tendency towards higher rates than the corresponding mono-cultures, though there was no significant difference between both groups. Albumin production was detected in all experimental groups from day 9 onwards (Figure 7B). In HCM-I/II control cultures, secretion rates slowly increased up to 2.0 ± 0.4 ng/h/ 10^6 initial cells on day 17, while cultures maintained using the test media clearly showed a steeper increase, attaining 6- to 10-fold higher values as compared with the control. The highest levels of albumin secretion were detected in the co-culture groups with maximal values of 22 ng/h/ 10^6 initial cells on day 17. Cells co-cultured with HUVEC in the presence of HCM-I/II + EGM complete produced significantly more albumin than cells in HCM-I/II control cultures ($p = 0.0058$). As a further parameter to assess the functionality of the differentiated cells, urea secretion was measured over time (Figure 7C). Relatively high values were detected at the beginning of differentiation, which decreased until day 9 and then increased again in all experimental groups until day 17. The highest values of urea secretion were detected in co-cultures with HCM-I/II + EGM supplements. Further, urea secretion was significantly increased in the co-culture with HCM-I/II + EGM complete as compared to the corresponding medium control ($p = 0.0467$).

2.2.5. Functional Analysis of Different Cytochrome P450 (CYP) Isoenzymes

To determine the effect of different culture media and/or co-culture with HUVEC on the functionality of hiPSC-derived HLC, the activity of different pharmacologically relevant CYP isoenzymes was investigated by analyzing isoenzyme-specific product formation rates after application of a substrate cocktail (Figure 8). All measured CYP activities were clearly higher in HCM-I/II + EGM complete or in HCM-I/II + EGM supplements maintained with or without HUVEC as compared with HCM-I/II control cultures. Only for CYP1A2 differentiation with HCM-I/II + EGM complete in co-culture with HUVEC resulted in product formation rates similar to the HCM-I/II control (Figure 8A). And differentiation using HCM-I/II + EGM supplements maintained with or without HUVEC showed higher activities than HCM-I/II + EGM complete. CYP2B6 showed significantly higher activities for HCM-I/II + EGM complete with and without HUVEC and for HCM-I/II + EGM supplements when compared with HCM-I/II control ($p < 0.05$; Figure 8B). Activity patterns for CYP3A4 were similar showing significantly higher activities for both co-cultures and for mono-cultures using HCM-I/II + EGM supplements ($p < 0.05$; Figure 8C).

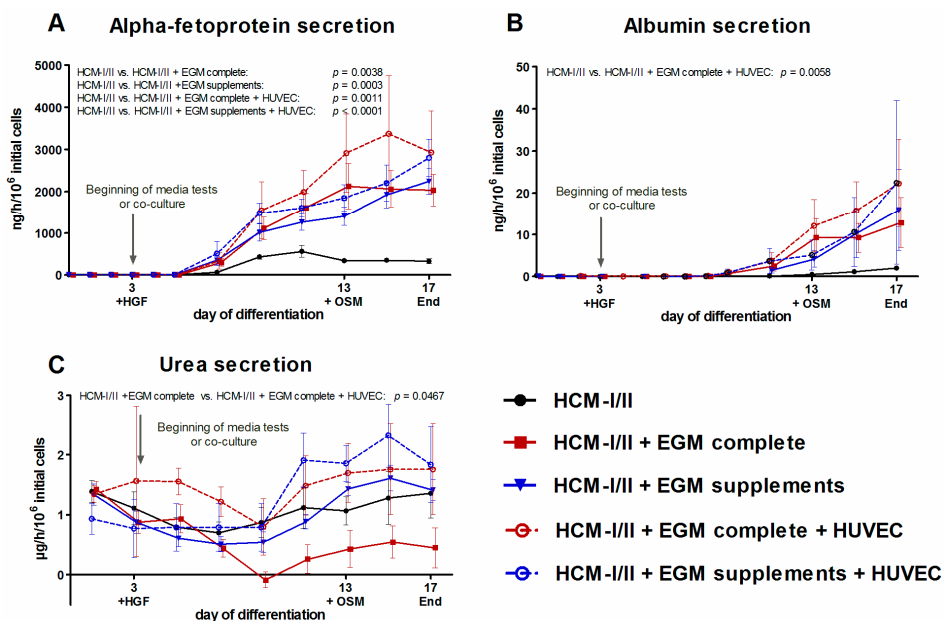


Figure 7. Effect of different media compositions and/or co-culture with human umbilical vein endothelial cells (HUVEC) on secretion of stage-specific markers during differentiation of human induced pluripotent stem cells (hiPSC). Differentiation of definitive endodermal cells was performed over 14 days using hepatocyte culture medium (HCM-I/II), a 1:1 mixture of hepatocyte culture medium and endothelial cell growth medium, consisting of basal medium and supplements (HCM-I/II + EGM complete) or HCM enriched with endothelial cell growth supplements (HCM-I/II + EGM supplements) with or without HUVEC addition. Graphs show the secretion of α -fetoprotein (AFP, A), secretion of albumin (B) and secretion of urea (C). The area under the curve was calculated and differences between HCM and all other groups as well as differences between test media and their corresponding co-cultures were detected using the unpaired, two-tailed Student's *t*-test, $n = 8$; Co-cultures: $n = 3$; mean \pm standard error of the mean.

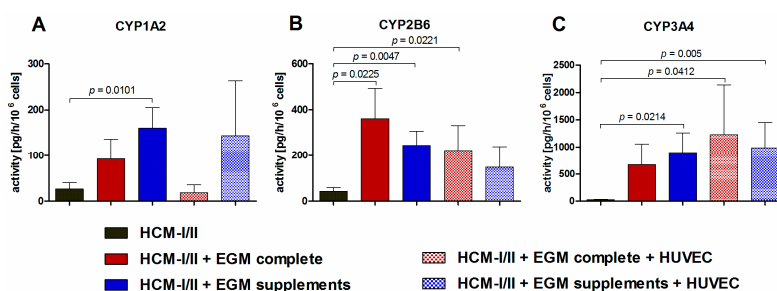


Figure 8. Effect of different media compositions and/or co-culture with human umbilical vein endothelial cells (HUVEC) on activities of cytochrome P450 (CYP) isoenzymes after hepatic differentiation of human induced pluripotent stem cells (hiPSC). Differentiation of definitive endodermal cells was performed over 14 days using hepatocyte culture medium (HCM-I/II), a 1:1 mixture of hepatocyte culture medium and endothelial cell growth medium, consisting of basal medium and supplements (HCM-I/II + EGM complete) or HCM enriched with endothelial cell growth supplements (HCM-I/II + EGM supplements) with or without HUVEC addition. The graphs show activities of CYP1A2 determined by measuring the conversion rates of phenacetin to acetaminophen (A), activities of CYP2B6 determined by measuring the conversion rates of bupropion to 4-OH-bupropion (B) and activities of CYP3A4 determined by measuring the conversion rates of midazolam to 1-OH-midazolam (C) over 6 h. Differences between HCM and all other groups and differences between test media and their corresponding co-cultures were detected using the unpaired, two-tailed Student's *t*-test, HCM: $n = 8$; HCM-I/II + EGM complete and HCM-I/II + EGM Supplements: $n = 7$; co-cultures: $n = 3$; mean \pm standard error of the mean.

3. Discussion

To date, the use of hiPSC-derived HLC in pharmacological drug screening and toxicity testing is limited by their low hepatic functionality due to a heterogeneous phenotype of HLC [26] resembling rather fetal than adult primary human hepatocytes [11]. To improve the differentiation outcome of hiPSC/hESC, several approaches have been focusing on co-culture with non-parenchymal cell types during the differentiation process, using various cell types and culture systems. A major precondition to a functional co-culture system is the use of a suitable culture medium, which meets the requirements of hiPSC as well as those of co-cultured cell types. In the present study, the influence of different culture medium compositions on HUVEC and hiPSC-derived DE cells maintained separately or in co-culture with each other was investigated. Culture media tested included media in use for hiPSC differentiation (HCM), media for HUVEC culture (ECM) and different mixtures of both.

The results from testing different media compositions in HUVEC mono-cultures showed that HUVEC did not survive using pure HCM-I, whereas use of HCM-I + EGM complete resulted in a similar growth behavior as EGM complete, and use of HCM-I + EGM supplements also supported HUVEC growth, although at a reduced level. These findings are in accordance with studies by Takebe et al. [25], who successfully employed HCM and EGM (both from Lonza) for co-culture of hiPSC with HUVEC and mesenchymal stem cells. The observation that HUVEC did not grow in HCM-I can be explained by the fact that this medium lacks some of the ingredients of EGM complete (Table S3), e.g., bovine hypothalamic extract containing the potent endothelial mitogen endothelial cell growth factor (ECGF) [27]. ECGF is even more efficient in combination with heparin [28] also being part of EGM complete, but not being present in HCM. Furthermore, HCM does not contain basic fibroblast growth factor (bFGF), which binds to heparin leading to dimerisation of bFGF receptors [29] and selective induction of endothelial cell proliferation [30]. Insulin, which is included in HCM, but not in EGM complete, is also reported to increase mitosis in endothelial cells [31], but this effect maybe counteracted by other factors. For example, transferrin, which is also part of HCM, was shown to have no influence on endothelial cell proliferation [32], but may play a role in promoting oxidant-induced apoptosis [33]. Furthermore, HCM contains ascorbic acid, which was reported to anticipate oxidative stress-induced apoptosis in endothelial cells [34]. In addition, the reduced proliferation of HUVEC cultivated in HCM-I + EGM supplements compared with cultivation in EGM complete might be associated with the higher glucose concentration of HCM-I + EGM supplements medium (10 mM), as high glucose concentrations have been shown to increase apoptosis and oxidative stress in endothelial cells [35]. In particular constant exposure to glucose levels above 7 mM, which is defined as hyperglycemia in the blood, is not physiological and may harm the endothelium [36].

Based on the results from media testing in HUVEC mono-cultures both, HCM-I/II + EGM complete and HCM-I/II + EGM supplements were tested for their suitability to induce hepatic differentiation in hiPSC-derived DE cells in presence or absence of HUVEC. The results were compared with those from using pure HCM-I/II.

As indicated by stage-specific marker expression and CYP activities, both test media improved the hepatic differentiation of hiPSC as compared with pure HCM-I/II, regardless whether HUVEC were present or not. The favorable effects of EGM complete or EGM supplements on hepatic differentiation of hiPSC may be due to some of the factors contained in those media (Table S3). In particular, the growth factor bFGF contained in EGM supplements has been shown to support the differentiation of DE cells into hepatoblasts in a concentration-dependent manner [37] and has been employed in some studies [17,38]. This may explain the distinctly increased gene expression of the hepatoblast marker *AFP* in cultures treated with HCM-I/II + EGM supplements, since this medium contains the highest amount of bFGF. The secretion of *AFP* was significantly higher in all test groups as compared with the control cultures maintained in pure HCM-I/II. A higher grade of hepatoblast differentiation may consequently lead to an increased hepatic maturation, as indicated by distinctly increased albumin secretion rates in all test groups. The albumin secretion detected in the test groups, when calculated for the same time interval (days), was more than twice as high compared to other

studies [9,16,39,40], while Baxter et al. and Gieseck et al. reported even higher albumin secretion rates of up to 1.5 g/day/10⁶ cells [11,22]. However, it has to be considered that the authors of these studies have been using different cell lines and culture protocols, which might have influenced the differentiation outcome and albumin secretion.

Potential reasons for the observed variability in the present data sets can be seen in influencing factors showing some variations among the experiments, e.g., passage number and seeding efficiency of different cell batches. In addition the usage of different batches of medium compounds may cause some variances. For example, B27 supplement used for the definitive endodermal differentiation step showed substantial variation between specific lots of B27 supplements in neuronal cell cultures [41] and also in hepatic differentiation experiments [42].

The gene expression of the epithelial marker *KRT18* was only slightly increased in differentiated HLC compared with undifferentiated hiPSC; however, immunoreactivity for KRT18 was clearly observed in hiPSC-derived HLC cultures. Both, gene and protein expression of KRT18, were barely influenced by the medium composition or addition of HUVEC. In contrast, the gene expression of the hepatic transcription factor *HNF4A* was distinctly increased in all groups compared with the use of pure HCM-I/II. This observation might again be explained by the effect of bFGF contained in HCM-I/II + EGM complete and HCM-I/II + EGM supplements since gene expression of *HNF4A* was shown to be induced by BMP4/bFGF supplemented media [10,43]. In addition, there are data indicating that the expression of *HNF4A* can be influenced by exposure to glucocorticoids [44], which are contained at a higher level in both test media as compared with pure HCM-I/II. Interestingly there was a discrepancy between protein expression of HNF4A as analyzed by immune fluorescence staining and gene expression of that factor. This could be explained by post-translational modifications of the protein that may reduce the sensitivity of the antibody used for immune fluorescence staining. Yokoyama et al. reported eight different post-translational modifications sites and observed that one of these sites is even changing in response to varying glucose levels [45], as occurring in different culture medium compositions used in this study. The nuclear receptor HNF4A is also responsible for the transcriptional activation of several CYP isoenzymes such as CYP1A2 [46] and CYP3A4 [47]. Both, the significantly increased *HNF4A* expression and the higher hydrocortisone concentration in both test media can explain the significant increase in CYP activities observed in the present study. Glucocorticoids are known to induce CYP2B, CYP2C and CYP3A in humans [48]. CYP activities were significantly increased in cultures differentiated in the optimized co-culture media as compared to the HCM-I/II control group. Maximal activities reached up to 10% of the activities of primary human hepatocytes cultured for 24 h, which were determined in a previous study of the authors [23].

The presence of HUVEC in hiPSC co-cultures could be confirmed by light-microscopy. In addition, HUVEC were detected at the end of hepatic differentiation by gene and protein expression of the endothelial cell marker PECAM1. It was reported that heparin, which is included in EGM supplements, enhances HGF production at a post-transcriptional level in HUVEC [49]. This may promote hepatic maturation [50] and proliferation [10,51] in co-cultures. However, in the present study, no supportive effect of HUVEC on the hepatic differentiation of hiPSC was observed.

An overview of current in vitro co-culture approaches for hepatic differentiation of human pluripotent stem cells is provided in Table 1. So far, the use of HUVEC to support hepatic differentiation of hiPSC was reported only in co-cultures together with either human mesenchymal stem cells [25] or adipose derived stem cells [52]. Takebe and colleagues created highly functional liver buds, which were able to rescue drug-induced lethal liver failure in immunodeficient mice. Additionally they observed that culturing hiPSC-derived HLC with endothelial cells alone failed to form three-dimensional transplantable tissues. Ma and coworkers observed significantly increased *ALB*, *HNF4A* and transthyretin gene expression in their co-culture model compared with hiPSC mono-cultures [52]. Interestingly, in contrast to the present study, both studies [25,52] omitted the epidermal growth factor (EGF) in the HCM used for differentiation. Since EGF was shown to stimulate cell proliferation in HUVEC in a dose-dependent manner [53,54], EGF should not have a negative

effect on HUVEC during co-culture experiments. Another study applied hiPSC-derived endothelial cells for co-culture during hepatic differentiation of hiPSC and was able to show significantly increased albumin secretion [55].

To increase the effect of HUVEC co-culture on hepatic maturation of hiPSC in the here described model, influencing factors such as the number of HUVEC in relation to hiPSC-derived DE cells, and the culture technique should be optimized. For example, Transwells [56] or niches separated by different extracellular matrices [55,57] can be used to provide a larger growth area for HUVEC, in a separate compartment from hiPSC (Table 1). Another approach would be the detachment of hiPSC-derived DE cells, which can then be mixed with HUVEC and reseeded [25,58,59]. These approaches would also enable to add the HUVEC at a later stage of differentiation, namely the hepatic endoderm stage as described *in vitro* by Takebe et al. [25] and *in vivo* by Matsumoto et al. [24]. Since in the present study HUVEC were expected to adhere in free spaces between the DE cells, the co-culture was initiated before spreading of DE cells resulting in a decrease of the available adhesion area for HUVEC.

As becomes apparent in Table 1, the most frequently used cell type in current co-culture approaches for hepatic differentiation of human pluripotent stem cells are murine embryonic fibroblasts [57,59–61], which increased hepatic gene expression and functionality. In the present study HUVEC were chosen as a well-established and standardized cell source for parenchymal-endothelial cell co-cultures. Furthermore, the umbilical vein is the major afferent vessel in the fetal liver [62,63] and HUVEC might thereby be important for the embryonic liver development. In this context, HUVEC were already successfully applied as early supporters of hepatic differentiation in previous studies [25,52]. Another interesting approach would be the usage of tissue-specific endothelial cells for support of hepatic differentiation through the secretion of tissue-specific factors. It was shown for several organs that tissue-specific endothelial cells orchestrate organ development as well as regeneration after injury before building a functional vasculature [64]. Ding et al. could show that liver sinusoidal endothelial cells release factors, which initiate and sustain liver regeneration induced by partial hepatectomy in mice [65]. Furthermore, there is evidence that adult hepatocytes also play a role in stem cell fate decision during liver regeneration by releasing growth factors such as HGF, Wnt and FGFs [66]. Hence, another strategy would be the co-cultivation with primary adult hepatocytes during hepatic differentiation.

In future studies the present findings should be verified using additional hiPSC lines to identify a potential dependency on donor-specific and epigenetic characteristics of individual hiPSC lines. In addition, a closer investigation of individual factors and compounds in the culture media mixtures would be helpful to create well-defined culture media formulations and to facilitate the further improvement of co-culture media.

Table 1. Studies on hepatic differentiation of human induced pluripotent stem cells (hiPSC) or human embryonic stem cells (hESC) in co-culture with different cell types.

Cell Type Used for Co-Culture with hiPSC/hESC	Ratio (hiPSC/hESC-Derived Cells:Co-Cultured Cell Type(s))	Co-Culture Method	Culture Medium Applied	Ref.
Murine hepatic stromal cell line MLSgt20	1:1	Self-aggregation in microwells	DMEM + FBS + differentiation factors	[58]
Murine embryonic fibroblasts (3T3-J2)	0.04:1	Seeding of DE cells onto mitomycin-treated 3T3-J2 feeder cells	Hepatocyte culture medium + FBS	[60]
Murine embryonic fibroblasts (swiss 3T3)	Not specified	Hepatoblast monolayer covered with 3T3 cell sheet	L15 medium + differentiation factors	[61]
HUVEC and mesenchymal stem cells	10:7:2	Spontaneous formation of 3D liver buds	HCM (without EGF) + EGM, 1:1	[25,67]
hiPSC-derived endothelial cells	2 : 1	Multicomponent hydrogel fibers containing galactose for HLC and collagen for endothelial cells	Not specified	[55]
Hepatic stellate cell line TWNT-1	Not specified	Cell inserts	DMEM-F12 + knockout serum replacer + DMSO	[56]
Murine embryonic fibroblasts (3T3-J2)	2:1 or 2.5:1 for cryopreserved HLC	Micropatterned co-culture containing collagen coating and matrigel overlay	RPMI + B27 supplement + differentiation factors	[57]
Murine embryonic fibroblasts (3T3-J2)	2:1	Self-aggregation in microwells	RPMI + B27 supplement + differentiation factors	[59]
Primary rat hepatocytes	1:2	Microfluidic co-culture	DMEM + FBS + maintenance factors and IMDM + FBS + DMSO + differentiation factors	[66]
HUVEC and adipose derived stem cells	1:1:0.02	3D bioprinting of in vivo like liver lobule structures	HCM (without EGF) + EGM-2, 1:1	[52]
HUVEC	2:1	HUVEC grow in free spaces of hiPSC-derived DE cell monolayers	HCM + EGM complete, 1:1 and HCM + EGM Supplements	Present study

4. Materials and Methods

4.1. Culture of HUVEC

Cryopreserved HUVEC (PromoCell GmbH, Heidelberg, Germany) were thawed as recommended by the manufacturer and were cultivated in endothelial cell growth medium (PromoCell GmbH), consisting of basal medium and supplements (EGM complete) and 0.05 mg/mL gentamycin (Merck, Darmstadt, Germany) on cell culture dishes (ThermoScientific, Waltham, MA, USA) at 37 °C in a 5% CO₂ atmosphere. The cells were passaged according to the manufacturer's instructions when they reached around 95% confluence. The composition of EGM complete as provided by the manufacturer is shown in Table S3.

4.2. Culture and Hepatic Differentiation of hiPSC

The hiPSC line DF6-9-9T [68] (WiCell Research Institute, Madison, WI, USA) was cultured under feeder-free conditions on Nunclon™ six-well cell culture plates (ThermoScientific Nunc™, Schwerte, Germany) coated with 8.68 µg/cm² Matrigel (growth factor reduced, Corning, NY, USA). Cells were expanded with mTeSR™1 medium (Stemcell Technologies, Vancouver, BC, Canada) containing 0.05 mg/mL gentamycin (Merck, Darmstadt, Germany).

Hepatic differentiation of hiPSC was performed according to protocols from Hay et al. [15,18,69] with some modifications, as described previously [23]. Briefly, when hiPSC reached a confluence of approximately 70%, differentiation into DE cells was induced with Roswell Park Memorial Institute (RPMI) 1640 culture medium (Merck) supplemented with 100 ng/mL activin A (Peprotech, London, UK), 50 ng/mL Wnt3a (R&D Systems, Minneapolis, MN, USA), 1 µM sodium butyrate (Sigma-Aldrich, St. Louis, MO, USA) and 2% (*v/v*) B27 supplements without insulin (Life Technologies, Carlsbad, CA, USA) for three days. Subsequently DE cells were differentiated into hepatoblasts over 13 days with hepatocyte culture medium consisting of basal medium and single quotes (Lonza, Walkersville, MD, USA) and 10 ng/mL HGF (Peprotech, Rocky Hill, NJ, USA). For further maturation to hepatocyte-like cells 10 ng/mL OSM (Peprotech) were added during the last four days of differentiation. The hepatoblast differentiation medium is referred to as HCM-I and the maturation medium is referred to as HCM-II throughout the whole manuscript. The composition of HCM as provided by the manufacturer is shown in Table S3.

4.3. Culture Medium Testing in Mono-Cultures of HUVEC

For testing of different culture media, HUVEC were seeded at a density of 4×10^3 cells/cm² and cultured over 14 days in the presence of 100% EGM complete (positive control), 100% HCM-I, HCM-I and EGM complete at a ratio of 1:1 (HCM-I + EGM complete) or HCM-I enriched with endothelial cell growth supplements (HCM-I + EGM supplements).

4.4. Co-Culture of hiPSC-Derived DE cells with HUVEC

For co-culture experiments, hiPSC were differentiated into DE cells as described above. Further differentiation was carried out in HCM-I/II + EGM complete or in HCM-I/II + EGM supplements with HUVEC added to the DE cells at a ratio of 1:2 (5×10^5 HUVEC + 1×10^6 DE cells). In parallel, DE cells were differentiated in HCM-I/II + EGM complete or in HCM-I/II + EGM supplements without HUVEC. An overview of culture media and culture medium combinations used for testing in HUVEC or hiPSC cultures is provided in Table 2.

Table 2. Culture media and culture medium combinations used for testing in cultures of human umbilical vein endothelial cells (HUVEC) or human induced pluripotent stem cells (hiPSC).

Component	EGM complete	HCM-I	HCM-II	HCM-I/II + EGM Complete	HCM-I/II + EGM Supplements
Hepatocyte culture medium (HCM) Bullet Kit	-	100% (v/v)		50% (v/v)	97.5% (v/v)
Endothelial cell growth medium (EGM)	97.5% (v/v)	-		48.75% (v/v)	-
EGM Supplements	2.5% (v/v)	-		1.25% (v/v)	2.5% (v/v)
Human hepatocyte growth factor, recombinant	-	10 ng/mL	10 ng/mL	10 ng/mL	10 ng/mL
Human oncostatin M, recombinant	-	-	10 ng/mL	10 ng/mL ¹	10 ng/mL ¹
Gentamycin	0.05 mg/mL	0.05 mg/mL	0.05 mg/mL	0.05 mg/mL	0.05 mg/mL

¹ only added to media containing HCM-II.

4.5. Analyses of Biochemical Parameters

The metabolic activity of HUVEC was assessed by daily measurement of glucose and lactate concentrations with a blood gas analyzer (ABL 700, Radiometer, Copenhagen, Denmark). Potential cell damage was detected by analyzing the release of LDH using an automated clinical chemistry analyzer (Cobas[®] 8000; Roche Diagnostics, Mannheim, Germany). The secretion of the albumin precursor protein AFP and urea during hiPSC differentiation was detected also using an automated clinical chemistry analyzer (Cobas[®] 8000, Roche Diagnostics). Albumin secretion, as a marker for mature hepatocytes, was quantified using an ELISA Quantitation kit and 3',5,5'-tetramethylbenzidine substrate (both from Bethyl Laboratories, Montgomery, TX, USA) according to the manufacturer's instructions.

4.6. Gene Expression Analysis

RNA was isolated from undifferentiated hiPSC, HLC, HUVEC, or HLC-HUVEC co-cultures. Isolation of RNA and subsequent cDNA synthesis were performed as described elsewhere [70], using PureLink[™] RNA Mini Kit (Life Technologies) and High Capacity cDNA Reverse Transcription Kit (Applied Biosystems, Foster City, CA). Each cDNA template was mixed with PCR Master mix (Applied Biosystems) and human-specific primers and probes (TaqMan Gene Expression Assay system, Life Technologies, Table 3). Quantitative real-time PCR (qRT-PCR) was performed using a Realtime cycler (Mastercycler ep Realplex 2, Eppendorf, Hamburg, Germany). The expression of specific genes was normalized to that of the housekeeping gene glyceraldehyde-3-phosphate dehydrogenase (*GAPDH*) and fold changes of expression levels were calculated with the $\Delta\Delta C_t$ method [71].

Table 3. Applied Biosystems TaqMan Gene Expression Assays[®].

Gene Symbol	Gene Name	Assay ID
<i>AFP</i>	α fetoprotein	HS00173490_m1
<i>ALB</i>	albumin	HS00910225_m1
<i>GAPDH</i>	glyceraldehyde-3-phosphate dehydrogenase	HS03929097_g1
<i>HNF4A</i>	Hepatocyte nuclear factor 4, α	Hs00230853_m1
<i>KRT18</i>	Keratin 18	Hs02827483_g1
<i>PECAM1</i>	platelet and endothelial cell adhesion molecule 1	Hs00169777_m1
<i>POU5F1</i>	POU domain, class 5, transcription factor 1	HS00999632_g1
<i>VWF</i>	von Willebrand factor	Hs00169795_m1

4.7. Immunocytochemical Staining

Immunofluorescence staining was performed as described elsewhere [70]. Antibodies used are listed in Table 4. Staining of hiPSC-derived cultures was performed in 24-well plates (lumox[®], Sarstedt, Nümbrecht-Rommelsdorf, Germany), while HUVEC were cultured and subsequently fixed on chamber slides (Thermo Scientific™ Nunc™ Lab-Tek™ II Chamber Slide™ System) for immunocytochemical analysis.

Table 4. Primary and secondary antibodies used for immunofluorescence staining.

Antibody Type and Specificity	Protein Symbol	Species	Manufacturer	Article-No.	Final Conc. (µg/mL)
Primary Antibody					
Cytokeratin 18	CK18	mouse	Santa Cruz	Sc-6259	2
Hepatocyte nuclear factor 4 α	HNF4A	rabbit	Santa Cruz	Sc-8987	4
Platelet endothelial cell adhesion molecule 1	PECAM1	mouse	Abcam	ab24590	5
POU domain, class 5, transcription factor 1	OCT3	rabbit	Santa Cruz	Sc-9081	2
Von Willebrand factor	VWF	rabbit	Abcam	ab6994	35.5
Secondary antibody					
Alexa Fluor®488 anti-mouse		goat	Life Technologies	A-11029	2
Alexa Fluor®594 anti-rabbit		goat	Life Technologies	A-11037	2

Fluorescence microscopic pictures were analysed by means of the open source image processing program ImageJ recording at least 5 visual fields for each group.

4.8. Measurement of Cytochrome P450 (CYP) Isoenzyme Activities

Activities of the pharmacologically relevant CYP isoenzymes CYP1A2, CYP2B6 and CYP3A4 were measured in hiPSC after completion of hepatic differentiation as described previously [23]. Briefly, a cocktail containing the CYP substrates phenacetin (CYP1A2), bupropion (CYP2B6) and midazolam (CYP3A4) was added to the cultures and the formation of the corresponding isoenzyme specific products was analyzed by LC-MS as described previously [23].

4.9. Statistical Evaluation

Experiments were performed in three to eight repeats, as indicated in the figure legends, and results are presented as mean ± standard error of the mean. The area under the curve was calculated for time-courses of biochemical parameters and differences between culture media and/or co-cultures were detected with a subsequent unpaired, two-tailed Student's *t*-test. Differences were judged as significant, if the *p*-value was less than 0.05.

5. Conclusions

In summary, the application of co-cultures to generate functional hiPSC-derived HLC is a relatively new and complex research field. Our study shows that the establishment of a functional co-culture model requires an intense study of surrounding aspects influencing the cell maintenance. Particular attention should be given to the composition of the applied media, as our results show that the effect of the co-culture medium outweighed the effect of the co-culture itself.

Supplementary Materials: Supplementary materials can be found at www.mdpi.com/1422-0067/18/8/1724/s1.

Acknowledgments: The research leading to these results has received support from the Innovative Medicines Initiative Joint Undertaking under grant agreement no. 115439, resources of which are composed of financial contribution from the European Union's Seventh Framework Programme (FP7/2007-2013) and EFPIA companies' in kind contribution. This article reflects only the author's views and neither the IMI JU, EFPIA, nor the European Commission is liable for any use that may be made of the information contained therein.

Author Contributions: Nora Freyer conceived, designed and performed the experiments and wrote the manuscript; Selina Greuel contributed to performance of experiments and writing of the manuscript; Fanny Knöspel contributed to data evaluation, provided useful discussion and revised the manuscript; Nadja Strahl contributed to performance of the experiments and analyzed the experimental data; Leila Amini contributed to performance of the experiments and writing of the manuscript and analyzed the experimental data; Frank Jacobs performed CYP analysis, provided useful discussion and revised the manuscript; Mario Monshouwer contributed to the study design and to the preparation of the manuscript, and Katrin Zeilinger contributed to the design of experiments, evaluation of results and writing of the manuscript.

Conflicts of Interest: The authors declare no conflict of interest.

Abbreviations

AFP	α -fetoprotein
ALB	Albumin
bFGF	Basic fibroblast growth factor
BMP	Bone morphogenetic proteins
CYP	Cytochrome P450
DE	Definitive endoderm
DMEM	Dulbecco's modified eagle's medium
DMSO	Dimethyl sulfoxide
ECGF	Endothelial cell growth factor
EGF	Epidermal growth factor
EGM	Endothelial cell growth medium
FBS	Fetal bovine serum
FGF	Fibroblast growth factor
GAPDH	Glyceraldehyde-3-phosphate dehydrogenase
HCM	Hepatocyte culture medium
hESC	Human embryonic stem cells
HGF	hepatocyte growth factor
hiPSC	Human induced pluripotent stem cells
HLC	Hepatocyte-like cells
HNF4A	Hepatocyte nuclear factor 4 α
HUVEC	Human umbilical vein endothelial cells
KRT18	Cytokeratin 18
L15	Leibovitz's
LDH	Lactate dehydrogenase
OSM	Oncostatin M
PECAM1	Platelet and endothelial cell adhesion molecule 1
POU5F1	POU domain, class 5, transcription factor 1
RPMI	Roswell Park Memorial Institute
VWF	Von Willebrand factor

References

1. Yi, F.; Liu, G.H.; Izpisua Belmonte, J.C. Human induced pluripotent stem cells derived hepatocytes: Rising promise for disease modeling, drug development and cell therapy. *Protein Cell* **2012**, *4*, 246–250. [[CrossRef](#)] [[PubMed](#)]
2. Passier, R.; Orlova, V.; Mummery, C. Complex tissue and disease modeling using hiPSCs. *Cell Stem Cell* **2016**, *18*, 309–321. [[CrossRef](#)] [[PubMed](#)]
3. Suter-Dick, L.; Alves, P.M.; Blaauuboer, B.J.; Bremm, K.D.; Brito, C.; Coecke, S.; Flick, B.; Fowler, P.; Hescheler, J.; Ingelman-Sundberg, M.; et al. Stem cell-derived systems in toxicology assessment. *Stem Cells Dev.* **2015**, *24*, 1284–1296. [[CrossRef](#)] [[PubMed](#)]
4. Larrey, D. Epidemiology and individual susceptibility to adverse drug reactions affecting the liver. *Semin. Liver Dis.* **2002**, *22*, 145–155. [[CrossRef](#)] [[PubMed](#)]

5. Sgro, C.; Clinard, F.; Ouazir, K.; Chanay, H.; Allard, C.; Guilleminet, C.; Lenoir, C.; Lemoine, A.; Hillon, P. Incidence of drug-induced hepatic injuries: A French population-based study. *Hepatology* **2002**, *36*, 451–455. [[CrossRef](#)] [[PubMed](#)]
6. Takayama, K.; Kawabata, K.; Nagamoto, Y.; Kishimoto, K.; Tashiro, K.; Sakurai, F.; Tachibana, M.; Kanda, K.; Hayakawa, T.; Furue, M.K.; et al. 3D spheroid culture of hESC/hiPSC-derived hepatocyte-like cells for drug toxicity testing. *Biomaterials* **2013**, *34*, 1781–1789. [[CrossRef](#)] [[PubMed](#)]
7. Ware, B.R.; Berger, D.R.; Khetani, S.R. Prediction of drug-induced liver injury in Micropatterned Co-cultures Containing iPSC-Derived Human Hepatocytes. *Toxicol. Sci.* **2015**, *145*, 252–262. [[CrossRef](#)] [[PubMed](#)]
8. Yu, Y.; Liu, H.; Ikeda, Y.; Amiot, B.P.; Rinaldo, P.; Duncan, S.A.; Nyberg, S.L. Hepatocyte-like cells differentiated from human induced pluripotent stem cells: Relevance to cellular therapies. *Stem Cell Res.* **2012**, *9*, 196–207. [[CrossRef](#)] [[PubMed](#)]
9. Song, Z.; Cai, J.; Liu, Y.; Zhao, D.; Yong, J.; Duo, S.; Song, X.; Guo, Y.; Zhao, Y.; Qin, H.; et al. Efficient generation of hepatocyte-like cells from human induced pluripotent stem cells. *Cell Res.* **2009**, *19*, 1233–1242. [[CrossRef](#)] [[PubMed](#)]
10. Si-Tayeb, K.; Noto, F.K.; Nagaoka, M.; Li, J.; Battle, M.A.; Duris, C.; North, P.E.; Dalton, S.; Duncan, S.A. Highly efficient generation of human hepatocyte-like cells from induced pluripotent stem cells. *Hepatology* **2010**, *51*, 297–305. [[CrossRef](#)] [[PubMed](#)]
11. Baxter, M.; Withey, S.; Harrison, S.; Segeritz, C.P.; Zhang, F.; Atkinson-Dell, R.; Rowe, C.; Gerrard, D.T.; Sison-Young, R.; Jenkins, R.; et al. Phenotypic and functional analyses show stem cell-derived hepatocyte-like cells better mimic fetal rather than adult hepatocytes. *J. Hepatol.* **2015**, *62*, 581–589. [[CrossRef](#)] [[PubMed](#)]
12. Takayama, K.; Mizuguchi, H. Generation of human pluripotent stem cell-derived hepatocyte-like cells for drug toxicity screening. *Drug Metab. Pharmacokinet.* **2017**, *32*, 12–20. [[CrossRef](#)] [[PubMed](#)]
13. Sullivan, G.J.; Hay, D.C.; Park, I.H.; Fletcher, J.; Hannoun, Z.; Payne, C.M.; Dalgetty, D.; Black, J.R.; Ross, J.A.; Samuel, K.; et al. Generation of functional human hepatic endoderm from human induced pluripotent stem cells. *Hepatology* **2010**, *51*, 329–335. [[CrossRef](#)] [[PubMed](#)]
14. Vosough, M.; Omidinia, E.; Kadivar, M.; Shokrgozar, M.A.; Pournasr, B.; Aghdami, N.; Baharvand, H. Generation of functional hepatocyte-like cells from human pluripotent stem cells in a scalable suspension culture. *Stem Cells Dev.* **2013**, *22*, 2693–2705. [[CrossRef](#)] [[PubMed](#)]
15. Hay, D.C.; Fletcher, J.; Payne, C.; Terrace, J.D.; Gallagher, R.C.; Snoeys, J.; Black, J.R.; Wojtacha, D.; Samuel, K.; Hannoun, Z.; et al. Highly efficient differentiation of hESCs to functional hepatic endoderm requires ActivinA and Wnt3a signaling. *Proc. Natl. Acad. Sci. USA* **2008**, *105*, 12301–12306. [[CrossRef](#)] [[PubMed](#)]
16. Cai, J.; Zhao, Y.; Liu, Y.; Ye, F.; Song, Z.; Qin, H.; Meng, S.; Chen, Y.; Zhou, R.; Song, X.; et al. Directed differentiation of human embryonic stem cells into functional hepatic cells. *Hepatology* **2007**, *45*, 1229–1239. [[CrossRef](#)] [[PubMed](#)]
17. Brolén, G.; Sivertsson, L.; Björquist, P.; Eriksson, G.; Ek, M.; Semb, H.; Johansson, I.; Andersson, T.B.; Ingelman-Sundberg, M.; Heins, N. Hepatocyte-like cells derived from human embryonic stem cells specifically via definitive endoderm and a progenitor stage. *J. Biotechnol.* **2010**, *145*, 284–294. [[CrossRef](#)] [[PubMed](#)]
18. Hay, D.C.; Zhao, D.; Fletcher, J.; Hewitt, Z.A.; McLean, D.; Urruticochea-Uriguen, A.; Black, J.R.; Elcombe, C.; Ross, J.A.; Wolf, R.; et al. Efficient differentiation of hepatocytes from human embryonic stem cells exhibiting markers recapitulating liver development in vivo. *Stem Cells* **2008**, *26*, 894–902. [[CrossRef](#)] [[PubMed](#)]
19. Takayama, K.; Inamura, M.; Kawabata, K.; Katayama, K.; Higuchi, M.; Tashiro, K.; Nonaka, A.; Sakurai, F.; Hayakawa, T.; Furue, M.K.; et al. Efficient generation of functional hepatocytes from human embryonic stem cells and induced pluripotent stem cells by HNF4 α transduction. *Mol. Ther.* **2012**, *20*, 127–137. [[CrossRef](#)] [[PubMed](#)]
20. Doddapaneni, R.; Chawla, Y.K.; Das, A.; Kalra, J.K.; Ghosh, S.; Chakraborti, A. Overexpression of microRNA-122 enhances in vitro hepatic differentiation of fetal liver-derived stem/progenitor cells. *J. Cell Biochem.* **2013**, *114*, 1575–1583. [[CrossRef](#)] [[PubMed](#)]
21. Deng, X.G.; Qiu, R.L.; Wu, Y.H.; Li, Z.X.; Xie, P.; Zhang, J.; Zhou, J.J.; Zeng, L.X.; Tang, J.; Maharjan, A.; et al. Overexpression of miR-122 promotes the hepatic differentiation and maturation of mouse ESCs through a miR-122/FoxA1/HNF4a-positive feedback loop. *Liver Int.* **2014**, *34*, 281–295. [[CrossRef](#)] [[PubMed](#)]

22. Gieseck, R.L., III; Hannan, N.R.; Bort, R.; Hanley, N.A.; Drake, R.A.; Cameron, G.W.; Wynn, T.A.; Vallier, L. Maturation of induced pluripotent stem cell derived hepatocytes by 3D-culture. *PLoS ONE* **2014**, *9*, e86372. [[CrossRef](#)] [[PubMed](#)]
23. Freyer, N.; Knöspel, F.; Strahl, N.; Amini, L.; Schrade, P.; Bachmann, S.; Damm, G.; Seehofer, D.; Jacobs, F.; Monshouwer, M.; et al. Hepatic differentiation of human induced pluripotent stem cells in a perfused three-dimensional multicompartiment bioreactor. *BioRes. Open Access* **2016**, *5*, 235–248. [[CrossRef](#)] [[PubMed](#)]
24. Matsumoto, K.; Yoshitomi, H.; Rossant, J.; Zaret, K.S. Liver organogenesis promoted by endothelial cells prior to vascular function. *Science* **2001**, *294*, 559–563. [[CrossRef](#)] [[PubMed](#)]
25. Takebe, T.; Sekine, K.; Enomura, M.; Koike, H.; Kimura, M.; Ogaeri, T.; Zhang, R.R.; Ueno, Y.; Zheng, Y.W.; Koike, N.; et al. Vascularized and functional human liver from an iPSC-derived organ bud transplant. *Nature* **2013**, *499*, 481–484. [[CrossRef](#)] [[PubMed](#)]
26. Godoy, P.; Schmidt-Heck, W.; Natarajan, K.; Lucendo-Villarín, B.; Szkolnicka, D.; Asplund, A.; Björquist, P.; Widera, A.; Stöber, R.; Campos, G.; et al. Gene networks and transcription factor motifs defining the differentiation of stem cells into hepatocyte-like cells. *J. Hepatol.* **2015**, *63*, 934–942. [[CrossRef](#)] [[PubMed](#)]
27. Maciag, T.; Cerundolo, J.; Ilsley, S.; Kelley, P.R.; Forand, R. An endothelial cell growth factor from bovine hypothalamus: Identification and partial characterization. *Proc. Natl. Acad. Sci. USA* **1979**, *76*, 5674–5678. [[CrossRef](#)] [[PubMed](#)]
28. Thornton, S.C.; Mueller, S.N.; Levine, E.M. Human endothelial cells: Use of heparin in cloning and long-term serial cultivation. *Science* **1983**, *222*, 623–625. [[CrossRef](#)] [[PubMed](#)]
29. Spivak-Kroizman, T.; Lemmon, M.A.; Dikic, I.; Ladbury, J.E.; Pinchasi, D.; Huang, J.; Jaye, M.; Crumley, G.; Schlessinger, J.; Lax, I. Heparin-induced oligomerization of FGF molecules is responsible for FGF receptor dimerization, activation, and cell proliferation. *Cell* **1994**, *79*, 1015–1024. [[CrossRef](#)]
30. Kang, S.S.; Gosselin, C.; Ren, D.; Greisler, H.P. Selective stimulation of endothelial cell proliferation with inhibition of smooth muscle cell proliferation by fibroblast growth factor-1 plus heparin delivered from fibrin glue suspensions. *Surgery* **1995**, *118*, 280–286. [[CrossRef](#)]
31. Montagnani, M.; Golovchenko, I.; Kim, I.; Koh, G.Y.; Goalstone, M.L.; Mundhekar, A.N.; Johansen, M.; Kucik, D.F.; Quon, M.J.; Draznin, B. Inhibition of phosphatidylinositol 3-kinase enhances mitogenic actions of insulin in endothelial cells. *J. Biol. Chem.* **2002**, *277*, 1794–1799. [[CrossRef](#)] [[PubMed](#)]
32. Carlevaro, M.F.; Albin, A.; Ribatti, D.; Gentili, C.; Benelli, R.; Cermelli, S.; Cancedda, R.; Cancedda, F.D. Transferrin promotes endothelial cell migration and invasion: implication in cartilage neovascularization. *J. Cell. Biol.* **1997**, *136*, 1375–1384. [[CrossRef](#)] [[PubMed](#)]
33. Kotamraju, S.; Chitambar, C.R.; Kalivendi, S.V.; Joseph, J.; Kalyanaraman, B. Transferrin receptor-dependent iron uptake is responsible for doxorubicin-mediated apoptosis in endothelial cells: Role of oxidant-induced iron signaling in apoptosis. *J. Biol. Chem.* **2002**, *277*, 17179–17187. [[CrossRef](#)] [[PubMed](#)]
34. Dhar-Masareño, M.; Cárcamo, J.M.; Golde, D.W. Hypoxia-reoxygenation-induced mitochondrial damage and apoptosis in human endothelial cells are inhibited by vitamin C. *Free Radic. Biol. Med.* **2005**, *38*, 1311–1322. [[CrossRef](#)] [[PubMed](#)]
35. Piconi, L.; Quagliaro, L.; Assaloni, R.; Da Ros, R.; Maier, A.; Zuodar, G.; Ceriello, A. Constant and intermittent high glucose enhances endothelial cell apoptosis through mitochondrial superoxide overproduction. *Diabetes Metab. Res. Rev.* **2006**, *22*, 198–203. [[CrossRef](#)] [[PubMed](#)]
36. Tanaka, M.; Gong, J.; Zhang, J.; Yamada, Y.; Borgeld, H.J.; Yagi, K. Mitochondrial genotype associated with longevity and its inhibitory effect on mutagenesis. *Mech. Ageing Dev.* **2000**, *116*, 65–76. [[CrossRef](#)]
37. Ameri, J.; Ståhlberg, A.; Pedersen, J.; Johansson, J.K.; Johannesson, M.M.; Artner, I.; Semb, H. FGF2 specifies hESC-derived definitive endoderm into foregut/midgut cell lineages in a concentration-dependent manner. *Stem Cells* **2010**, *28*, 45–56. [[CrossRef](#)] [[PubMed](#)]
38. Touboul, T.; Hannan, N.R.; Corbinau, S.; Martinez, A.; Martinet, C.; Branchereau, S.; Mainot, S.; Strick-Marchand, H.; Pedersen, R.; Di Santo, J.; et al. Generation of functional hepatocytes from human embryonic stem cells under chemically defined conditions that recapitulate liver development. *Hepatology* **2010**, *51*, 1754–1765. [[CrossRef](#)] [[PubMed](#)]
39. Kim, J.H.; Jang, Y.J.; An, S.Y.; Son, J.; Lee, J.; Lee, G.; Park, J.Y.; Park, H.J.; Hwang, D.Y.; Kim, J.H.; et al. Enhanced Metabolizing Activity of Human ES Cell-Derived Hepatocytes Using a 3D Culture System with Repeated Exposures to Xenobiotics. *Toxicol. Sci.* **2015**, *147*, 190–206. [[CrossRef](#)] [[PubMed](#)]

40. Tasnim, F.; Phan, D.; Toh, Y.C.; Yu, H. Cost-effective differentiation of hepatocyte-like cells from human pluripotent stem cells using small molecules. *Biomaterials* **2015**, *70*, 115–125. [[CrossRef](#)] [[PubMed](#)]
41. Chen, Y.; Stevens, B.; Chang, J.; Milbrandt, J.; Barres, B.A.; Hell, J.W. NS21: Re-defined and modified supplement B27 for neuronal cultures. *J. Neurosci. Methods*. **2008**, *171*, 239–247. [[CrossRef](#)] [[PubMed](#)]
42. Cai, J.; DeLaForest, A.; Fisher, J.; Urick, A.; Wagner, T.; Twaroski, K.; Cayo, M.; Nagaoka, M.; Duncan, S.A. Protocol for Directed Differentiation of Human Pluripotent Stem Cells toward a Hepatocyte Fate. StemBook. 2012. Available online: <http://www.ncbi.nlm.nih.gov/books/NBK133278/PubMed> (accessed on 2 August 2017).
43. DeLaForest, A.; Nagaoka, M.; Si-Tayeb, K.; Noto, F.K.; Konopka, G.; Battle, M.A.; Duncan, S.A. HNF4A is essential for specification of hepatic progenitors from human pluripotent stem cells. *Development* **2011**, *138*, 4143–4153. [[CrossRef](#)] [[PubMed](#)]
44. Dean, S.; Tang, J.I.; Seckl, J.R.; Nyirenda, M.J. Developmental and tissue-specific regulation of hepatocyte nuclear factor 4-alpha (HNF4-alpha) isoforms in rodents. *Gene Expr.* **2010**, *14*, 337–344. [[CrossRef](#)] [[PubMed](#)]
45. Yokoyama, A.; Katsura, S.; Ito, R.; Hashiba, W.; Sekine, H.; Fujiki, R.; Kato, S. Multiple post-translational modifications in hepatocyte nuclear factor 4 α . *Biochem. Biophys. Res. Commun.* **2011**, *410*, 749–753. [[CrossRef](#)] [[PubMed](#)]
46. Martínez-Jiménez, C.P.; Castell, J.V.; Gómez-Lechón, M.J.; Jover, R. Transcriptional activation of CYP2C9, CYP1A1, and CYP1A2 by hepatocyte nuclear factor 4alpha requires coactivators peroxisomal proliferator activated receptor-gamma coactivator 1alpha and steroid receptor coactivator 1. *Mol. Pharmacol.* **2006**, *70*, 1681–1692. [[CrossRef](#)] [[PubMed](#)]
47. Tirona, R.G.; Lee, W.; Leake, B.F.; Lan, L.B.; Cline, C.B.; Lamba, V.; Parviz, F.; Duncan, S.A.; Inoue, Y.; Gonzalez, F.J.; et al. The orphan nuclear receptor HNF4alpha determines PXR- and CAR-mediated xenobiotic induction of CYP3A4. *Nat. Med.* **2003**, *9*, 220–224. [[CrossRef](#)] [[PubMed](#)]
48. Pascussi, J.M.; Gerbal-Chaloin, S.; Drocourt, L.; Maurel, P.; Vilarem, M.J. The expression of CYP2B6, CYP2C9 and CYP3A4 genes: A tangle of networks of nuclear and steroid receptors. *Biochim. Biophys. Acta* **2003**, *1619*, 243–253. [[CrossRef](#)]
49. Matsumoto, K.; Nakamura, T. Heparin functions as a hepatotrophic factor by inducing production of hepatocyte growth factor. *Biochem. Biophys. Res. Commun.* **1996**, *227*, 455–461. [[CrossRef](#)] [[PubMed](#)]
50. Behbahan, I.S.; Duan, Y.; Lam, A.; Khoobyari, S.; Ma, X.; Ahuja, T.P.; Zern, M.A. New approaches in the differentiation of human embryonic stem cells and induced pluripotent stem cells toward hepatocytes. *Stem Cell Rev.* **2011**, *7*, 748–759. [[CrossRef](#)] [[PubMed](#)]
51. Kang, L.I.; Mars, W.M.; Michalopoulos, G.K. Signals and cells involved in regulating liver regeneration. *Cells* **2012**, *1*, 1261–1292. [[CrossRef](#)] [[PubMed](#)]
52. Ma, X.; Qu, X.; Zhu, W.; Li, Y.S.; Yuan, S.; Zhang, H.; Liu, J.; Wang, P.; Lai, C.S.; Zanella, F.; et al. Deterministically patterned biomimetic human iPSC-derived hepatic model via rapid 3D bioprinting. *Proc. Natl. Acad. Sci. USA* **2016**, *113*, 2206–2211. [[CrossRef](#)] [[PubMed](#)]
53. Nakamura, M.; Nishida, T. Differential effects of epidermal growth factor and interleukin 6 on corneal epithelial cells and vascular endothelial cells. *Cornea* **1999**, *18*, 452–458. [[CrossRef](#)] [[PubMed](#)]
54. Gentilini, G.; Kirschbaum, N.E.; Augustine, J.A.; Aster, R.H.; Visentin, G.P. Inhibition of human umbilical vein endothelial cell proliferation by the CXC chemokine, platelet factor 4 (PF4), is associated with impaired downregulation of p21(Cip1/WAF1). *Blood* **1999**, *93*, 25–33. [[PubMed](#)]
55. Du, C.; Narayanan, K.; Leong, M.F.; Wan, A.C. Induced pluripotent stem cell-derived hepatocytes and endothelial cells in multi-component hydrogel fibers for liver tissue engineering. *Biomaterials* **2014**, *35*, 6006–6014. [[CrossRef](#)] [[PubMed](#)]
56. Javed, M.S.; Yaqoob, N.; Iwamuro, M.; Kobayashi, N.; Fujiwara, T. Generation of hepatocyte-like cells from human induced pluripotent stem (iPS) cells by co-culturing embryoid body cells with liver non-parenchymal cell line TWNT-1. *J. Coll. Physicians Surg. Pak.* **2014**, *24*, 91–96. [[PubMed](#)]
57. Berger, D.R.; Ware, B.R.; Davidson, M.D.; Allsup, S.R.; Khetani, S.R. Enhancing the functional maturity of induced pluripotent stem cell-derived human hepatocytes by controlled presentation of cell-cell interactions in vitro. *Hepatology* **2015**, *61*, 1370–1381. [[CrossRef](#)] [[PubMed](#)]

58. Ishii, T.; Yasuchika, K.; Fukumitsu, K.; Kawamoto, T.; Kawamura-Saitoh, M.; Amagai, Y.; Ikai, I.; Uemoto, S.; Kawase, E.; Suemori, H.; et al. In vitro hepatic maturation of human embryonic stem cells by using a mesenchymal cell line derived from murine fetal livers. *Cell Tissue Res.* **2010**, *339*, 505–512. [[CrossRef](#)] [[PubMed](#)]
59. Song, W.; Lu, Y.C.; Frankel, A.S.; An, D.; Schwartz, R.E.; Ma, M. Engraftment of human induced pluripotent stem cell-derived hepatocytes in immunocompetent mice via 3D co-aggregation and encapsulation. *Sci. Rep.* **2015**, *5*, 16884. [[CrossRef](#)] [[PubMed](#)]
60. Yu, Y.D.; Kim, K.H.; Lee, S.G.; Choi, S.Y.; Kim, Y.C.; Byun, K.S.; Cha, I.H.; Park, K.Y.; Cho, C.H.; Choi, D.H. Hepatic differentiation from human embryonic stem cells using stromal cells. *J. Surg. Res.* **2011**, *170*, 253–261. [[CrossRef](#)] [[PubMed](#)]
61. Nagamoto, Y.; Tashiro, K.; Takayama, K.; Ohashi, K.; Kawabata, K.; Sakurai, F.; Tachibana, M.; Hayakawa, T.; Furue, M.K.; Mizuguchi, H. The promotion of hepatic maturation of human pluripotent stem cells in 3D co-culture using type I collagen and Swiss 3T3 cell sheets. *Biomaterials* **2012**, *33*, 4526–4534. [[CrossRef](#)] [[PubMed](#)]
62. Collardeau-Frachon, S.; Scoazec, J.Y. Vascular development and differentiation during human liver organogenesis. *Anat. Rec.* **2008**, *291*, 614–627. [[CrossRef](#)] [[PubMed](#)]
63. Si-Tayeb, K.; Lemaigre, F.P.; Duncan, S.A. Organogenesis and development of the liver. *Dev. Cell* **2010**, *18*, 175–189. [[CrossRef](#)] [[PubMed](#)]
64. Rafii, S.; Butler, J.M.; Ding, B.S. Angiocrine functions of organ-specific endothelial cells. *Nature* **2016**, *529*, 316–325. [[CrossRef](#)] [[PubMed](#)]
65. Ding, B.S.; Nolan, D.J.; Butler, J.M.; James, D.; Babazadeh, A.O.; Rosenwaks, Z.; Mittal, V.; Kobayashi, H.; Shido, K.; Lyden, D.; et al. Inductive angiocrine signals from sinusoidal endothelium are required for liver regeneration. *Nature* **2010**, *468*, 310–315. [[CrossRef](#)] [[PubMed](#)]
66. Haque, A.; Gheibi, P.; Stybayeva, G.; Gao, Y.; Torok, N.; Revzin, A. Ductular reaction-on-a-chip: Microfluidic co-cultures to study stem cell fate selection during liver injury. *Sci. Rep.* **2016**, *6*. [[CrossRef](#)] [[PubMed](#)]
67. Takebe, T.; Zhang, R.R.; Koike, H.; Kimura, M.; Yoshizawa, E.; Enomura, M.; Koike, N.; Sekine, K.; Taniguchi, H. Generation of a vascularized and functional human liver from an iPSC-derived organ bud transplant. *Nat. Protoc.* **2014**, *9*, 396–409. [[CrossRef](#)] [[PubMed](#)]
68. Yu, J.; Hu, K.; Smuga-Otto, K.; Tian, S.; Stewart, R.; Slukvin, I.I.; Thomson, J.A. Human induced pluripotent stem cells free of vector and transgene sequences. *Science* **2009**, *324*, 797–801. [[CrossRef](#)] [[PubMed](#)]
69. Hay, D.C.; Zhao, D.; Ross, A.; Mandalam, R.; Lebkowski, J.; Cui, W. Direct differentiation of human embryonic stem cells to hepatocyte-like cells exhibiting functional activities. *Cloning Stem Cells* **2007**, *9*, 51–62. [[CrossRef](#)] [[PubMed](#)]
70. Knöspel, F.; Freyer, N.; Stecklum, M.; Gerlach, J.C.; Zeilinger, K. Periodic harvesting of embryonic stem cells from a hollow-fiber membrane based four-compartment bioreactor. *Biotechnol. Prog.* **2016**, *32*, 141–151. [[CrossRef](#)] [[PubMed](#)]
71. Livak, K.J.; Schmittgen, T.D. Analysis of relative gene expression data using real-time quantitative PCR and the 2(-Delta Delta C(T)) Method. *Methods* **2001**, *25*, 402–408. [[CrossRef](#)] [[PubMed](#)]



Mein Lebenslauf wird aus datenschutzrechtlichen Gründen in der elektronischen Version meiner Arbeit nicht veröffentlicht.

Mein Lebenslauf wird aus datenschutzrechtlichen Gründen in der elektronischen Version meiner Arbeit nicht veröffentlicht.

KOMPLETTE PUBLIKATIONSLISTE

Greuel S, Hanci G, Böhme M, Miki T, Schubert F, Sittinger M, Mandenius CF, Zeilinger K, Freyer N. Effect of inoculum density on human-induced pluripotent stem cell expansion in 3D bioreactors. *Cell Prolif.* 2019 May 8:e12604. doi: 10.1111/cpr.12604. [Epub ahead of print] IF: 4.936

Greuel S, Freyer N, Hanci G, Böhme M, Miki T, Werner J, Schubert F, Sittinger M, Zeilinger K, Mandenius CF. Online measurement of oxygen enables continuous non-invasive evaluation of human induced pluripotent stem cell (hiPSC) culture in a perfused 3D hollow-fiber bioreactor. *J Tissue Eng Regen Med.* 2019 Apr 29. doi: 10.1002/term.2871. [Epub ahead of print] IF: 4.089

Freyer N, Knöspel F, Damm G, **Greuel S**, Schneider C, Seehofer D, Stöhr T, Petersen KU, Zeilinger K. Metabolism of remimazolam in primary human hepatocytes during continuous long-term infusion in a 3-D bioreactor system. *Drug Design, Development and Therapy.* 2019 Apr 2 (13), 1033-1047. doi: 10.2147/DDDT.S186759. IF: 2.935

Freyer N*, **Greuel S***, Knöspel F, Gerstmann F, Storch L, Damm G, Seehofer D, Foster Harris J, Iyer R, Schubert F, Zeilinger K. Microscale 3D Liver Bioreactor for In Vitro Hepatotoxicity Testing under Perfusion Conditions. *Bioengineering (Basel).* 2018 Mar 15;5(1). pii: E24. doi: 10.3390/bioengineering5010024. IF: none *These authors contributed equally to this study

Meier F, Freyer N, Brzeszczynska J, Knöspel F, Armstrong L, Lako M, **Greuel S**, Damm G, Ludwig-Schwellinger E, Deschl U, Ross JA, Beilmann M, Zeilinger K. Hepatic differentiation of human iPSCs in different 3D models: A comparative study. *Int J Mol Med.* 2017 Dec;40(6):1759-1771. doi: 10.3892/ijmm.2017.3190. IF: 2.784

Freyer N, **Greuel S**, Knöspel F, Strahl N, Amini L, Jacobs F, Monshouwer M, Zeilinger K. Effects of Co-Culture Media on Hepatic Differentiation of hiPSC with or without HUVEC Co-Culture. *Int J Mol Sci.* 2017 Aug 7;18(8). pii: E1724. doi: 10.3390/ijms18081724. IF: 3.687

DANKSAGUNG

Die vorliegende Arbeit wurde in der Arbeitsgruppe von Frau Dr. Katrin Zeilinger am Berlin-Brandenburger Centrum für Regenerative Therapien (BCRT) im Zeitraum November 2015 bis Juni 2019 angefertigt. Die Forschung mit den resultierenden Ergebnissen wurde durch das BMBF unter der Fördervertragsnummer 13GW0129A gefördert. Diese Arbeit gibt lediglich die Ansichten des Autors wieder; das BMBF haftet nicht für die etwaige Benutzung der darin gemachten Angaben.

An dieser Stelle möchte ich mich ganz ausdrücklich bei allen Unterstützern dieser Arbeit bedanken.

Zu aller Erst bedanke ich mich bei Dr. Katrin Zeilinger, die mir nicht nur die Durchführung der Arbeit in ihrer Arbeitsgruppe ermöglicht hat, sondern mich von Beginn bis Ende des Projekts, selbst nach ihrem Ausscheiden aus der Forschung, beraten und begleitet hat; selten fühlte ich mich so gut betreut. Besonders bedanken möchte ich mich auch bei Prof. Dr. Michael Sittinger, der mir durchweg unterstützend zur Seite stand. Auch bei Prof. Dr. Carl-Fredrik Mandenius bedanke ich mich herzlich für die hervorragende Zusammenarbeit.

Zudem bedanke ich mich bei meinen ehemaligen Arbeitskollegen, die mich liebevoll in ihre Gruppe aufnahmen und für eine sowohl produktive, als auch offene und freundliche Arbeitsatmosphäre sorgten. Gerne denke ich an die gemeinsame Zeit im Labor und die spannenden Diskussionen am Mittagstisch zurück. Insbesondere bedanken möchte ich mich an dieser Stelle bei Dr. Nora Freyer, die mich nicht nur geduldig in die Bioreaktortechnologie und Stammzellkultur eingearbeitet hat, sondern mir jederzeit mit Rat und Tat (und manchmal einem Tee) zur Seite stand. Auch bedanken möchte ich mich bei Güngör Hanci und Mike Böhme, deren Master- bzw. Bachelor-Arbeit zum Gelingen dieser Dissertation beigetragen haben.

Zu guter Letzt bedanke ich mich ganz besonders bei meiner lieben Familie, durch deren bedingungslose Unterstützung diese Arbeit erst ermöglicht wurde. Mein größter Dank gilt meinem Mann Linus, der die tagtäglichen Höhen und Tiefen aufzufangen wusste und der nie den Glauben an mich oder den Erfolg dieser Arbeit verlor.